Cellular Origin and Molecular Expression Mechanisms of Virus-induced Type I Interferon in Vivo

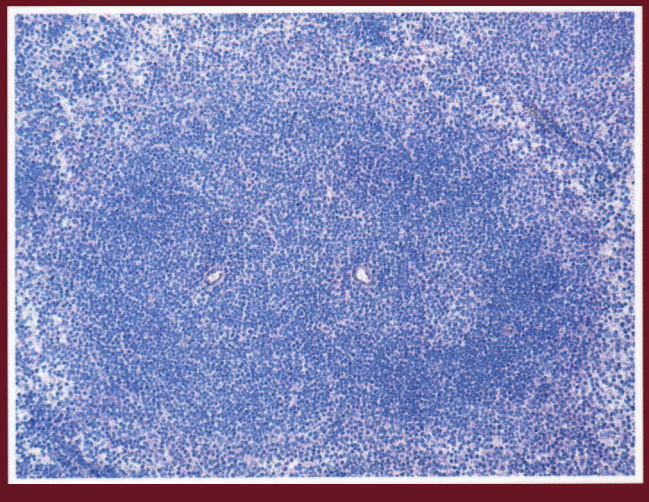

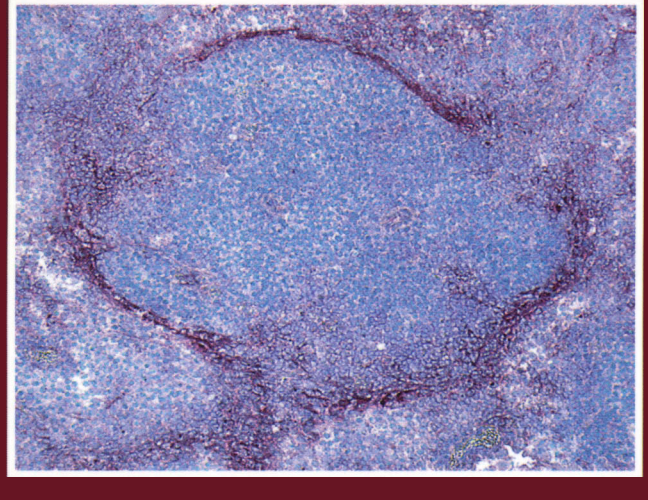

Winfried Barchet

Cellular origin and molecular expression mechanisms of virus-induced type I interferon *in vivo*

Inaugural-Dissertation

zur

Erlangung des Doktorgrades

der Mathematisch-Naturwissenschaftlichen Fakultät

der Universität zu Köln

Vorgelegt von

Winfried Barchet

aus Schorndorf

2002

Berichterstatter: Prof. Dr. Klaus Rajewsky
Prof. Dr. Jonathan Howard

Tag der mündlichen Prüfung: 14.05.02

To the memory of my father

"The trouble with facts is that there are so many of them"

Anonymous

"There is an intrinsic simplicity of nature and the ultimate contribution of science resides in the discovery of unifying and simplifying generalizations, rather than in the description of isolated situations – in the visualization of simple, overall patterns rather than in the analysis of patchworks."

Salvador Luria
General Virology, 1953

Summary

An effective type I interferon (IFN-α/β) response is critical for the control of many viral infections. *In vivo,* the majority of type I IFN is produced by a rare cell type, referred to as professional interferon producing cell (IPC). The phenotype of the murine IPC in viral pathogenesis *in vivo*, and the molecular mechanism by which high-level IFN-α production is regulated in IPCs have not been characterized previously.

Recent analysis of Newcastle disease virus (NDV) infected fibroblasts (MEFs) in cell culture established the model of autocrine feedback regulation of type I IFN production. In this model, induction of IFN-α subtype genes - except α4 - was dependent on type I IFN receptor (IFNAR) triggering and interferon regulatory factor (IRF)-7 upregulation. Since in an acutely infected host, fibroblasts presumably do not produce the majority of type I IFN, we investigated the role of positive feedback regulation of type I IFN induction in viral pathogenesis *in vivo*. Surprisingly, vesicular stomatitis virus (VSV) and UV-inactivated herpes simplex virus (UV-HSV) treated mice mounted early IFN-α responses, largely independent of IFNAR feedback signaling and IRF-7 upregulation. Type I IFN was produced at high level by few cells located in the marginal zone (MZ) of the spleen. In contrast, high-level IFN production by cells in the MZ was not detected in mice stimulated with synthetic double stranded RNA (poly(I:C)). Moreover, IFN-α production in poly(I:C) treated mice was IFNAR dependent. These data are discussed in the context of an extended model of IFN-α induction based on the cell type involved in the production of IFN-α.

To identify professional IFN-α producing cell type(s) in the mouse, IFN-α2 or IRF-7 promoter driven reporter constructs based on bacterial artificial chromosomes (BACs) were generated by homologous recombination (ET-cloning). Currently transgenic mice, expressing these BAC reporters, are being made that will allow to trace the fate of IPCs *in vivo* and may give insights whether differentiated IPCs function as antigen presenting cells.

In a second approach to identify mouse IPCs, numerous populations of CD11c positive dendritic cells (DC) have been isolated from VSV infected mice and screened for IFN-α expression. Unlike all other fractions tested, the population of $CD11c^{int}CD11b^{-}GR\text{-}1^{+}$ DC was a major IFN-α producer. This DC subset had a morphology similar to the human plasmacytoid dendritic cells. Interestingly, these cells expressed IFN-α, irrespective of whether they were isolated from VSV infected IFNAR competent or deficient mice. Thus, VSV preferentially activates a specialized DC subset of mouse IPCs to produce high-level IFN-α largely independent of IFNAR feedback signaling.

VSV infection led to a prompt upregulation of MHC class II and CD86 molecules on the IPCs; a hallmark of DC maturation. However, the IPCs of acutely virus-infected mice rapidly disappeared from secondary lymphoid tissues. At the same time IPC counts were markedly increased in the bone marrow and slightly enhanced in several peripheral organs. IPC repopulation of the spleen occurred during the recovery phase from acute virus infection.

In conclusion, the mouse IPCs described here are capable of immediate IFN-α production upon viral stimulation and show several characteristics of dendritic cell types. However, activated IPCs disappear from secondary lymphoid tissues and are therefore unlikely to constitute a major antigen presenting cell during the initial activation of the adaptive immune response.

Contents

Cover picture: Rapid expression of type I interferon (IFN-α/β) is the key innate immune response to many viral infections. Type I IFN-producing cells in the marginal zone of the spleen were stained with polyclonal antibody directed against type I IFN within hours after viral infection (lower right panel). Unlike fibroblasts in cell culture, type I IFN-producing cells in the mouse are able to produce IFN-α independent of type I IFN receptor (IFNAR) feedback signaling. In both wild-type and IFNAR-/- mice the subset of $CD11c^{+}GR\text{-}1^{+}$ dendritic cells has been shown to be a major producer of type I IFNs after viral infection *in vivo*.
See also figures 3.14 and 3.26*f*.

Detailed Contents

List of Figures and Tables

1 Introduction

1.1 The Immune System

It is the task of the immune system to protect the host against invading infectious agents and thereby to prevent infectious disease. A plethora of microbial pathogens exists (viruses, bacteria, fungi, parasites and helminths). The successful combat of an invading infectious agent largely depends on the host's capacity to mount an appropriate protective immune response.

Classic definition divides the immune system into an innate and an adaptive branch. Innate immunity depends upon germline-encoded receptors to recognize features that are common to many pathogens. These receptors are referred to as pattern-recognition receptors (PRRs) and are expressed differentially by lineages or subtypes of cells. These cells are thus equipped to exert immediate antipathogen effector function. In contrast, adaptive immunity is based on the specific recognition of a defined antigen. Antigen-specific receptors of B- and T-cells (BCR and TCR) are generated by random gene-rearrangement and thus are clonally distributed, i.e. every naive B- and T-lymphocyte carries a unique receptor (Rajewsky, 1996). A specific response is generated by antigen dependent clonal selection and expansion (Burnet, 1966). Therefore the adaptive immune response has a necessarily slow onset, but it provides the important advantage of immunological memory as a consequence of the persistence of antigen-specific clones. This allows the rapid response of specific effector cells upon second encounter with a pathogen bearing the relevant antigen (Zinkernagel et al., 1996).
The receptors and ancient molecular pathways at the core of innate immunity can be traced even in insects and plants, thus appear to be used in immune defense in most if not all multicellular organisms. In comparison, adaptive immunity can be found in jawed fish and ‘higher’ vertebrates but not in other closely related fish species. Recent evidence proposed an explanation for the abrupt emergence of adaptive immunity with the integration of a retroposon into the genome (Agrawal et al., 1998; Hiom et al., 1998). This event may have introduced both the RAG genes and the RSS elements – the paradigm of variability due to DNA recombination - into a gene of the immunoglobulin family.

The harvest of decades of intense research led leading immunologists to conclude that “our understanding of the basic mechanisms governing the complex adaptive immune responses is reasonably complete” (Janeway et al., 2001). Yet it becomes clear, that the effector mechanisms of the adaptive immune system - as an in evolutionary terms recent addition to host defense - can only function properly within the framework of innate immunity. The innate and adaptive immune systems together provide a remarkably effective defense system. It ensures that although we are surrounded by potentially pathogenic micro-organisms, we become ill only relatively rarely. Many infections are handled successfully by the innate immune system and cause no disease, others that cannot be resolved by innate immunity trigger adaptive immunity and are then overcome successfully, followed by lasting immunological memory.

1.2 Innate Immunity

1.2.1 Phagocytes are the primary innate effectors

Elie Metchnikoff is considered the founding father of innate immunology. In early 1900 he discovered that many microorganisms could be engulfed and digested by phagocytic cells, which he called macrophages (Metchinkoff, 1905). In the mammalian immune system there are three types of phagocytes neutrophils, macrophages and dendritic cells (DCs). When the barrier of the epithelia are breached and microbes begin to replicate in the tissues of the host, macrophages and neutrophils provide a first line of defense and are essential for the control of common bacterial infections. It is mainly due to phagocytes that many infections are handled successfully by the innate immune system and cause no disease.
Immune systems of all species have one feature in common: they respond to infection by switching from a resting to an activated state. Thus, there must be key features of an infectious process that trigger immune responses. Pathogens reveal their presence to the cells of the innate immune system via so called pathogen-associated molecular patterns (PAMPs) that are usually embedded in structures that are essential to their bearers' survival. As such, PAMPs evolve slowly and tend to be shared by whole classes of bacteria, viruses or fungi. And, as different classes of microbe carry different PAMPs, a macrophage or dendritic cell can classify the invader, and respond appropriately.

1.2.2 Pattern Recognition Receptors

Receptors on innate immune cells mediate a number of different functions. Many are phagocytic receptors (such as the mannose receptor (CD14), DC lectins or the scavenger receptors) that stimulate ingestion of the pathogens they recognize. Some are chemotactic receptors (e.g. IL-8R or the CXCRs and the CCRs). A third function is to induce effector molecules that contribute to the induced responses of innate immunity and molecules that influence the initiation and nature of any subsequent adaptive immune response. The Toll-like receptors (TLRs) are the best-studied family of molecules serving this purpose. The Toll pathway has been discovered for its role in Drosophila development (Anderson et al., 1985) and only recently it was shown to also participate in defense against infection in adult flies (Hoffmann and Reichhart, 2002), and a similar pathway is used by plants in their defense against viruses (Asai et al., 2002). The necessary DNA sequences are found in all three classes of organisms: invertebrates, vertebrates, and plants. What invertebrates and plants share in common with the vertebrates are the genes that encode intracellular signaling pathways leading from the cell surface to the activation of the transcription factor NF-κB. Each organism has a cassette of genes that encode the proteins of this pathway, supporting the notion that the activation of NF-κB is the original and central signaling pathway of activation in innate immunity (Silverman and Maniatis, 2001).

The central components of the Toll pathway are summarized in Fig. 1.1. The signaling pathway via MyD88 leads to activation of NF-κB transcription factor and c-Jun NH_2 terminal kinase (Jnk) via p38 mitogen-activated protein kinases (MAPKs). In the case of LPS stimulation also MyD88-independent activation of NF-κB and Jnk is observed (Kawai et al., 2001).

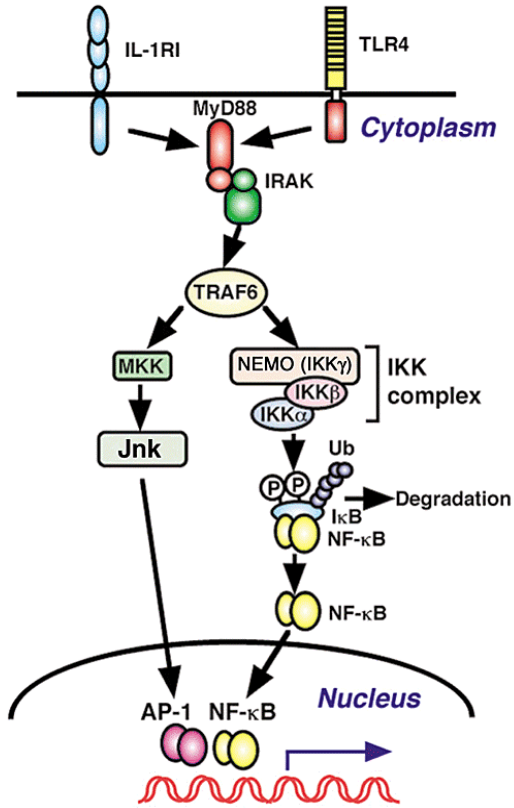

Fig. 1.1 The IL-1R–TLR signaling pathway. Molecular components involved in IL-1R and TLR4 signaling are shown. Activated IL-1R1 or TLR4 associates with a cytoplasmic adaptor molecule, MyD88, through the homophilic interaction between their TIR domains. MyD88 also possess the death domain, which mediates the association with a serine-threonine kinase (IRAK). Subsequently, another adaptor molecule, TRAF6, is activated and in turn activates MAPK kinases (MKKs) and the IKK complex. MKK can lead to AP-1 activation through Jnk. The IKK complex induces phosphorylation of IκB, which renders IB competent for being ubiquitinated and degraded. IB degradation liberates NF-κB and allows it to translocate into the nucleus where it can induce target gene expression. (From Akira Nat. Immunol. 2001) Note that the activation of both NF-κb and the MAPK kinase pathway are prerequisites for IFN-β promoter activation (Chapter 1.6).

So far, ten family members (TLR1-TRL10) have been identified, each able to recognize a specific pathogen component. For most TLRs activating components have been defined, leaving TLR1, TLR8 and TLR10 without a known ligand (Table 1). Importantly, also cellular components released from damaged tissue, e.g. fibronectin or heat-shock proteins (Hsps), have been shown to activate TLRs (Basu et al., 2000; Okamura et al., 2001). These and other cytosolic molecules may serve as endogenous danger signals (Gallucci and Matzinger, 2001), leading to the concept that the immune system does not operate independently of the tissues that it defends.

TLR	Recognized PAMP	Example Pathogens	Reference
TLR1	?		
TLR2 / TLR(2/X) (heterodimer)	Lipoproteins, Glycophosphatidyl-inositol	*M. tuberculosis, Borrelia burgdorfei, Treponema pallidum, Mycoplasma fermentans*	(Means et al., 1999; Means et al., 1999; Underhill et al., 1999)
TLR2 / TLR6	MALP-2 Peptidoglycan (PGN)	Gram-positive bacteria, mycoplasma	(Takeuchi et al., 2001)
TLR3	Double stranded RNA	Most viruses	(Alexopoulou et al., 2001)
TLR4	LPS	Outer membranes of Gram-negative bacteria, *Salmonella*	(Kurt-Jones et al., 2000; Medzhitov et al., 1997)
	Viral Protein	respiratory syncytial virus	
TLR5	Flagellin	Flagellated bacteria, *Listeria monocytogenes*	(Hayashi et al., 2001)
TLR7	(Imidazoquinoline, Immiquimod)	?, viruses?	(Hemmi et al., 2002)
TLR8	?		
TLR9	CpG-DNA	most bacteria, DNA-viruses	(Hemmi et al., 2000)
TLR10	?		

Table 1.1 Toll-like receptors specifically recognize conserved patterns of pathogens

Activation of TLRs leads to the release of several inflammatory mediators, including chemokines, from resident tissue macrophages and dendritic cells, and modulates the expression of chemokine receptors on dendritic cells. The most important innate cytokines that are produced after TLR stimulation include IL-12, TNF-α and the type I IFNs. Data from knockout mice indicate that MyD88 is a critical component in the signaling pathway that leads to production of inflammatory cytokines. MyD88-deficient macrophages are unresponsive to all TLR ligands in terms of cytokine production (Akira et al., 2001; Kawai et al., 1999). Different TLRs seem to activate similar but distinct signaling pathways. Thus, pathogens can determine the nature of the immune response through differential activation of TLRs and the subsequent patterns of cytokine and chemokine expression may be the first point at which the immune system tailors its response to specific pathogens.

1.2.3 Local amplification at the site of the infection

Three critical processes in both innate and adaptive immune defense are recognition, amplification, and control. After the initial recognition of pathogen infection, the numerous signals of the local inflammatory reaction constitute a first amplification process that serves

to attract, activate and enhance other innate immune mechanisms. Most importantly, activated macrophages and dendritic cells secrete, and are themselves affected by, early cytokines (TNF-α, IL-1, IL-6, IL-12 and the type I interferons) and inducible chemokines (e.g. IL-8, MCP-1). These are for example required for the production of the respiratory burst of neutrophils that generates reactive oxygen and nitrogen intermediates (Bogdan, 2001), or for the activation of cytotoxicity in NK cells (Biron, 1997). Other important players in the local immune amplification include inducible cell adhesion molecules, some opsonins, and the complement system.

Most recently, local immunoregulatory mechanisms have been highlighted by the discovery of several receptor families, expressed on myeloid cells. So far, three members of the DAP12 adapter associated TREM family of activating receptors have been described. They are encoded by an innate immune gene complex on chromosome 17 in the mouse. TREM-1 triggering strongly amplifies LPS mediated inflammation and septic shock (Bouchon et al., 2001a), while TREM-2 signaling mediates NF-κB independent maturation of DCs (Bouchon et al., 2001b). Another group of molecules involved in modulating the activity of macrophages and DCs are the members of the receptor tyrosine kinase Tyro-3 family (Tyro-3, Axl, and Mer) (Lu and Lemke, 2001). Finally lysophosphatidylcholine that is released from the membranes of damaged cells is known to promote chemotaxis and later also regulates T-cell activity via the immunoregulatory receptor G2A (Kabarowski et al., 2001). Thus the cells of the innate immune system, and especially antigen presenting cells (APCs), integrate and process a complex set of signals at the site of infection (Lo et al., 1999), and eventually transport this ‘information’ together with pathogen derived antigen to the secondary lymphoid organs (Lanzavecchia and Sallusto, 2001).

1.3 Innate links to adaptive Immunity

The primary adaptive immune response takes place in the draining lymph nodes or the spleen and not in the infected tissue itself. Adaptive immunity is initiated when an innate immune response fails to eliminate a new infection, and antigen and activated antigen-presenting cells are delivered to the draining lymphoid tissues. Indeed, the ability to overcome innate immune defenses is a key feature that distinguishes pathogenic from non-pathogenic microorganisms. The cells of the innate immune system and the cytokines they produce, however, play a crucial part as mediators in the initiation and subsequent direction of adaptive immune responses.

1.3.1 Dendritic cells as mediators

Dendritic cells (DCs) are professional APCs that can activate naïve T cells. They are widely considered the most important mediators between innate and adaptive immunity, because they physically travel from the site of local infection to the regions in secondary lymphoid organs where the initial activation of naïve lymphocytes takes place (Fig. 1.2).
Dendritic cells enter peripheral tissues in an immature state. There, DC maturation can be induced by inflammatory cytokines and by microbes or - if they are ligands of TLRs - their

products. DC maturation is characterized by the production of proinflammatory cytokines (e.g. IL-12 and TNF-α), up-regulation of costimulatory molecules (CD40, CD80 and CD86) and altered expression of chemokine receptors (CCR2, CCR5 and CCR7). Mature DCs show increased antigen-presenting capacity and migrate from the peripheral tissues to draining lymph nodes or the spleen, where they instruct the adaptive immune response by stimulating T lymphocytes (Cella et al., 1997).

1.3.2 Cytokines and Chemokines as mediators

Early innate cytokines may also influence the nascent adaptive response either directly, or indirectly via effects on antigen presenting cells. Importantly, the cytokines present during the initial proliferative phase of T-cell activation shape the functional differentiation of CD4 T cells (Moser and Murphy, 2000). While IL-12 in combination with autocrine or NK-cell derived IFN-γ leads to the differentiation of Th-1 cells (Hsieh et al., 1993), IL-6 together with IL-4 promotes the generation of Th-2 cells (Rincon et al., 1997). In addition, a multitude of chemokines orchestrates the migration and the homing of both innate and adaptive immune cells and hence enables the encounters required for the generation of an adaptive response (reviewed in Luster, 2002).

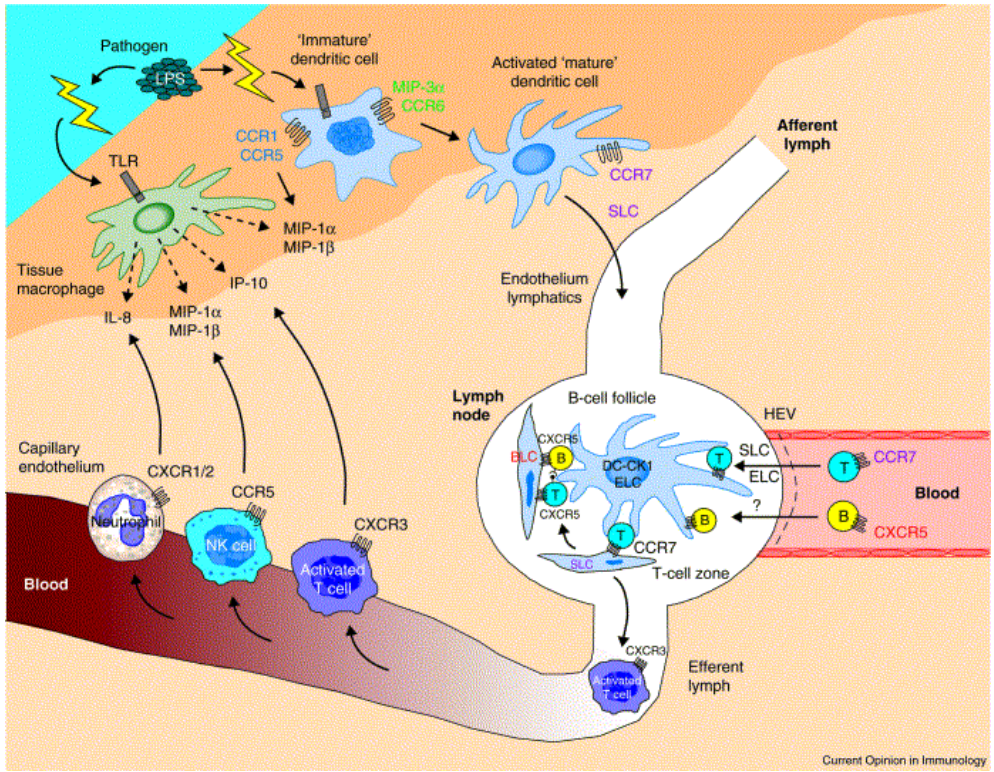

Fig. 1.2 Dendritic cells and cytokines link the local innate immune response with the adaptive response in the lymph node. Immature dendritic cells home to peripheral tissues, where they acquire antigen. Once activated by a pathogen stimulus they mature and migrate to secondary lymphoid organs. In this graph, special emphasis is given to the chemokines involved in the orchestrated migration of innate and adaptive immune cells (Adapted from Luster AD Curr Op Imm 2002).

1.4 Viruses

Viruses have been known as distinct biological entities for little more than a century. The fundamental characteristic of this class of pathogens is their absolute dependence on a living host organism for reproduction. Viruses enter permissive cells, and the infecting genome contains the information necessary to redirect the cell to the production of all the components necessary to assemble new virus particles.
The innate immune response is crucial in antiviral defense because it can be activated quickly and can begin functioning within hours of a viral infection. Such rapid action contrasts with the activation of the adaptive response, which is orders of magnitude slower than the replication cycles of some viruses.
Conversely viruses serve as valuable tools for studying the mechanisms of innate and adaptive immune defense *in vivo*. In the following, the two model pathogens used in this study to characterize the type I IFN response of a virus-infected host are briefly described.

1.4.1 Vesicular stomatitis Virus (VSV)

Vesicular stomatitis virus belongs to the family of Rhabdoviridae, whose members are widely distributed in nature and have a broad host range. In addition to plant rhabdoviruses more than 70 rhabdoviruses of vertebrates have been identified (Shope and Tesh, 1987). Rabies virus is the best-known member of this family of viruses and is of importance to public health as it causes invariably lethal infection in unvaccinated humans. VSV serotype Indiana (VSV-IND) can infect insects and mammals and caused widespread epizootics in cattle and swine in Central America and Mexico (Wagner, 1987). VSV in humans may cause influenza-like disease that is very rarely fatal and almost invariably caused by laboratory infection or by transmission from infected animal cadavers (Tesh and Johnson, 1975). Since VSV has been commonly used as a model in basic virologic and immunologic studies, much is known about its molecular biology and immunology making it an ideal candidate virus for experimental purposes.
Like other rhabdoviruses, VSV particles are bullet shaped (Fig. 1.3 a), approximately 180 nm in length and 65 nm in width. The genome of the VSV-Indiana (VSV-IND) serotype consists of an unsegmented single strand RNA of 11162 nucleotides (Schubert et al., 1984). The membrane of one VSV particle is composed of ~50% host cell derived lipid and 50% protein consisting of 1828 molecules of unglycosylated peripheral matrix protein (M) and 1205 molecules of externally oriented glycoprotein (G) (Thomas et al., 1985). For the survival of VSV infected mice a functional type I IFN response is critical (Steinhoff et al., 1995) that is followed by a potent B cell as well as a cytotoxic T cell (CTL) response. However, only the antibody response is involved in antiviral protection. Interestingly, all VSV neutralizing antibodies are directed against one major antigenic site of the protein moiety of the viral glycoprotein (VSV-G) (Kalinke et al., 1996; Roost et al., 1996) and are detectable in the serum already 2 days after infection (Bachmann et al., 1994).

1.4.2 Herpes Simplex Virus (HSV)

Herpes simplex virus is a member of the Herpesviridae and belongs to the most intensively characterized viruses at the clinical, molecular and structural level (Corey, 1998). Other family members - besides HSV itself - that are of relevance for human pathology include Epstein-Barr virus (EBV), causing acute infectious Mononucleosis and Varicella Zoster the causative agent of chickenpox. In nature, herpes simplex viruses infect exclusively humans, whereas under tissue culture conditions they infect and replicate in most mammalian cell lines. In fact, herpes simplex virus infections are very common, affecting an estimated 40% of the population. There are two types of herpes simplex virus, type I and type II. Most often type I infections involve the mouth and type II the genitalia.
Of interest is that HSV evades the immune system by entering latency in which neither viral proteins nor particles are detectable (Stevens, 1989). Herpes simplex virus acutely infects epithelia and spreads to sensory neurons serving the area of infection. After an effective immune response controls the epithelial infection, the virus persists in the sensory neurons. Environmental stress and/or alteration of the immune status may reactivate viral replication and thus leads to recurrent HSV infections.
The HSV virion particle (Fig. 1.3 b) is 150 - 200 nm in diameter composed of about 40 polypeptides, lipids derived from the host-cell nuclear membrane and complex carbohydrates. The HSV genome is a linear, double-stranded molecule of approximately 150 kb, organized in two segments: Unique Long (UL) and Unique Short (US). The laboratory strain HSV strain F shows a strongly reduced infectivity for humans. The risk of laboratory infection may be reduced further as HSV is sensitive to UV inactivation. Importantly, inactivated HSV (UV-HSV) retains its ability to induce type I IFNs.

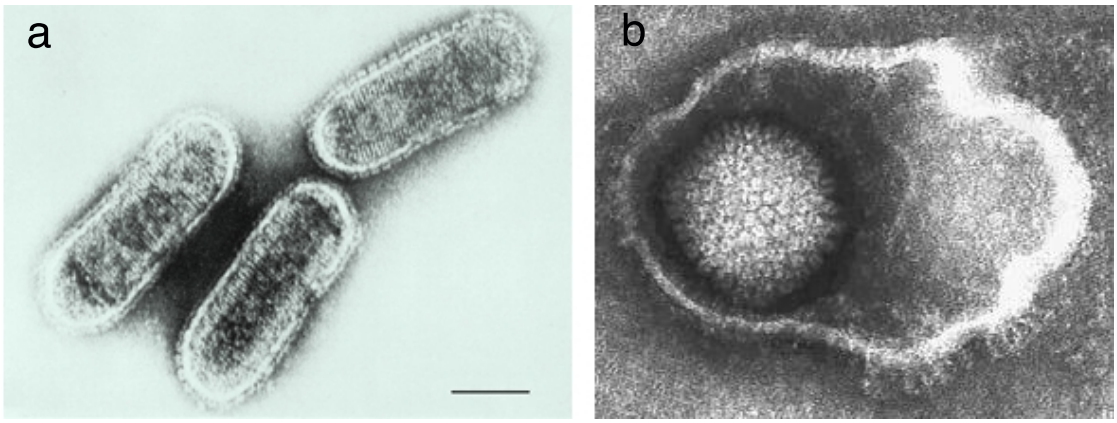

Fig. 1.3 Electron micrographs of vesicular stomatitis virus (a) and herpes simplex virus (b). (**a**) Vesicular stomatitis virus particles are bullet shaped and ca. 180 nm in length. The exposed surface is, with the exception of the flat end of the bullet, densely packed with repeated glycoprotein molecules. (**b**) Herpesviruses have an envelope surrounding an icosahedral capsid, approximately 100 nm in diameter, which contains the dsDNA genome. When the envelope breaks and collapses away from the capsid, virions have a typical "fried-egg" appearance (Micrographs by Dr Frank Fenner and Dr Linda M Stannard).

1.5 Type I IFNs are the primary antiviral cytokine

IFNs were identified by their ability to protect cells against viral infection (Isaacs and Lindenmann, 1957). For a broad spectrum of viruses a functional type I IFN response is critical for the survival of the infected host (Gresser et al., 1976; Muller et al., 1994). Type I interferons (IFN-α/β) constitute a family of highly homologous cytokines, comprising in the mouse at least 11 IFN-α isoforms and one IFN-β, which are all located on the same chromosome (9p in humans and 4q in mice). IFN-γ is the only known type II IFN and shares no obvious structural homology with type I IFNs. Rather than being induced directly by virus infection it is synthesized in response to recognition of infected cells by activated T-lymphocytes and NK cells. However, functional similarities between type I and type II IFNs exist due to a broad overlap in the types of genes that they induce (reviewed in Boehm et al., 1997; http://immunol.annualreviews.org/cgi/content/full/15/1/749/DC1).

1.5.1 Type I IFN receptor signaling

The biologic activity of all IFN-α subtypes and of IFN-β is mediated by binding to the common type I IFN receptor (IFNAR), a heterodimer consisting of the α-chain (IFNAR-1) and the β-chain (IFNAR-2) (Lutfalla and Uze, 1994; Uze et al., 1990). IFN proteins bind to the IFNAR with high affinity (equilibrium dissociation constant [Kd] of about $1 \cdot 10^{-10}$ M). IFNAR signaling activates a JAK-STAT signaling pathway (Darnell, 1997; Leonard and O'Shea, 1998). Activation of the cytoplasmic tyrosine protein kinases Jak1 and Tyk2 leads to phosphorylation of Stat1 and Stat2 transcription factors that heterodimerize, translocate to the nucleus and assemble with the DNA-binding protein IRF-9 (also known as p48) to form the ISGF-3 complex. The ISGF-3 complex binds with high affinity to the IFN-stimulated response element (ISRE, consensus sequence $^{A}/_{G}$NGAAANNGAAACT) found in the promoters of a multitude of IFN stimulated target genes, whose products are responsible for type I IFN mediated effects and may drastically alter cell homeostasis (Fig. 1.4).

1.5.2 Type I IFN function

Similar to other early cytokines, type I IFN mediated effects are pleiotropic and can be classified into 1) direct antiviral, 2) feedback and amplification and 3) immunomodulatory effects.

Type I IFNs stimulate an ‘antiviral state’ in target cells, able to directly block or impair virus replication due to the synthesis of enzymes that interfere with cellular or viral processes. IFNs also slow the growth of target cells and make them more susceptible to apoptosis (Tanaka et al., 1998). In the case of IFN-sensitive viruses (e.g., picorna-, orthomyxo-, retro-, pox-, herpes-, adeno-, papilloma-, and hepadnaviruses), both viral and cellular protein synthesis stops abruptly in IFN treated, infected cells, but not in uninfected cells. This defense is carried out by at least two cellular proteins, dsRNA-activated protein

kinase (PKR) and ribonuclease L (RNase L) (reviewed in Sen, 2001). IFN first promotes the increased expression and accumulation of an inactive protein that subsequently can become activated when the cell is infected. If the cell is infected, PKR proenzyme can be activated by viral dsRNA. Activated PKR then phosphorylates the alpha subunit of the eIF2 translation initiation factor (eIF2a), effectively rendering it incapable of contributing to new protein synthesis in the cell. RNase L is a nuclease capable of degrading most cellular and viral RNA species. RNase L is activated by unusual poly(A) oligomers, which are produced by the 2'-5'-oligo(A) synthetase, but only when activated by dsRNA. Further direct antiviral molecules are Mx proteins of a family of IFN inducible GTPases that are active against various negative strand RNA viruses by inhibiting the viral polymerase. Yet, recent studies involving the generation of mice that are triply deficient in RNase L, PKR and Mx1 indicate that there are additional direct anti-viral effects of IFNs (Zhou et al., 1999).

Type I IFNs synergize with other pro-inflammatory stimuli (i.e. PAMPs, cytokines, chemokines and costimulatory molecules) to attract and activate further innate effectors to the site of the infection. Importantly, type I IFNs synergize with IL-12 in the activation and cytotoxicity of NK cells. Together with GM-CSF or TNF-α, type I IFNs support the activation and maturation of monocytes (Paquette et al., 1998) and resting DCs (Cella et al., 1999; Luft et al., 1998), respectively. In macrophages autocrine type I IFN is required for the enhancement of phagocytosis by M-CSF and IL-4 (Sampson et al., 1991) and stimulates antibody-dependent cytotoxicity. In addition, type I IFNs positively or negatively regulate the production of various cytokines (e.g. TNF, IL-1, IL-6, IL-8, IL-12 and IL-18) by macrophages (Taylor and Grossberg, 1998). Recently it has been shown, that type I IFNs may also regulate their own expression (Harada et al., 1996; Yoneyama et al., 1996). The molecular basis for this feedback mechanism is described in chapter 1.6.

Finally, type I IFNs are known to enhance antigen presentation by upregulating the expression of MHC class I molecules and modulate key facets of the adaptive immune response. An elaborate interplay of positive and negative type I IFN effects influences the production of IL-12 and IFN-γ that are the prime cytokines in shaping the outcome of T-helper cell responses (Biron, 2001). IFN-induced IL-15 can stimulate the division of memory T cells (Zhang et al., 1998), whilst type I IFN may directly promote the survival of activated T cells (Marrack et al., 1999). Furthermore type I IFNs have been shown to exert potent adjuvant activity on the differentiation of DCs from monocytes (Santini et al., 2000) and on the generation of antigen-specific antibody responses (Le Bon et al., 2001). Due to complex and situation dependent interactions with other regulating stimuli, type I IFNs immunomodulatory effects are least well understood and offer ample opportunity for future study.

Besides viruses also certain bacterial or protozoan pathogens induce the production of type I IFNs *in vivo* (Diefenbach et al., 1998; Havell, 1993; Nakane and Minagawa, 1982). Conversely, recombinant IFN-β protected mice against an infection with *L. monocytogenes, Trypanosoma cruzi or T. gondii* (Fujiki and Tanaka, 1988; Kierszenbaum and Sonnenfeld, 1984; Orellana et al., 1991). However, compared to viral infections, the role of type I IFNs for the defense against non-viral pathogens has been considerably less well studied and the function of endogenously produced IFN-α/β remains to be determined.

1.6 Feedback regulation of type I IFN production

Viral infection or stimulation with IFN inducers results in the activation of three different signaling pathways: 1) activation of the NF-κB signaling pathway, via phosphorylation and degradation of the cytoplasmic I-κB inhibitor mediated by the IKK complex; this activation allows free NF-κB to translocate to the nucleus and bind to the PRDII element. 2) activation of the Interferon Regulatory Factors (IRFs), in particular IRF-3 and IRF-7 by phosphorylation and binding to PRDIII-I. 3) activation of the ATF-2/c-Jun transcription complex through phosphorylation by MEKK1 kinase, and binding to PRDIV element. Each of these factors is activated by serine phosphorylation in virus-infected cells, though the kinases involved in the activation of IRF-3 and IRF-7 have not yet been defined. Signaling by all three pathways leads to transcriptional activation of the IFN-β gene via the assembly of an enhanceosome (Thanos and Maniatis, 1995; Wathelet et al., 1998). The high mobility group proteins HMGI(Y) function as architectural proteins. Their interactions with ATF-2/c-Jun and NF-κB are required for virus induction of the IFN-β gene, and for cooperative assembly and stability of the enhanceosome (Yie et al., 1999). The requirements for the expression of the IFN-α subtype genes are less well studied. It is known however, that IFN-α promoter regions contain PRD-like elements (PRD-LE) that allow the binding of members of the IRF family, but most lack the binding site for NF-κB. This suggests a differential regulation of IFN-β and IFN-α promoter activity.

The molecular mechanisms of type I IFN induction were intensively investigated by analyzing virus stimulated mouse embryonic fibroblasts (MEFs) derived from gene targeted mice deficient of factors involved in the type I IFN signaling cascade. MEFs from mice lacking IFN-β, IFNAR-1, Stat-1, or IRF-9 showed a defective IFN-α response (Erlandsson et al., 1998; Harada et al., 1996; Marie et al., 1998; Sato et al., 1998). This suggested that following the production of early IFN-β, and possibly IFN-α4, expression of other IFN-α genes was dependent on type I IFN receptor feedback signaling.

1.6.1 Interferon regulatory factors (IRFs)

The members of the interferon regulatory factor (IRF) family share a high degree of homology in the N-terminal DNA binding domain and generally bind the DNA sequence GAAANNGAAANN; the C-terminal portion of the IRF proteins is unique to each member. Two members of the IRF family - IRF-3 and IRF-7 - have been shown to play a key role in the sequential induction of type I IFN genes. Virus mediated serine phosphorylation leads to IRF-3 activation and translocation to the nucleus (Sato et al., 1998). There, IRF-3 is part of an enhanceosome complex promoting the expression of IFN-β, and presumably of IFN-α4. Early type I IFN is secreted and triggers IFNAR signaling in an autocrine fashion. Among other type I IFN induced genes, IFNAR signaling strongly upregulates IRF-7 expression (Marie et al., 1998; Sato et al., 1998).

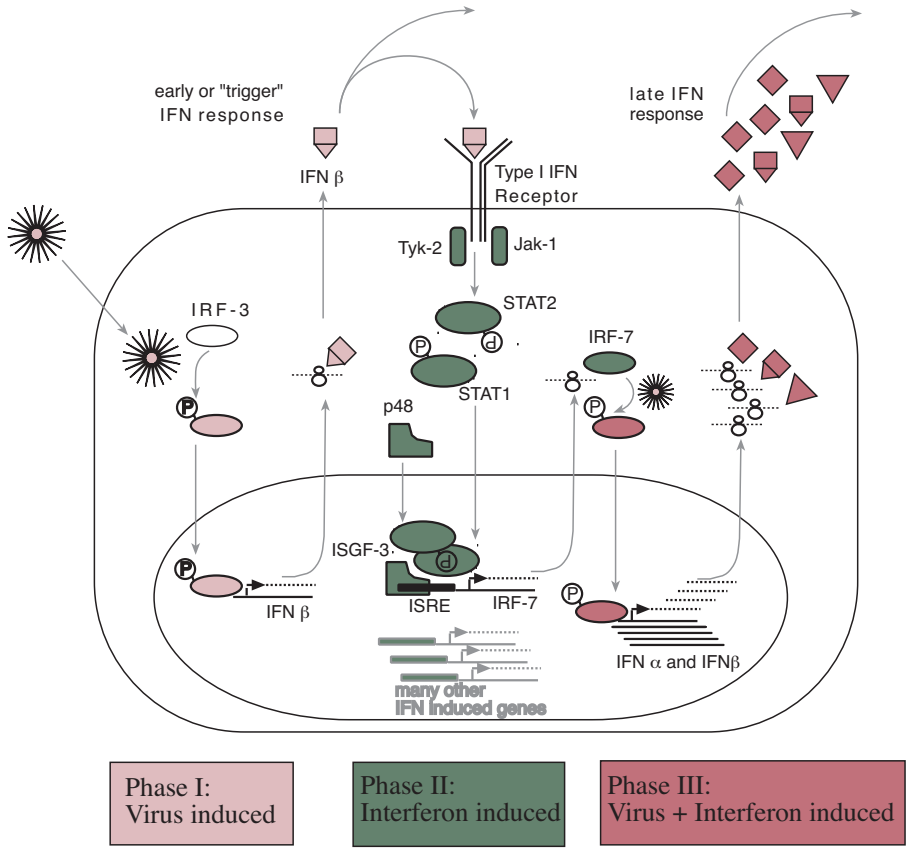

Fig. 1.4 Model for the positive feedback regulation of type I IFN production. In phase I virus-mediated activation of interferon regulatory factor-3 (IRF-3) leads to the low-level induction of IFN-β. Autocrine signaling via the type I IFN receptor in phase II activates a large number of IFN stimulated genes. One of these genes codes for IRF-7, a transcription factor critically required for the induction of IFN-α genes. IRF-7 activation in phase III is again mediated by the viral stimulus. Activated IRF-7 upregulates many IFN-α subtypes and thereby allows for a pronounced production of "late" type I interferons.

Virus infection leads to IRF-7 activation by phosphorylation that drives the expression of the majority of IFN-α subtypes, and hence amplifies the type I IFN response (Fig. 1.4). It appears, that several pathways may lead to IRF-3 and IRF-7 activation. Some viruses, such as type I herpes simplex virus (HSV), induce an IFN response independent of viral replication whereas others, e.g. vesicular stomatitis virus (VSV), lose the ability to induce type I IFN upon inactivation. Furthermore, a variety of non-viral IFN inducers have been described, including procaryotic DNA motifs (CpG-DNA), synthetic double-stranded RNA (poly(I:C)), lipopolysaccharide (LPS), and imiquimod derivatives (Bauer et al., 2001; Megyeri et al., 1995).

1.7 The major IFN-α producing cell (IPC)

In cell culture virtually any cell type can produce type I IFN in response to appropriate stimulation. Yet, depending on the expression of pattern recognition receptors distinct cell types are stimulated by different IFN inducers. For example CpG but not poly(I:C) treated human $CD11c^-$ dendritic cells (DCs) produce type I IFN, whereas a reverse correlation was found for $CD11c^+$ DCs (Bauer et al., 2001; Kadowaki et al., 2001). Accordingly, $CD11c^-$ DCs express the Toll-like receptor (TLR)-9 and $CD11c^+$ DCs express TLR-3 (Bauer et al., 2001; Kadowaki et al., 2001), which have been shown to be involved in the recognition of CpG or poly(I:C), respectively (Alexopoulou et al., 2001; Hemmi et al., 2000). Differential expression of TLRs on DCs is presumably involved in the fine-tuning of host immune responses. So far, the major IFN producing cell (IPC) has not been defined in the context of infection with specific pathogens. Several studies addressed the nature of the human IPC (Ferbas et al., 1994; Sandberg et al., 1991; Svensson et al., 1996), which eventually was defined as the subset of $CD11c^-$ plasmacytoid DCs (Cella et al., 1999; Siegal et al., 1999). There are indications, that upon stimulation of mice certain macrophages (Eloranta and Alm, 1999) or DC subsets can produce type I IFN (Asselin-Paturel et al., 2001; Hochrein et al., 2001; Nakano et al., 2001).

1.7.1 Plasticty of the myeloid lineage - IPCs and other dendritic cell subsets

The cells of the immune system originate from precursor cells residing in the bone marrow, where many of them also mature. There is however, a significant degree of plasticity in cell types that are found in the periphery, both in the blood and solid organs. This feature was demonstrated most impressively by the analysis of PAX5 deficient cells, which are arrested at the pro-B cell stage. These can de-differentiate and give rise not only to DCs, NK cells and T cells but also to myeloid and erythroid cells (Rolink et al., 1999; Schaniel et al., 2002). Dendritic cells have a remarkable heterogeneity related to both tissue localization and functional maturation state. Differential expression of DC lineage markers led to the notion that the mouse and human possess surprisingly divergent DC compartments. Fortunately, recent progress allowed for most subtypes the definition of similar populations in both species (for review see Ardavin et al., 2001). Yet, despite extensive research on the development of dendritic cells, their origin and the differentiation pathways that generate DCs *in vivo* remain largely unknown. Monocytes in human blood are attracted to sites of inflammation where they extravasate and differentiate into dendritic cells under the aegis of local cytokines such as type I IFNs (Randolph et al., 1999; Santini et al., 2000). Other examples of stimulation dependent DC plasticity and the discovery of common progenitors of myeloid and lymphoid DC subsets (Martin et al., 2000; Traver et al., 2000) have led to a model of instruction on top of lineage heritage for the generation of DC diversity (Lanzavecchia and Sallusto, 2001; Liu et al., 2001). Similarly, it is not clear whether the professional interferon producing cells alias plasmacytoid- T-cells, monocytes or DCs, define a discrete lineage of cells destined to differentiate into dendritic cells or whether they constitute a multipotent precursor to a set of different immunocytes (Galibert et al., 2001).

1.8 Aim of the Thesis

The model of type I IFN receptor (IFNAR) feedback for the regulation of IFN-α production has been established recently from studies of mouse embryonic fibroblasts (MEFs) infected in cell culture. Yet, in an acutely infected host, fibroblasts presumably do not produce bulk quantities of type I IFN.

Here we study the requirement of type I IFN receptor signaling and IRF-7 upregulation for the production of IFN-α during viral infection *in vivo*. We hypothesize that *in vivo* the majority of type I IFN is contributed by a distinct cell type, referred to as professional interferon producing cell (IPC). The phenotype of IPCs in the mouse and the mechanism by which high-level IFN-α production is regulated in these cells have not been characterized previously. In order to identify professional interferon producing cells (IPCs) in the mouse a two-tier strategy is pursued. One approach aims at genetically marking IPCs in transgenic mice by the expression of reporter genes under the control of the IFN-α2 or IRF-7 promoter. The second strategy tries to identify the mouse IPC population by cell sorting using surface markers for dendritic cell subsets. Both approaches can be applied to study the origin and fate of mouse IPCs. Especially, it will be important to investigate whether mouse IPCs may function as antigen presenting cells and thus link innate and adaptive immune responses against viruses and other pathogens.

2 Materials and Methods

2.1 Mice

2.1.1 General maintenance and breeding

Type I interferon receptor deficient mice (IFNAR-/-) on the SV129 background (Muller et al., 1994) and IFN-β-/- mice on the Balb/c background (Erlandsson et al., 1998) were bred under specific pathogen free conditions (SPF). Unmutated SV129 mice (referred to as WT) were obtained from the SPF-breeding colony of the European Mutant Mouse Archive (EMMA), Monterotondo, Italy. C57BL/6 mice were purchased at IFFA-Credo (Saint Germain-sur-l'Abresle, France). Experimental mouse work was done under SPF conditions in compliance with regulations of the Ministerio della Sanità, Rome, Italy (decreto ministeriale n˚ 15/2001-b, 3/3.1).

2.1.2 Spleenectomy

Mice were anesthetized via i.p. injection of Avertin (2.5%, ~0.3 ml). Fur was shaved around the site of the intervention. The skin was washed with Betadine and a horizontal incision of ~1 cm was made using scissors. The connective tissue under the skin was loosened with blunt end forceps and a < 1 cm horizontal cut was made in the peritoneal wall. The spleen was gently pulled onto the exterior surface of the peritoneum. Using a heated forceps, the artery attached to the hilium of the spleen closest to the stomach and then the efferent venule on the other side of the spleen were cauterized. Then connective tissue was cut away and the spleen removed. The peritoneal wall was closed with 2 separate sutures and the skin was closed with an additional 2 - 3 sutures. The animal was placed in a fresh pre-warmed cage was observed during the wake up time. The quality of the sutures is of prime importance as animals scratch and gnaw at the wound and a reopening of the cut is fatal. Animals were checked twice daily and were used for the experiments 3 - 5 days after the surgery.

2.1.3 Preparation of single cells suspension from various tissues

Blood was collected by retro orbital bleeding using a Pasteur pipette partially filled with heparinized PBS (8 mM Na_2HPO_4-$2H_2O$, 3 mM NaH_2PO_4-H_2O, 150 mM NaCl) 3% FCS. Peritoneal cavity cells were obtained by flushing 10 ml ice cold PBS 3% FCS through the peritoneal wall using a syringe with an 18 gauge needle. Bone marrow was flushed from femurs and tibiae, after the edges of the bones had been clipped off, using PBS 3% FCS and a syringe with a 26 gauge needle. Livers were rinsed from blood by injection of 10 ml PBS into the vena cava before explanting. Spleens, peripheral lymph nodes (Inguinal, axillary and brachial), mesenteric lymph nodes, peyers patches, thymi and kidneys and lungs were collected into 15 ml Falcon tubes containing 3 - 5 ml PBS 3% FCS and then passed through a nylon mesh using a steel plunger. Cells were resuspended in 10 ml PBS

3% FCS. Debris was allowed to settle and the supernatant decanted into a fresh 15 ml Falcon tube. Suspensions from livers and kidneys contained large quantities of cellular debris requiring prolonged and repeated settling of debris and decanting followed by extensive washing of the cells. On pelleted blood and kidney samples red blood cell lysis was performed on ice for 10 min using ACK lysing buffer (150 mM NH_4Cl, 10.0 mM $KHCO_3$, 0.1 mM Na_2EDTA pH 7.4). In all other cases, cells were washed once with PBS 3% FCS and counted using a Neubauer counting chamber (Bender/Hobein, #631A1110).

2.2 Cell culture

2.2.1 Cell Culture of cell lines

All tissue culture reagents used were purchased from Gibco-BRL (www.lifetech.com) unless otherwise stated. Catalog numbers are: DMEM #41965-039, D-MEM #10938-025, MEM #31095-029. Fetal calf serum (FCS) was used heat inactivated for 60 min at 56 °C. Further additives for culture media were 0.1 mM 2β-mercaptoethanol (Fluka, #63690), 2 mM L-glutamine (Gibco, #25030-024). Standard cell culture was performed in antibiotic free media. For short-term assays under non-sterile conditions 1% penicillin-streptomycin (Gibco, #15140-130) was added to the media. Cells were usually cultured in T175 flasks (Falcon BD, #353028).

- *BHK cells* (BHK-21), baby hamster kidney fibroblast cells were obtained from the ATCC (#CCL-10) and were cultured in DMEM 5% FCS.
- *L929 cells* (H-2^b), mouse fibroblasts were obtained from the ATCC (#CCL-1) and were propagated in DMEM 10% FCS.
- *MC 57 G cells* (H-2^b), methylcholanthren transformed mouse fibrosarkoma cells were originally provided by Dr. B. B. Knowles (Philadelphia, USA). These cells were cultured in MEM 5% FCS
- *Vero cells*, African green monkey kidney epithelial cells were obtained from the ATCC (#CCL-81) and were propagated in DMEM 5% FCS.

Confluent cells were split by washing the adherent cell monolayer for 10 min with PBS (Gibco, #14190-169). Cells were then detached by incubation with Trypsin/EDTA (Gibco, #25300-054) for 5 min at 37 °C. Single cell suspension was prepared by adding medium containing 10% FCS and repeated pipe ting followed by the removal of excess cells.

2.2.2 Freezing and thawing of cells

Cells from a confluent flask were trypsinized, washed once and taken up in freezing medium (DMEM 10% FCS, 10% DMSO). Aliquots were placed in a freezing container filled with isopropanol and remained for 3 days at –80 °C before storage in the liquid nitrogen tank. Aliquots were thawed by brief incubation in a water bath at 37 °C, were washed once in DMEM 10% FCS and then seeded at various dilutions into 6 well plates.

2.2.3 Generation of mouse embryonic fibroblasts (MEFs)

Wild type and IFNAR-/- MEFs were derived from day 13 embryos (Torres and Kühn, 1997). Embryos were collected in PBS, heads and livers were removed. The remainder was placed in 4 ml 0.125% trypsin/EDTA and minced into small pieces and incubated for 30 min at 37 °C. The reaction was stopped by adding Dulbecco's MEM supplemented with 10% FCS and single cell suspension was prepared by vigorous pipeting. After removal of cell debris, by settling and decanting, cells were seeded in T175 flasks with 25 ml MEM 10% FCS. Cells were grown to confluence and every 2 - 3 days one flask was split into 5 T175 flasks. After 2 - 4 passages MEF cells were frozen for later use (see 2.2.2)
For the IFN production experiments MEFs were seeded in 6 cm petri dishes and after adhering o.n. the cell monolayers were infected with VSV at a multiplicity of infection (moi) of 10. After 1 h of incubation at 37 °C the virus suspension was replaced by Dulbecco's MEM 10% FCS.

2.3 Viruses

2.3.1 Production and Purification of VSV

Vesicular stomatitis virus Indiana (VSV) (Mudd-Summers isolate) was originally obtained from D. Kolakofsky (University of Geneva, Geneva, Switzerland) and was grown on BHK (ATCC CCL-49) cells and plaqued on Vero cells (see 2.3.3). Confluent T175 flasks were infected with a low multiplicity of infection (moi 0.1, by adding 3 ml of diluted virus/T175 flask), incubated for 1h at RT with occasional shaking. Then 27 ml MEM 2% FCS were added and incubated at 37˚C, 5% CO_2 for 48 h. Supernatants were pooled and cell debris was removed by centrifugation. Stocks were maintained at –80 °C in MEM containing 2% FCS.

2.3.2 Production and Purification of HSV

HSV strain F originally obtained by ATCC was grown on Vero cells. HSV was purified from cell culture supernatant by PEG 40.000 (Serva #33139.01) precipitation. Following several pelleting steps for 1 h at 43.000 g virus was resuspended in PBS and titrated on Vero cells. After UV irradiation (1.2 Joule/cm^2) complete HSV inactivation was verified by plaquing on Vero cells.

2.3.3 Plaque Assay for VSV and HSV

One day before the assay Vero cells (diluted to $2 \cdot 10^5$/ml in MEM 5% FCS, 3 ml per well) were seeded in 6 well cell culture plates. Serial ten-fold dilutions of the virus-containing sample were prepared in MEM 5% FCS. It is important to mix well in each dilution and to change tips after every transfer. The medium on the Vero cell monolayer was replaced with 1 ml of virus dilution. The plates were then incubated for 1 h at 37 °C. Each well was carefully overlaid with 1 ml 1% Methylcellulose/1% DMEM. After overnight incubation at 37 °C, medium was flicked off into 10% bleach and the cell-monolayer was stained for 1h

with crystal violet solution. Color was flicked off and plates were washed extensively with tap water and air-dried. Plaques were counted and the pfu determined using the following formula: pfu virus = ∑plaques of three consecutive wells x (dilution factor of the well with the lowest dilution counted / 1.11).

2.4 Assay methods

2.4.1 Expression analysis by RT-PCR.

Preparation of total RNA was performed using the TRIZOL reagent (Gibco #15596) according to the manufacturer's instructions. Tissue samples were snap-frozen and homogenized in Trizol using a Polytron PT 1200 C (Kinematica, Switzerland). On cultured cell monolayers and FACS-sorted cells Trizol was applied directly. From samples containing small cell numbers, directly sorted into Trizol, total RNA was prepared after adding 200 µg Glycogen (Boehringer Mannheim, #901393) as carrier followed by shearing of genomic DNA by two passes through a 26 gauge needle. Reusable Plastic materials were rinsed with RNAase ZAP (Ambion #9780) to reduce the risk of introducing RNase. To eliminate possible DNA contamination total RNA was incubated for 15 minutes at 37 °C with 10 units of DNase (Boehringer Mannheim, #776785). cDNA was prepared using Superscript II (Gibco #18064-014) and oligo dT primer (Gibco, #18418-012) according to the manufacturer's instructions. To estimate relative amounts of specific mRNAs, PCRs were performed with serially five-fold diluted cDNA using published primers for IFN-α (consensus primers annealing with all IFN-α subtypes) and IRF-7 (Marie et al., 1998). The mRNA content was normalized by RT-PCR analysis with GAPDH-specific primers from the same publication. The absence of contaminating DNA was verified by PCR analysis of RNA preparations not treated with reverse transcriptase. Taq Polymerase (#M1668) and dNTPs (#U1201/1221/1211/1231) were ordered from Promega. PCR reactions were performed in MicroAmp tubes (Perkin Elmer, #N801-0535/-0580). The PCR-Machine used was a MJ Research PTC-200, DNA engine, Biozym Diagnostik GmbH, Hess. Oldendorf.

Gene	Primer Name	Primer Sequence	PCR conditions
IFN-α subtypes	#18 IFNa-up	ATG GCT AGR CTC TGT GCT TTC CT	Product length: 524 bp 94 °C-5', 94 °C-30'', 53 °C-30'', 72 °C-1'06'', 30 cycles, 72 °C-10'
	#19 IFNa-do	AGG GCT CTC CAG AYT TCT GCT CTG	
IFN-β	#98 IFNb-up	CAT GAA CAA CAG GTG GAT CCT CCA CGC	Product: 560 bp 94 °C-5', 94 °C-30'', 60 °C-30'', 72 °C-60'', 30 cycles, 72 °C-10'
	#99 IFNb-do	TCA GTT TTG GAA GTT TCT GGT AAG TCT TCG	
GAPDH	#34GAPDH-up	ACC ACA GTC CAT GCC ATC AC	Product length: 452 bp 94 °C-5', 94 °C-30'', 60.5 °C-30'', 72 °C-55'', 25 cycles, 72 °C-10'
	#35GAPDH-do	TCC ACC ACC CTG TTG CTG TA	
IRF-3	#50 IRF3-up	CCA GGT CTT CCA GCA GAC ACT	Product length: 557 bp 94 °C-5', 94 °C-15'', 60.0 °C-15'', 72 °C-1', 30 cycles, 72 °C-10'
	#51 IRF3-do	TAG GCT GGC TGT TGG AGA TGT	
IRF-7	#52 IRF7-up	CAG CGA GTG CTG TTT GGA GAC	Product length: 360 bp 94 °C-5', 94 °C-30'', 61 °C-30'', 72 °C-43'', 30 cycles, 72 °C-10'
	#53 IRF7-do	AAG TTC GTA CAC CTT ATG CGG	
IRF-5	#180 5'IRF-5a	ATT CAG CGG GAA GTC AAG ACG AAG	Product length: bp 94 °C-5', 94 °C-15'', 60.0 °C-15'', 72 °C-1', 30 cycles, 72 °C-10'
	#181 3'IRF-5a	GGG CCA CCA CAT TGC TAT ATC AGT C	
VSV-GP	#136 5VSVGP	CCA TGA AGT GCC TTT TGT ACT	Product length: 495 bp 94 °C-5', 94 °C-15'', 60.0 °C-15'', 72 °C-1', 30 cycles, 72 °C-10'
	#137 3VSVGP	ATT GCT GCA TTT TCC GTT GAT	

Table 2.1 PCR primers used for semiquantitative RT-PCR

2.4.2 Sequencing of subcloned PCR-product and sequence analysis

The 524 bp PCR product of the IFN-α consensus primer PCR on cDNA was purified via agarose gel electrophoresis and gel-extraction (Qiaex II, Qiagen #20051). Purified fragment was A:T-ligated into the pGEMT vector (Promega #A3600). 5 ml of the ligation was transfected by heat-shock into $CaCl_2$ competent bacteria (see 2.5.2) and plated on LB-Ampicillin plates. Single colonies were picked after o.n. incubation at 37 °C and mini-preparations by alkaline lysis. Clones with the integration of the correct fragment were determined by Pvu II digest. Selected clones sequencing reaction was prepared using ABI-Systems Big-Dye or Dye terminator chemistry. All kits were used according to the manufacturer's instructions. Sequencing reactions were purified by ethanol precipitation and were resuspended in formamide (Merck, #1.09684). Sequences were obtained on an ABI-Systems 310 capillary sequencer or a 373 gel sequencer, respectively and analyzed using the Sequencher (Gene Codes Corporation) software. Contigs of homologous fragments were compared to published IFN-α sequences (EMBL accession numbers: M68944, M13660, K01238, X01973, X01971, X01972, M13710, D00460, M28587, L38698). Sequence identity to the published IFN-α subtype was assumed when the sequence analyzed contained less than 10 mismatches / 300 bp.

2.4.3 Quantification of type I IFN in blood sera (CPE-assay)

The IFN bioassay was based on the protection of L929 cells from the cytopathic effect of VSV (CPE inhibition assay). Mouse blood sera were obtained by retro-orbital bleeding followed by centrifugation at 4300 rpm in Microtainer serum separator tubes (Becton Dickinson, #365960). To inactivate potential viral contamination, 1:5 pre-diluted serum samples from VSV infected mice were UV-irradiated with 1.2 Joule/cm^2. Duplicates of serially two-fold diluted sera were transferred to 24 h pre-incubated semiconfluent monolayers of L929 cells in 96-well plates. After 24 h incubation at 37 °C supernatants were removed and VSV was added at a MOI of 0.05. After 48 h incubation at 37 °C, supernatants were taken away and protected cells were stained with 0.5% crystal violet in 5% formaldehyde, 50% ethanol, and 0.8% sodium chloride. Following extensive washing with water and air drying, the dye was extracted from stained cells with 100 ml/well 0.1 M sodium citrate in 50% ethanol, pH 4.2 and the crystal violet content was determined on an ELISA reader at 570 nm. In the CPE inhibition assay an international mouse IFN-α/β reference standard of 100 IU/ml (Gu02-901-511, NIAID Repository) and recombinant IFN-αA standards (PBL Biomedical Laboratories, #12100) of 100, 500, 2500, and 10000 IU/ml were included. For IFN quantification the 50% protective serum dilution was indicative. A $\log_2 5$ titer corresponded to 1000 IU IFN-αA. The contribution of IFN-β or IFN-α to the total type I IFN activity was determined by pre-incubating sera for 1 h with excess amounts of neutralizing anti-IFN-α (clone 4E-A1, Yamasa Shoyu) or anti-IFN-β (clone 7F-D3, Yamasa Shoyu) monoclonal antibodies. Protection from cytopathic effect due to IFN-γ was formally excluded by an IFN-γ Elisa (Endogen #KM-IFNG) indicating that the IFN-γ content of all samples tested was below the detection threshold of the assay (see 2.4.4).

2.4.4 Quantification of IFN-γ in blood sera (ELISA)

For the determination of IFN-γ content in mouse blood sera the Endogen minikit IFN-γ Elisa (KM-IFNG) was used according to the manufacturer's instructions with the modifications described here. The required number of wells of a plate were coated o.n. with anti-IFN-γ antibody and then blocked and washed. IFN-γ standard was diluted and used in serial twofold dilution starting at 4000 pg/ml. Serum samples were tested in 1:5 and 1:50 dilution. 50 µl of the dilutions were added to the wells and incubated for 1h at 37 °C. After washing wells were incubated for 1h at RT with biotinylated anti-IFN-γ detection antibody and then washed again. Incubation with Streptavidin-HRP (Endogen Cat. #N-200) was carried out at 1:10.000 dilution for 30 min followed by washing. TMB substrate at RT was then added and incubated in the dark for 30 min and then the reaction was terminated by adding Stop-Solution. The plate was measured immediately at 450 nm.

2.4.5 Flow cytometric analysis

Freshly prepared single cell suspensions were pre-incubated with Fc-Block reagent (BD Pharmingen #553142) and stained as indicated with the following mABs in PBS 3% FCS: FITC conjugated CD5, CD11b, CD19, DX-5, CD40, CD54, CD69, CD80, CD86, Rat

IgG2a isotype control (BD Pharmingen) or CD62L, CD90, B220, CD8, MHCII, Ly6C (Southern Biotechnology Associates); PE conjugated CD4, IL-3R, Sca-1, Gr-1, Rat IgG2a isotype control (BD Pharmingen), Ly6C (Southern Biotechnology Associates) or F4/80 (Serotec); Cychrome conjugated B220 (BD Pharmingen); Biotin conjugated CD11b, CD11c (BD Pharmingen) mABs were followed by streptavidin-Cychrome (BD Pharmingen). Stainings were performed either in 6 ml FACS tubes (Falcon, BD) or in 96 well round bottom plates followed by transfer into PPN-96 tubes (Micronic, #M226C2). Red blood cells and cell debris were excluded by a morphological gate (FSC/SSC), or by appropriate setting of the FSC threshold, respectively and 300.000 – 1.2 Mio events were acquired on a Becton Dickinson FACScalibur and analyzed using CellQuest (Becton Dickinson) software.

2.4.6 Intracellular cytokine staining for IFN-α

Single cell suspensions were prepared from the spleens of C57BL/6 mice, untreated or VSV infected for 6 h. To accumulate intracellular IFN the cells were incubated for 2h at 37 °C 4% CO_2 in DMEM 10% FCS containing 10 µg/µl Brefeldin A (Sigma, #B7651). Cells were fixed in 2% paraformaldehyde (Sigma, #P6148) for 15 min on ice. A permeabilization buffer consisting of PBS 0.5% Saponin (Sigma, #S7900) 1% FCS was used for all following washes and incubation steps. Cells were washed twice and then permeabilized for 20 min at RT. Monoclonal rat anti-mouse IFN-α antibody (Serotec, #MCA1431) was used at 10 µg/ml for 30 min at RT. After extensive washing PE-labeled monoclonal goat anti-rat antibody (Southern Biotechnology Associates) was used at 1:50 dilution and incubated for 30 min at RT. Cells were washed in PBS 3% FCS (without saponin) and measured on a FACScalibur cytometer (Becton Dickinson). Controls were performed omitting the primary antibody or using an isotype control. Moreover, control stainings were performed on cells from uninduced mice.

2.4.7 Kinetics of IPC turnover in spleen and bone marrow

Mice were injected i.p. with 1 mg bromodeoxyuridine (BrdU, Sigma #B5002) dissolved in PBS and were fed thereafter with drinking water containing 1 mg/ml BrdU. MACS enriched $CD11c^+$ cells from spleen or BM were stained intracellularly with FITC conjugated anti-BrdU mAb and contemporaneously on the cell surface with fluorescent mABs using the BrdU Flow Kit (BD Pharmingen #559619) according to the manufacturer's instructions.

2.4.8 Labeling of cells for adoptive transfer cells using CFSE

Single cell suspensions were incubated with a 1/1000 dilution of carboxyfluoroscein succinimidyl ester (CFSE 0.5 mM (Molecular Probes #C-1157) in DMSO (Fluka #41641) at 37 °C for 10 min. In order to obtain less intense staining 1/10.000 dilutions were used. Cells were washed once using ice cold DMEM 10% FCS and injected intravenously in a volume of 500 µl (Lyons and Parish, 1994).

2.4.9 Flow cytometric cell sorting of DC subsets (FACS)

Single cell suspension of 3 - 5 spleens was prepared and $CD11c^+$ cells were enriched by magnetic adsorption cell sorting (MACS, Miltenyi Biotech). Three-color stainings were made using anti-CD11c-Biotin, anti-CD11b-FITC and anti-GR-1-PE conjugated monoclonal antibodies followed by Streptavidin-APC (all from Pharmingen, San Diego, California). 4 - 10 · 10^4 cells of each subset were sorted from about 10^7 cells on a MoFlo cytometer (Cytomation, Fort Collins, Colorado).

2.4.10 Magnetic adsorption cell sorting (MACS)

Cells were enriched from spleen and BM suspensions by magnetic adsorption cell sorting (Midi MACS, LS+ separation columns, Miltenyi Biotech #424-01) according to the manufacturer's instructions. The following MACS MicroBeads were used: MHC Class II (Ia) #524-01, CD45R (B220) #522-01, CD11b (Mac-1) #496-01, and CD11c (N418) #520-01. To remove cell clumps Pre-Separation Filters (Filcons 30 µm, #414-07) were used. PBS 10% FCS 1 mM EDTA was used as MACS-buffer at all stages.

2.4.11 May-Grünwald Giemsa staining of single cells

May-Grünwald-Giemsa staining consists of a mixture of methylene blue (which dyes acidic cell components blue), azure (which dyes basic cell components red and violet) and eosin (which dyes alkaline cell components orange-red). In May Grünwald Giemsa stains residual RNA, cytoplasm and nucleoli are blue, DNA and primary granula red and violet as well as hemoglobin and eosinophilic granula are orange-red.
Single cell suspension of FACSorted cells was briefly incubated at 37 °C to ensure natural morphology of the cells. About 10.000 cells were diluted in 300 µl RPMI-Hepes medium and were spun onto a microscope slide (Assistant #2406/1) for 10 min at 500 rpm in a Cytospin centrifuge (Shandon) according to the manufacturer's instructions. Slides were air dried for 10 min at RT. Slides were fixed for 2.30 min at RT in 100% methanol, dried for 10 min at RT and then incubated for 3 min in concentrated May-Grünwald solution (Fluka, #63590). The slides were then incubated for 3 min in 50% May-Grünwald solution diluted in tap water, followed by 10 min incubation in 7% Giemsa solution (Fluka, #48900). The slides were rinsed with tap water, dried and enclosed with Eukitt before analysis by brightfield light microscopy.

2.4.12 Immunohistochemistry

Freshly removed organs were immersed in Hank's balanced salt solution (HBSS 10x, Gibco #14065-031) and snap frozen in a large volume of liquid nitrogen. Tissue sections of 5 mm thickness were cut in a cryostat, placed on siliconized glass slides, air dried, fixed with acetone for 10 min, and stored at –80 °C. Interferon was stained using a polyclonal sheep anti-mouse IFN-α/β antiserum (PBL Biomedical Labs, New Brunswick, NJ, #RDI-PB32105) or monoclonal rat anti-mouse IFN-α antibody (Serotec #MCA1431). The primary sheep antibody was detected with affinity purified biotinylated donkey anti-sheep

Ig antibodies (Jackson ImmunoResearch Labs, West Grove, PA #713-066-147) and alkaline phosphatase labeled avidin/biotin complexes (ABC/AP Dako, Glostrup, Denmark #K0391). The primary monoclonal rat antibody was detected with affinity-purified peroxidase labeled goat anti-rat Ig antibody (Jackson #112-035-102). For signal amplification by catalyzed reporter deposition, biotinylated thyramine (Bobrow et al., 1989) and 3% H_2O_2 was added for 7 min, and covalently bound biotin was revealed by ABC/AP. For the staining of cell differentiation markers, sections were incubated with rat monoclonal antibodies against red pulp macrophages (F4/80, Biomedicals, Augst, Switzerland) marginal zone macrophages (ERTR-9; van Vliet et al., 1985) and against marginal zone metallophils (MOMA-1, Biomedicals, Augst, Switzerland). Primary rat antibodies were revealed by sequential incubation with goat antibodies to rat immunoglobulins (Caltag Labs, San Francisco, CA) and alkaline phosphatase labeled donkey antibodies to goat immunoglobulins (Jackson). Alkaline phosphatase was visualized using naphthol AS-BI (6-bromo-2-hydroxy-3-naphtholic acid-2-methoxy anilide) phosphate and new fuchsin as substrate. Endogenous alkaline phosphatase was blocked by levamisole. The dilutions of secondary antibodies were made in TBS (50 mM Tris-HCl (pH 7.4), 150 mM NaCl) containing 5% normal mouse serum. Incubations were done at RT. for 30 min; TBS was used for all washing steps. Color reactions were performed at RT for 15 min with reagents from Sigma Chemical Co. (St. Louis, MO). Sections were counterstained with hemalum and coverslips mounted with glycerol and gelatin.

2.4.13 In situ hybridization of IRF-7 mRNA

In situ hybridisation was performed according to Neubüser et al. (Neubuser et al., 1995). Spleens were fixed overnight in freshly prepared 4% paraformaldehyde (PFA) in phosphate-buffered saline (PBS) and then embedded in paraffin wax. Sections were cut at 5-7 µm and mounted onto Superfrost-Plus slides. The IRF-7 riboprobe was generated by cloning a 351 bp RT-PCR product into pBluescript followed by Digoxygenin-11-UTP-labeling using the Boehringer RNA labeling kit. Paraffin sections were dewaxed and rehydrated, fixed in 4% PFA in PBS for 20 min, digested with 10 µg/ml proteinase K in 20 mM Tris/HCl, pH 7.0, 1 mM EDTA for 10 min, and refixed in 4% PFA in PBS for 20 min. Hybridization solution contained the digoxygenin-11-UTP-labeled riboprobe (1 ng/µl) in 40% formamide, 5X SSC, 1X Denhardt's solution, 100 µg/ml each of denatured salmon testis DNA and tRNA. Hybridization occurred over night at 65° C under a siliconized coverslip. Coverslips were floated off in 5X SSC, followed by a 40 min wash in 0.5X SSC, 20% formamide at 60°C and a 15-min wash in NTE (0.5 M NaCl, 10 mM Tris/HCl, pH 7.0, 5 mM EDTA). The sections were treated with 20 µg/ml RNase A in NTE for 30 min at 37° C and washed in NTE for 15 min, in 0.5X SSC, 20% formamide for 20 min at 60 °C, and then in 2X SSC for 25 min. Antibody incubation and detection were performed according to the manufacturer's description (Boehringer Mannheim) Sections were mounted in Eukitt and photographed under a Zeiss DMRXA microscope.

2.5 Molecular biology methods and standard cloning

All cloning strategies were designed and first carried out *in silico* using the Gene Construction Kit 2 software (www.textco.com/products/gck2.html). This was especially important for the correct design of long oligo-nucleotide PCR primers used for ET-cloning. Standard cloning steps of plasmid vectors and the basic molecular biology techniques were performed according to the protocols from Molecular Cloning (Sambrook et al., 1989). The bacteria strain XL-1 blue was used for the amplification of plasmid DNA. Isolation of plasmid DNA was performed using an alkaline lysis method (Birnboim and Doly, 1979). For cleaner preparations of plasmid Qiagen columns (Qiagen, Hilden) were used. All enzymes used for restriction digests and cloning purposes were from New England Biolabs (NEB, Beverly, USA) unless otherwise stated. DNA was recovered from agarose gel slices with QIAEXII gel extraction kit (Qiagen, Hilden) according to the manufacturer's instructions. The restriction enzymes used were from New England Biolabs (NEB). Agarose Electrophoresis was performed in TAE buffer (0.04 M Trisbase 0.04 M Acetate, 0.002 M EDTA) using SeaKem LE Agarose (Biozym, #50004) containing 4 µl / 100 ml Ethidium bromide (Sigma #E-8751). 1 kb ladder (Gibco #15615-16) was used as DNA size marker.

2.5.1 Preparation of $CaCl_2$ competent cells for transfection by heat-shock

A 5 ml starter culture of bacteria (strains HB101, DH5α or XL-1 blue) was grown o.n. at 37 °C. 0.5 ml of the o.n. culture were used to inoculate 20 ml LB medium and grown at 37 °C on a shaker for approximately 4 h until an OD_{600} of 0.4 was reached. Cells were spun for 10 min at 4000 rpm and washed once with 10 ml cold 10 mM NaCl and then incubated for 20 min in 10 ml cold 50 mM $CaCl_2$. After centrifugation the cell pellet was resuspended in 1 ml $CaCl_2$ 15% Glycerol. Aliquots of 200 µl were snap frozen in liquid N_2 and stored until use at - 80 °C.

2.5.2 Transfection by heat-shock

Competent bacteria were thawed on ice and mixed with the plasmid DNA. After incubation for 30 min on ice cells were heat shocked for 1 min at 42 °C. After another 5 min on ice cells were either incubated shaking for 1 h at 37 °C in 1 ml LB medium or plated directly.

2.5.3 Transformation using Flp expressing E. coli

The 294-Flp bacteria used to excise frt-flanked regions in plasmids or BACs were obtained from Francis Stewart and were originally generated by integrating the 707-Flp plasmid into *E. coli* (Buchholz et al., 1998). Competent bacteria were transfected by heat shock or by electroporation (see chapter 2.6.2) and incubated in LB medium for 1 h at 37 °C. Cells were then plated on selection plates. Single colonies were picked and used to inoculate 5 ml LB medium with appropriate antibiotics. Incubation was performed at 30 °C overnight to reduce Flp expression and increase plasmid yield. Mini preparations were checked for the loss of frt-flanked regions by restriction digest and loss of Kanamycin resistance.

2.5.4 Southern Blot analysis

For the Southern blot assay 1 µg of BAC DNA were digested with the respective restriction enzyme and separated o.n. on a 0.7% agarose gel. After capillary blotting on a nylon membrane (Hybond N+, Amersham #RPN2020B), membranes were pre-incubated in hybridization-buffer (1% BSA, 1 mM EDTA 0.5M Na-phosphate buffer pH 7.2, 7% SDS) at 65°C for 30 minutes. DNA probes were labeled by random priming (Gibco Life Technologies, #18187-013) with ^{32}P α-dGTP (Amersham) Unincorporated nucleotides were removed by centrifugation on a Sepharose Microspin G-50 column (Pharmacia, #27-5330-01). Probes were added to hybridization-buffer and allowed to hybridize with the membrane overnight. Filters were washed four times for 30 min in wash buffer (1 mM EDTA, 40 mM Na-phosphate, pH 7.2, 1% SDS) at 65 °C and then exposed on a radiosensitive phosphoimager screen (Molecular Dynamics) or to autoradiographic film overnight at -80°C.

2.5.5 Colony hybridization

For colony hybridisation a circular nitrocellulose filter was placed on the plate with transformed cells until the filter was completely wetted. The position of the filter was marked using needle punches. The filter was removed and then placed sequentially in 10% SDS for 10 sec, then in 0.5 M KOH, 1 M NaCl for 2 min and in 0.5 M Tris-HCl pH 7.5, 1M NaCl for 5 min. The filter was washed in 4x SSC buffer, the remainders of colonies were rubbed off and the filter rinsed in fresh 4x SSC. Filters were baked for 1 h at 80 °C. Hybridisation was performed as described in 2.5.3. Colonies were regrown by incubating the bacterial plates at 37 °C

2.5.6 Colony PCR

Colony PCR was performed by picking a bacterial colony and suspending it in 200 µl ddH_2O. After an incubation of 10 min, 10 µl of the suspension were used as template in a standard 50 µl PCR reaction using appropriate screening primers. Colonies were regrown by incubating the bacterial plates at 37 °C.

2.6 ET-cloning and BAC handling techniques

A detailed protocol for the preparation of competent cells and for performing ET cloning experiments can be found at the following web address:
http://www.embl-heidelberg.de/ExternalInfo/stewart/ETprotocols.html.
Here the most relevant steps are summarized. As developed so far, the host for ET-cloning can be either (i) a strain which endogenously expresses RecE/RecT (see 2.6.1) or (ii) a strain in which RecE/RecT or Redα/Redβ are expressed from an exogenously introduced plasmid (see2.6.5).

2.6.1 Generation of PCR fragments for ET-cloning

PCR reactions were performed using the primer pairs listed below. When the amplified DNA fragment was destined to be part of the construct, PCR was carried out using the proofreading cloned Pfu-polymerase (Stratagene, #S600159) either alone or in 1:1 mixture with Taq-polymerase. For ET-subcloning Taq-polymerase (Promega) based PCR was sufficient. PCR product was purified by gel-extraction or using the Qiaquick PCR purification kit (Qiagen, #28104). When required, contaminating plasmid used as PCR template was removed by 1 h DpnI digest followed by Phenol:CH_3Cl extraction and ethanol precipitation. For electroporation PCR products were diluted to 0.3 - 1 µg/µl.

2.6.2 Electroporation of competent cells

Gene Pulser 0.1 cm electroporation cuvettes (Biorad, #165-2089) were precooled on ice for at least 5 min. Electrocompetent cells were thawed on ice and 50 µl of cells were mixed with 0.5 - 2 ml of the DNA-containing solution (BAC, plasmid, PCR-product or a fragment excised from a plasmid). Cells were electroporated at 2.3 kV (2.5 kV for the strain YZ300) on a Bio-Rad Gene Pulser (25 µF with pulse controller set to 200 Ohms), usually with time constants between 4.5 and 4.8. 1 ml of LB medium was added and transferred back into the eppendorf tube. Cells were then incubated at 37 °C for 1 to 1.5 hours under shaking, and plated on suitable antibiotic selection plates.

2.6.3 Primer pairs used for ET-recombination

sub-gfp5 139 mer
5′- TCG ACC AGG ATG GGC ACC ACC CCG GTG AAC AGC TCC TCG CCC TTG CTC ACC
ATT GTG GGT CTT GCA GAG GTT GAT GGC TCT CTG GAC TGT GTG TTT GAG TCT TCT
GGC GCG CCT TAC GCC CCG CCC TGC CAC TCA TCG C –3′

sub-gfp3, 160-mer
5'- CCG CCG GGA TCA CTC TCG GCA TGG ACG AGC TGT ACA AGT AAG AAG TTC CTA
TTC TCT AGA AAG TAT AGG AAC TTC AGA TCT GTG TGA GAC AAA GTG TGG AGA GAC
CTC CCC TGG ACT AGA AAC TGC ATC TCA GCG GCC GCA CAA CTT ATA TCG TAT GGG
G -3'

---

sub-geok5, 75-mer
5'- TCC TCT AGA GTC CAG ATC FTC CGG GTA CCG AGC TCC TGT GCC AGA CTC TGG
TTA CGC CCC GCC CTG CCA CTC ATC -3'

sub-geok3, 115-mer
5'- TCC CGA TTC GCA GCG CAT CGC CTT CTA TCG CCT TCT TGA CGA GTT CTT CTG
AGA AGT TCC TAT TCT CTA GAA AGT ATA GGA ACT TCA GAT CTA CAA CTT ATA TCG
TAT GGG GCT G -3'

PLAP-sub5, 87-mer
5'- TGC TTC CTC TGC TGG CCG GGA CCC TGC TGC TGC TGG AGA CGG CCA CTG CTC
CCT GAG CTA GCA CAA CTT ATA TCG TAT GGG GCT GAC -3'

PLAP-sub3, 84-mer
5'- TGC CCA GGG AGA GCT GTA GCC TCA GGC CCA GCA GCA GCA GCA GCA GCA GCA
TGC TAG CTT ACG CCC CGC CCT GCC ACT CAT CGC -3'

---

n-ires5, 28-mer
5'- TGA GCG GGT ACC CAG AGT AAT GAC ATG G -3'

n-ires3, 42-mer
5'- TAG TCG GTA CCT TAA TTA AGC TAG CCA AGC GTG GGC TGT ACC -3'

5-NRF2EMCV,74-mer
5'- CCG ATT CGC AGC GCA TCG CCT TCT ATC GCC TTC TTG ACG AGT TCT TCT GAC
CAG AGT CTG GCA CAG GAG CTC GG -3'

3-NRF2EMCV,74-mer
5'- CCC AGG GAG AGC TGT AGC CTC AGG CCC AGC AGC AGC AGC AGC AGC AGC ATG
GTT GTG GCA AGC TTA TCA TCG TG -3'

---

newlRF7hom5',145-mer
5'- AGA CAG TTT TAC TGT TCG TGA TGA TAT ATT TTT ATC TTG TGC AAT GTA ACA
GAC CCT GCA GGC AGA GCA GCC ACG CTG GGG TTA GGG CTA ATG TAA GGG ACA CAG
GAC CCA ATA CCT CGA GAC AAC TTA TAT CGT ATG GGG CTG -3'

newlRF7hom3', 138-mer
5'- GAG CTT TAT TTT CAT GAT CTG TGT GTT GGT TTT TGT GTG CGG CGC GCC CTG
GGC TGT GGC CCG AGG GAG GTG GCC ACC TAG TGG AGT TAA CCT GCC ACC CCC AGA
GGC TCT AGA TTA CGC CCC GCC CTG CCA CTC ATC -3'

2.6.4 Preparation of competent bacteria (strain YZ300) for ET-cloning experiments

YZ300 cells ($RecA^+$strain JC8679 that carries the *sbc*A mutation) from glycerol stock were streaked out on an LB plate. After o.n. growth at 37 °C a single colony was picked and an o.n. starter culture (5 ml LB medium) was inoculated. The following day 250 ml LB medium were inoculated with 1 ml of the starter culture. Bacteria were grown at 37 °C and harvested at an OD_{600} of < 0.35. The centrifuge and the rotors SA600 or SS34 (Sorvall) were pre-cooled by centrifuging for 10 min at -5 °C at 4,000 rpm. The cells were spun in a first round of centrifugation for 10 min at 7,000 rpm at -5 °C. After pouring away the supernatant, tubes were put on ice, and the cells resuspended in 5 to 10 ml ice-cold 10% glycerol using an ice-cold 10 ml pipette. 200 ml of 10% glycerol were added and the cells were centrifuged. This step was repeated twice. At the end, after pouring away the supernatant, the tubes were immediately dried with Kleenex tissue taking care not to touch the pellet. Cells were then resuspended in the residual liquid (the final resuspended volume usually amounted to 500 µl). 50 µl of cells were transferred into pre-cooled eppendorf tubes and frozen in liquid N_2 or used immediately. For transformation, competent cells were thawed on ice and mixed with 1 to 2 µl of the recombinogenic linear DNA fragment (PCR product and/or a fragment excised from a plasmid).

2.6.5 Preparation of competent cells containing BACs for ET-cloning experiments

E. coli cells (strain DH10B) harboring the relevant BAC were transformed with the ET expression plasmid (pBADabg (Muyrers et al., 1999) or pR6K116/BAD/abg (Zhang et al., 2000)) by the electroporation procedure (see 2.5.1) and then plated. Single colonies were picked and grown in 5 ml LB medium overnight. 0.7 ml of culture were then transferred into 70 ml of LB medium (without glucose) and grown at 37 °C under constant shaking. To ensure optimal harvesting conditions, bacterial growth curves of the clones under study have been monitored before the actual culture for competent bacteria was stared. When the cells reached OD600 = 0.1-0.15, 0.7 ml of a 10% L-arabinose (Sigma) solution were added to induce ET protein expression. After another 45-60 minutes, the cells usually have reached an OD600 of 0.3-0.4 and were ready for harvest. For BAC experiments, lower ODs (around 0.25) have actually yielded better results. The centrifuge and the rotors SA600 or SS34 (Sorvall) were cooled by centrifuging for 10 min at -5 °C at 4,000 rpm. 35 ml of cells were spun in a first round of centrifugation for 10 min at 7,000 rpm at -5 °C, while keeping the other 35 ml on ice. After pouring away the supernatant, the second 35 ml were added and recentrifuged. 10% glycerol with dH_2O was prepared, and cooled on ice for at least 3 hours before use. After pouring away the supernatant, tubes were put on ice, and the cells resuspended in 5 to 10 ml ice-cold 10% glycerol using an ice-cold 10 ml pipette. 25 more ml of 10% glycerol were added and the cells were centrifuged. This step was repeated twice. At the end, after discarding the supernatant, the tubes were immediately dried with Kleenex tissue taking care not to touch the pellet. Cells were then resuspended in the remaining liquid (the final resuspended volume usually amounted to l00 µl). 50 µl of cells were transferred into pre-cooled eppendorf tubes and frozen in liquid N_2 or used immediately. For transformation, competent cells were thawed on ice and mixed with 1 to 2 µl of the recombinogenic linear DNA fragment (PCR product and/or a fragment excised from a plasmid).

2.6.6 Preparation of BAC minipreps

Minipreparations of BAC DNA were performed as described by the Research Genetics BAC fact sheet. Cells from 1.5 ml o.n. culture were pelleted and resuspended in 100 µl Qiagen solution I. Tubes were placed on ice and 200 µl of Qiagen solution II were added. Tubes were inverted 7 times and incubated for 2 min on ice. 150 µl of Qiagen solution III added and the tubes inverted. After brief incubation tubes were spun at maximum speed for 6 min in a microfuge. Supernatant was transferred into a fresh tube and residual debris removed using a toothpick. After addition of 1 ml 100% ethanol the tube was respun for 6 min at maximum speed. After decanting the supernatant, DNA pellet was rinsed with 70% ethanol. Residual ethanol was removed by double aspiration and the pellet was air dried at 37 °C. The DNA pellet was resuspended in 20 µl ddH_2O. The BAC DNA obtained was sufficient for two analytic restriction digests.

2.6.7 Preparation of circular BAC for microinjection

Maxipreparations were carried out using the Qiagen large construct kit (Qiagen) according to the manufacturers instructions. Contamination with genomic bacterial DNA is minimized by exonuclease treatment. The final resuspension was performed using 200 µl DNA injection buffer. Usually 5 - 50 µg of BAC DNA was obtained as determined by spectrophotometry at 260 nm. For microinjection purified BAC was diluted to 1 - 2 ng/µl.

2.6.8 Preparation of linear BAC fragments for microinjection

To obtain linearized BAC fragments that lack the pBeloBAC 11 plasmid backbone, about 10 µg of a BAC maxipreparation were restriction digested for 3 h with Not I. The reaction was loaded on a 0.8% low melt agarose gel (Biozym, Large DNA Low Melt Agarose) devoid of ethidium bromide flanked by DNA size markers (left and right). The gel was run slowly at 50 V o.n.
Two slices on either side of the gel including the edges of the sample and the markers were cut and stained with ethidium bromide. Plastic wrap was used to avoid contact between the stained slices and the unstained body of the gel. On the UV-box, gel and slices were aligned and the insert band on the unstained body was cut at the height of the stained band on the side slices. The cut band was placed in eppendorf tubes. 30 µl of 5M NaCl solution were added and the tube was incubated for 30 min at RT. After a quick spin agarose was melted by full immersion of the tube for 7 min in a water bath heated to 68 °C. Then the tube was incubated o.n. at 42 °C with 5-10 units beta-agarase (Promega, Agar ACE, cat no M17 4A) added after the first 10 min of incubation. The tube was spun at full speed for 10 min and the supernatant was transferred into a fresh tube. For purification the BAC-fragment containing supernatant was placed into an Ultrafree-MC filter system (Millipore, 30 kD cut-off, cat no UFC3LTK25) and spun at 6000 rpm in an eppendorf centrifuge. Spinning was stopped when the volume was around 50 µl. For washing, DNA microinjection buffer was overlaid and spinning continued. The filter was incubated at 4 °C o.n. to allow the DNA to come off the membrane, followed by gentle resuspension using a pipet.

2.6.9 Screening for transgenic founders by PCR on genomic tail DNA

DNA was prepared form mouse tail-biopsies by incubation in Laird-Jaenisch (LJ) lysis buffer (100 mM Tris-Cl pH 8.5, 5 mM EDTA, 0.2% SDS, 200 mM NaCl) supplemented with proteinase K (1 mg/ml). Tissues/cells were incubated overnight at 55 °C and residual debris was pelleted by centrifugation and then removed. DNA was precipitated by addition of equal volume of isopropanol, washed with 70% ethanol, airdried and dissolved in TE (Tris-EDTA, pH 8.0). PCR reactions were performed as described in chapter 2.4.1 using 2 µl of template DNA. C57BL/6 tail DNA served as negative control and the same DNA spiked with IFN-α2 recombinant BAC was used as positive control. The PCR primer pairs used for screening are listed in Table 2.2. Note that for both primer pairs specific for the 5' and 3' transitions between the WT IFN-α2 sequence and the reporter construct also a PCR specific for the IFN-α2 WT sequence was performed as a positive control.

Fragment	Primer Name	Primer Sequence	PCR conditions
GFP	#20 GFP-5'	CAT CGA GCT GAA GGG CAT CGA C	Product length: ~ 500 bp 94 °C-5', 94 °C-15'', 60.0 °C-15'', 72 °C-1', 40 cycles, 72 °C-10'
	#21 GFP-3'	GTA CAG CTC GTC CAT GCC GAG AG	
5' Transitn Promoter / GFP	#107 5IFNa2a	AGA GAA CCT AGA GGA GAA GAC	Product length: 533 bp 94 °C-5', 94 °C-15'', 60.0 °C-15'', 72 °C-1', 40 cycles, 72 °C-10'
	#108 3IFNa2a	TCG GCC ATG ATA TAG ACG TTG	
5' WT Promoter / IFN-a2	#107 5IFNa2a	AGA GAA CCT AGA GGA GAA GAC	Product length: 392 bp 94 °C-5', 94 °C-15'', 60.0 °C-15'', 72 °C-1', 40 cycles, 72 °C-10'
	#109 3IFNa2b	GCT GCT GGT GGA GGT CAT TGC	
3' Transitn BetaGeoK / 3' UTR	#110 5IFNa2c	GAA CAA ATG GGT GCA GAT ACA	Product length: 308 bp 94 °C-5', 94 °C-15'', 60.0 °C-15'', 72 °C-1', 40 cycles, 72 °C-10'
	#111 3IFNa2c	GCT GAC CGC TTC CTC GTG CTT	
3' WT IFN-a2 / 3' UTR	#112 5IFNa2d	TGT GCT GCG AGA TCT TAC TCA	Product length: 525 bp 94 °C-5', 94 °C-15'', 60.0 °C-15'', 72 °C-1', 40 cycles, 72 °C-10'
	#111 3IFNa2c	GCT GAC CGC TTC CTC GTG CTT	
ECMV-IRES	#113 5IFNa2e	ACG TCT ATA TCA TGG CCG ACA	Product length: 519 bp 94 °C-5', 94 °C-15'', 60.0 °C-15'', 72 °C-1', 40 cycles, 72 °C-10'
	#114 3IFNa2e	CTT GCA TTC CTT TGG CGA GAG	
3' ΔfrtBAC GFP / 3' UTR	#113 5IFNa2e	ACG TCT ATA TCA TGG CCG ACA	Product length: ~ 500 bp 94 °C-5', 94 °C-15'', 60.0 °C-15'', 72 °C-1', 40 cycles, 72 °C-10'
	#111 3IFNa2c	GCT GAC CGC TTC CTC GTG CTT	

Table 2.2 PCR primers used in the screening for transgenic founders

3 Results

3.1 Type I IFN response to VSV infection in cultured MEFs

Tissue culture experiments have shown previously that the expression of all IFN-α genes, except IFN-α4, was dependent on type I IFN receptor feedback signaling in Newcastle disease virus (NDV) stimulated MEFs (Marie et al., 1998; Sato et al., 1998). To validate this finding under conditions of a productive virus infection, IFNAR competent (WT) and IFNAR deficient (IFNAR-/-) MEFs were VSV infected and IFN-α mRNA expression was monitored by RT-PCR analysis. Six hours after VSV infection WT MEFs showed significant upregulation of both IFN-β and the IFN-α subtype genes while in MEFs deficient of type I IFN feedback signaling no upregulation of IFN-α mRNA was detected. In IFNAR-/- MEFs also the expression IFN-β mRNA was impaired, albeit to a lesser extend. Similarly mRNA of the transcription factor IRF-7 was upregulated in WT MEFs but could not be detected in IFNAR-/- MEFs (Fig. 3.1). Upregulation of the transcription factor IRF-7 has been reported to be dependent on IFNAR feedback and has been shown to be critically required for IFN-α expression in NDV stimulated MEFs (Marie et al., 1998; Sato et al., 1998). Thus in VSV infected MEFs the IFN-α production is strictly dependent on IFNAR feedback signaling.

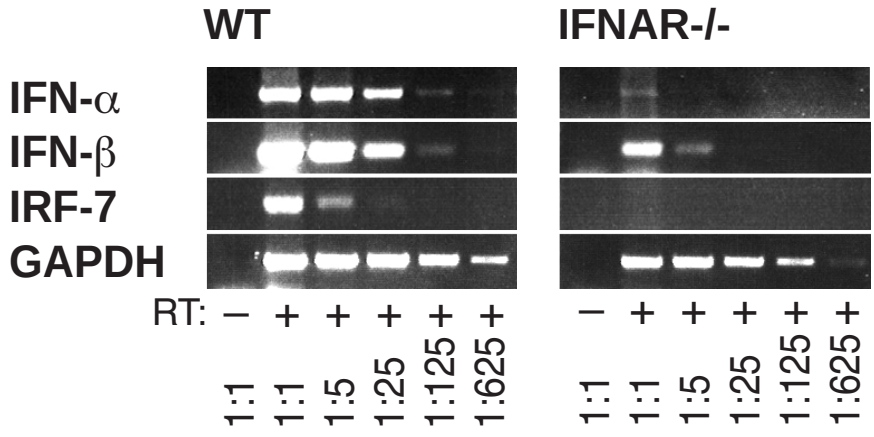

Fig. 3.1 Type I IFN receptor feedback is required for IRF-7 upregulation and IFN-α expression in VSV infected MEFs. MEFs derived from wild type (WT) or IFNAR deficient mice (IFNAR-/-) were infected with VSV at a multiplicity of infection of 10. Six hours after infection, total RNA of $1 \cdot 10^6$ cultured MEFs was extracted, and the mRNA content of different samples was normalized by a GAPDH-specific RT-PCR. The expression of IFN-α mRNA was monitored using consensus primers amplifying all IFN-α subtypes. Expression of IFN-β and IRF-7 mRNA was determined using specific PCR primers. The analysis was performed with serially 5 fold diluted cDNA samples starting with undiluted material.

3.2 Type I IFN response to VSV infection *in vivo*

To next examine IFN responses *in vivo*, IFN-α gene expression was analyzed in spleen from WT and IFNAR-/- mice infected with an intermediate dose of VSV ($2 \cdot 10^6$ pfu).
Surprisingly, expression of IFN-α mRNA was detected in the spleens of both WT and IFNAR-/- mice (Fig. 3.2 a). However, VSV replication is not controlled in IFNAR deficient mice, leading to highly elevated virus load already at the onset of measurable type IFN titers, while VSV titers in the sera of WT mice remained below the detection limit (Fig. 3.2c). The consequences of the discrepancy in viral load were apparent also when measuring type I IFN titers in the sera of VSV infected mice. After a delayed onset, IFN levels of IFNAR-/- mice rose up to, and eventually exceeded those measured in WT mice (Fig. 3.2 b).
Thus, to reduce the effect of differential replication of VSV in WT and IFNAR-/- mice, and to achieve a synchronized stimulation of IFN producing cells *in vivo*, in the following experiments mice were injected with an elevated dose of VSV ($2 \cdot 10^8$ pfu). Furthermore, the study was extended to incorporate also non-replicating inducers of type I IFNs.

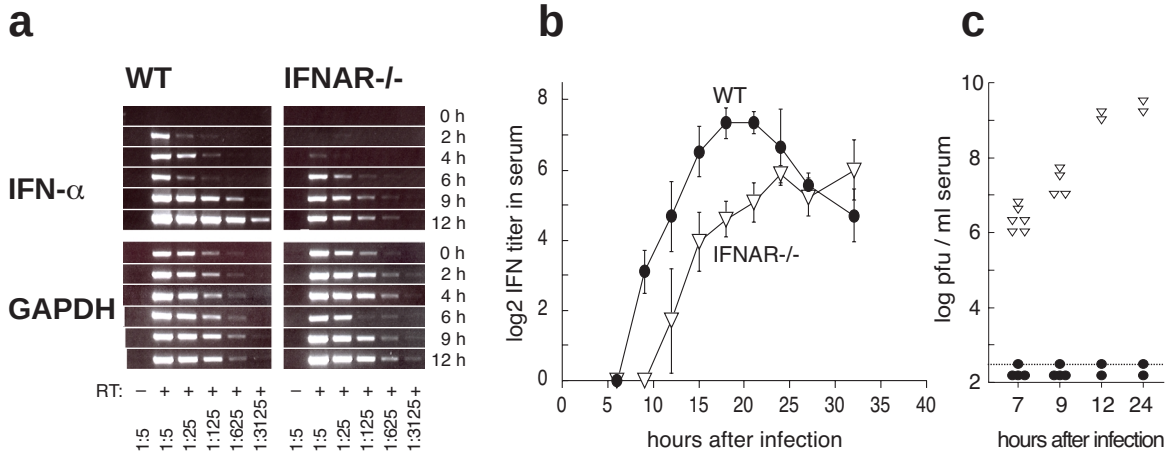

Fig. 3.2 IFNAR-/- mice infected with an intermediate dose of VSV show induced IFN-α expression, but the rapid increase in viral load precludes direct comparison with WT mice. WT mice (filled circles) and IFNAR-/- mice (open triangles) were i.v. stimulated with $2 \cdot 10^6$ pfu VSV. (**a**) At the time points indicated, total RNA from the spleen was prepared and RT-PCR using IFN-α consensus primers was performed as described in Fig. 3.1. (**b**) Mice were bled at the indicated time points and serum IFN titers were determined in a CPE protection assay. A log2 titer of 5 corresponds to 1000 IU of IFN-α. Data points represent mean titers (± sdev) of the sera of at least three mice. (**c**) Virus titers in the serum were determined by VSV plaque assay on serial 10 fold dilutions. The dotted line indicates the detection limit of the assay.

3.2.1 Requirement of type I IFN feedback signaling *in vitro* vs. *in vivo*

In order to directly compare the requirement of type I IFN receptor feedback for the production of IFN-α, the kinetics of IFN-α mRNA expression was monitored in MEFs infected with VSV at a moi of 10 (i.e. 10 pfu/cell) and in the spleens of mice acutely infected with $2 \cdot 10^8$ pfu VSV. WT fibroblasts showed elevated IFN-α mRNA levels beginning 4 h after VSV infection and peak expression between 9 h and 12 h (Fig. 3.3 a). Similar to NDV stimulated MEFs (Marie et al., 1998), VSV infected MEFs predominantly expressed IFN-α4 as determined by subcloning of RT-PCR products and sequence analysis of random clones (Fig. 3.4 a). In contrast, IFN-α upregulation was not observed in VSV infected MEFs lacking the type I IFN receptor (Fig. 3.3 a). Surprisingly, IFN-α mRNA was induced rapidly and to a similar extent in spleen of WT and IFNAR-/- mice. At later time points, IFN-α expression in spleen of IFNAR-/- mice decreased slightly, whereas spleen from WT mice showed a further increase in IFN-α expression (Fig. 3.3 b).

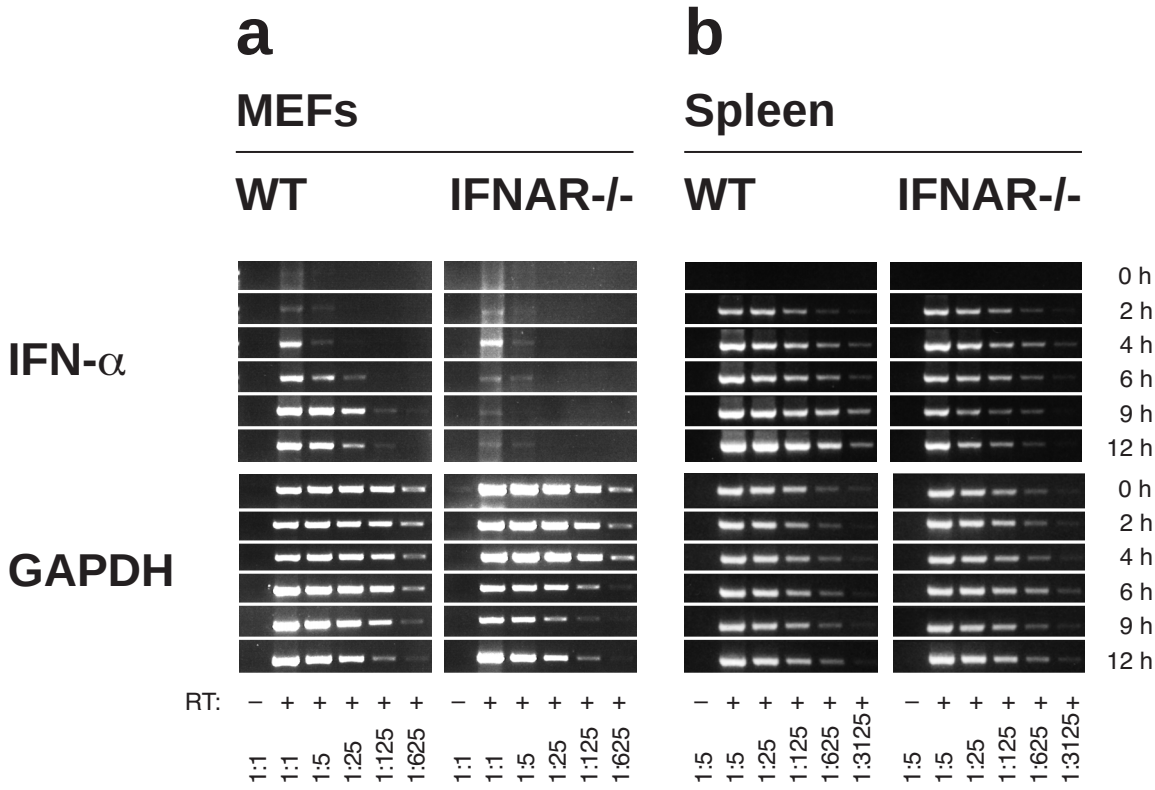

Fig. 3.3 VSV infection stimulates IFNAR independent production of IFN-α in mice, but not in mouse embryonic fibroblasts (MEFs). (**a**) MEFs derived from wild type (WT) or IFNAR deficient mice (IFNAR-/-) were infected with VSV at a multiplicity of infection of 10 and (**b**) WT and IFNAR-/- mice were i.v. injected with $2 \cdot 10^8$ pfu VSV. Total RNA of 10^6 cultured MEFs or of spleen tissue was extracted, and the mRNA content of different samples was normalized by a GAPDH-specific RT-PCR. The expression of IFN-α mRNA was monitored using consensus primers amplifying all IFN-α subtypes. The analysis was performed with serially 5 fold diluted cDNA samples starting with undiluted material; spleen derived samples were 5 fold prediluted.

The IFN-α subtype analysis revealed, that both VSV infected IFNAR competent and deficient mice showed abundant expression of IFN-α2 and α5, whereas IFN-α4 was found only rarely (Fig. 3.4 b and c). Thus, different IFN-α patterns found after VSV infection of MEFs and mice suggested that *in vivo* the majority of IFN-α is produced by a cell type different from fibroblasts. Moreover, similar IFN-α patterns found in WT and IFNAR-/- mice indicated a largely feedback-independent production of early IFN-α in VSV infected mice.

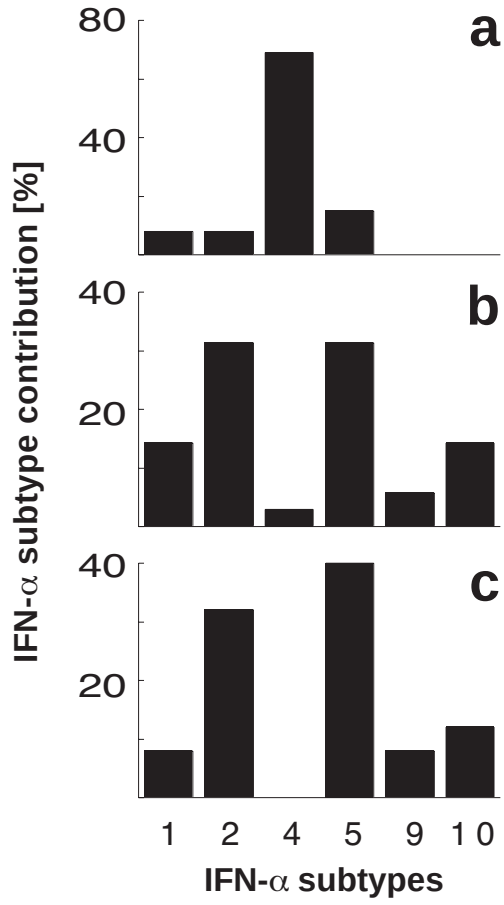

Fig. 3.4 Differential IFN-α expression profiles of VSV infected MEFs and mice. PCR products of the IFN-α expression analysis 6 h after VSV infection of (**a**) WT MEFs, (**b**) spleen of WT mice, or (**c**) spleen of IFNAR-/- mice were subcloned and DNA sequence of 13, 35, and 25 single clones was analyzed, respectively. IFN-α sequences were classified according to EMBL database entries. The sequence termed IFN-α10 corresponds to the IFN-αB sequence available on the EMBL database (accession No. L38698).

To correlate IFN-α mRNA levels and IFN serum activities, blood serum of VSV infected mice was taken and analyzed in a cytopathic effect (CPE) inhibition assay. As early as 4 h after VSV infection IFN activity was found in the serum of both WT and IFNAR-/- animals. Specific inhibition of IFN-α and/or IFN-β by neutralizing monoclonal antibodies in the CPE inhibition assay revealed a major contribution of IFN-α to the serum IFN activity, irrespective of whether IFNAR signaling was functional or not. Serum IFN titers of WT animals increased more rapidly than those of IFNAR-/- mice, eventually leading to about 30 fold higher IFN titers in WT animals than in IFNAR-/- mice (Fig. 3.5 a).

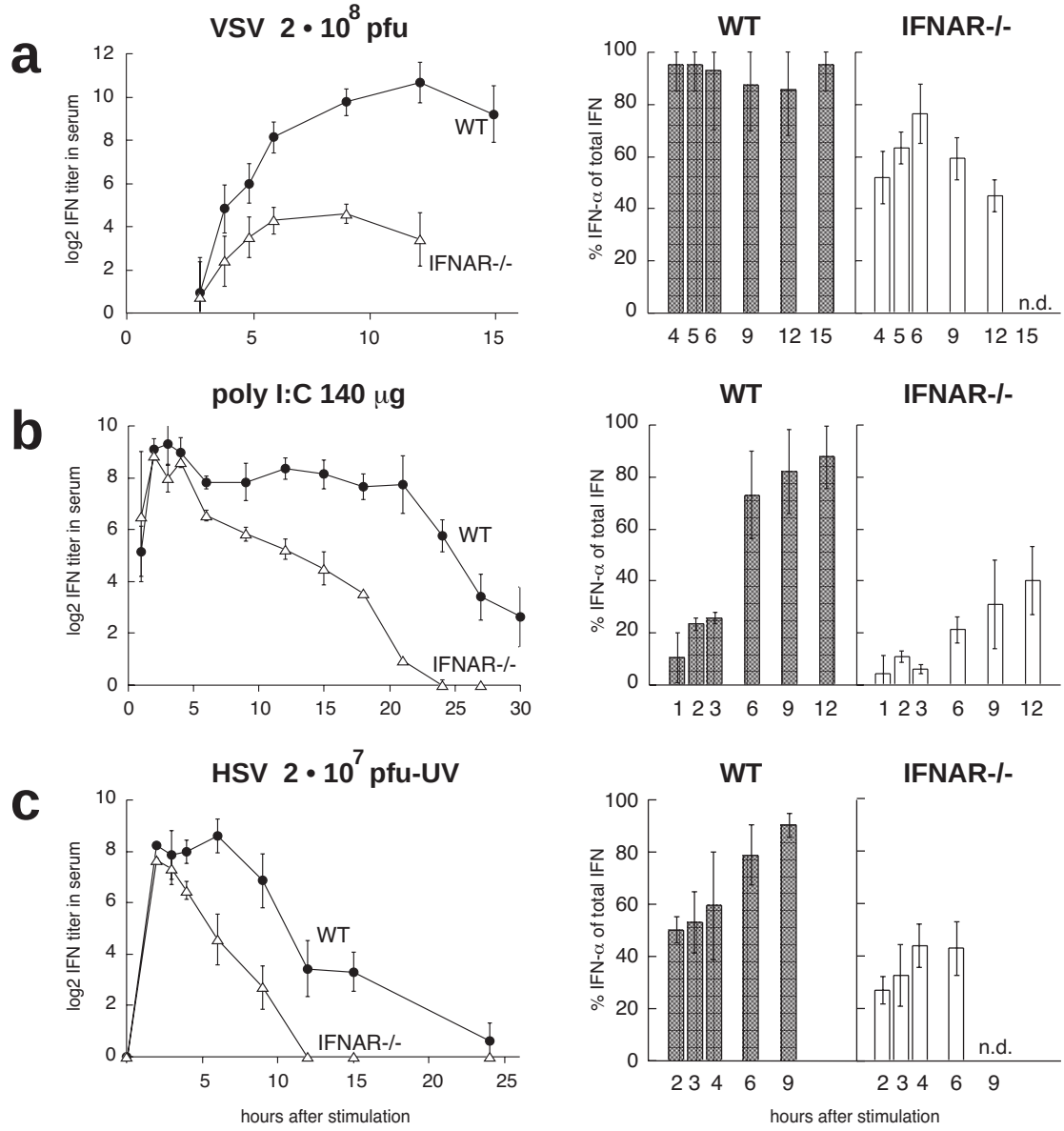

Fig. 3.5 Type I IFN activity in the serum of mice treated with VSV, poly(I:C), or UV-HSV. WT mice (filled circles) and IFNAR-/- (open triangles) mice were i.v. stimulated with (**a**) $2 \cdot 10^8$ pfu VSV, (**b**) 140 μg poly(I:C), or (**c**) $2 \cdot 10^7$ pfu UV-HSV. Mice were bled at the indicated time points and serum IFN titers were determined in a CPE protection assay. A log2 titer of 5 corresponds to 1000 IU of IFN-α. The contribution of IFN-α or IFN-β to the total IFN activity was determined by specific inhibition with monoclonal antibodies.

3.3 Type I IFN response induced by HSV *in vivo*

As mentioned before, virus replication is not controlled in VSV infected IFNAR deficient mice. The highly elevated virus load and increased cell death could have interfered with cytokine production in IFNAR-/- mice. Thus, we next analyzed type I IFN responses after stimulation with non-replicating virus. Since UV inactivated VSV does not induce type I IFN responses (data not shown), mice were injected with UV inactivated HSV. Two hours after the treatment, WT and IFNAR-/- mice showed similar peak IFN activity with about 50% and 35% IFN-α contribution, respectively. While the IFN response was short-lived in IFNAR-/- mice, IFN titers in WT mice were sustained for several hours, and a switch to a more pronounced IFN-α expression was found (Fig. 3.5 c). To verify the induction of early IFN-α in the absence of IFNAR-feedback signaling, mice deficient of the type I IFN receptor or IFN-β were intercrossed and IFNAR-/- IFN-β-/- double-knockout mice and IFNAR+/- IFN-β-/- littermates were stimulated with UV-HSV. Even in the absence of IFN-β initial IFN-α titers showed the same magnitude in receptor deficient and competent mice. At later time points IFN-α production was sustained and further enhanced in IFN receptor competent mice as compared to IFNAR-/- mice (Fig. 3.6). Thus, upon treatment with live VSV or UV inactivated HSV early IFNAR-independent IFN-α production is observed. Yet, at later time points IFNAR-feedback signaling is critical to sustain the production of IFN-α.

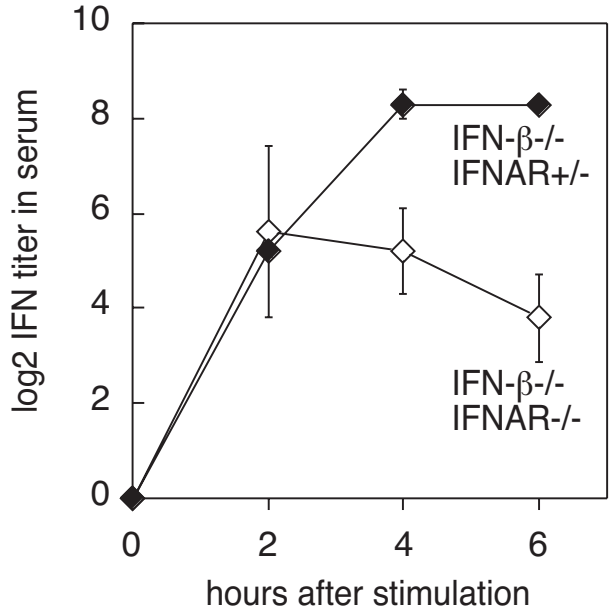

Fig. 3.6 IFN-α is produced in mice deficient of IFN-β and IFNAR. IFN-β deficient mice (filled diamonds) and double deficient mice lacking IFN-β and IFNAR (open diamonds) were i.v. injected with $2 \cdot 10^7$ pfu UV-HSV. Sera were taken at indicated time points and analyzed in a CPE protection assay. Mean IFN activity of 3 mice per time point is indicated. Results are shown of one out of two independent experiments. Note that the indicated IFN serum activities exclusively derived form IFN-α because the analyzed mice were IFN-β deficient.

3.4 Role of IRF-3 and IRF-7

The promoter regions of both IFN-β and the IFN-α subtype genes contain elements for the binding of members of the interferon regulatory factor (IRF) family. Recently the focus has been centered on IRF-3 and IRF-7 as the main regulators of type I IFN expression. IRF-3 and IRF-7 are considered key components of the type I IFN receptor feedback (Sato et al., 2000). In MEFS, expression of IRF-3 has been shown to be constitutive (Sato et al., 1998), thus allowing immediate induction of IFN-β and in some cases of IFN-α4. Also *in vivo*, IRF-3 expression was similar in the spleens of WT and IFNAR-/- mice and remained remarkably stable in the course of VSV infection (Fig. 3.7).

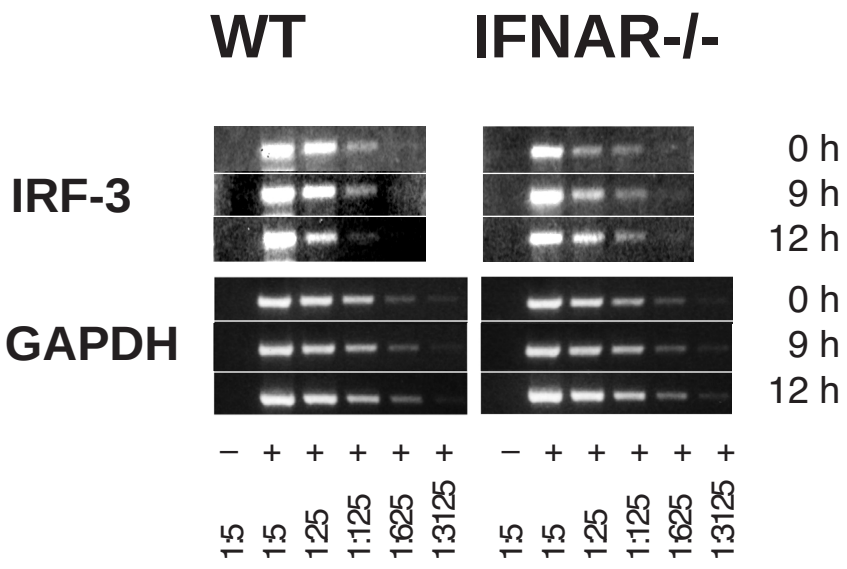

Fig. 3.7 Expression of IRF-3 mRNA in spleens of WT and IFNAR-/- mice is similar and is not altered during viral infection. Mice were infected intravenously with $2 \cdot 10^8$ pfu VSV. Total RNA was isolated at the time points indicated and RT-PCR was performed as described in Fig. 3.1.

In contrast, IRF-7 has been shown to be upregulated upon IFNAR triggering (Marie et al., 1998; Sato et al., 1998) and was proposed to be critically required for the expression of IFN-α subtype genes (Sato et al., 1998; Yeow et al., 2000). We therefore asked, whether early IFNAR-independent IFN-α was produced in the absence of IRF-7 induction. The RT-PCR analysis of IRF-7 mRNA levels in VSV infected WT and IFNAR-/- mice revealed a prompt IRF-7 upregulation only in WT mice but not in IFNAR deficient mice (Fig. 3.8). These experiments indicated that in VSV infected mice early IFN-α was induced in the absence of detectable IRF-7 upregulation. At later time points IFNAR-independent IRF-7 upregulation was observed (Fig. 3.9) which, however, did not suffice to promote a sustained production of IFN-α in IFNAR-/- mice.

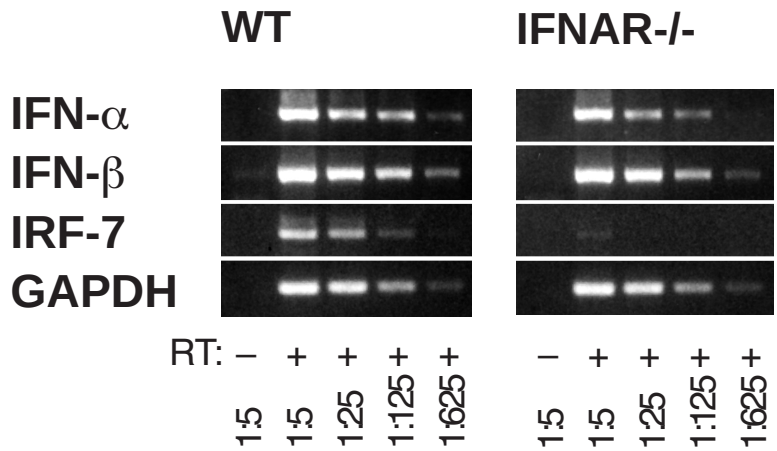

Fig. 3.8 VSV infected IFNAR-/- mice show an early induction of IFN-α before the onset of IRF-7 expression. Total RNA from spleen of IFNAR-/- or WT mice was isolated 3 hours after i.v. infection with $2 \cdot 10^8$ pfu VSV. RT-PCR was performed as described in Fig. 3.1.

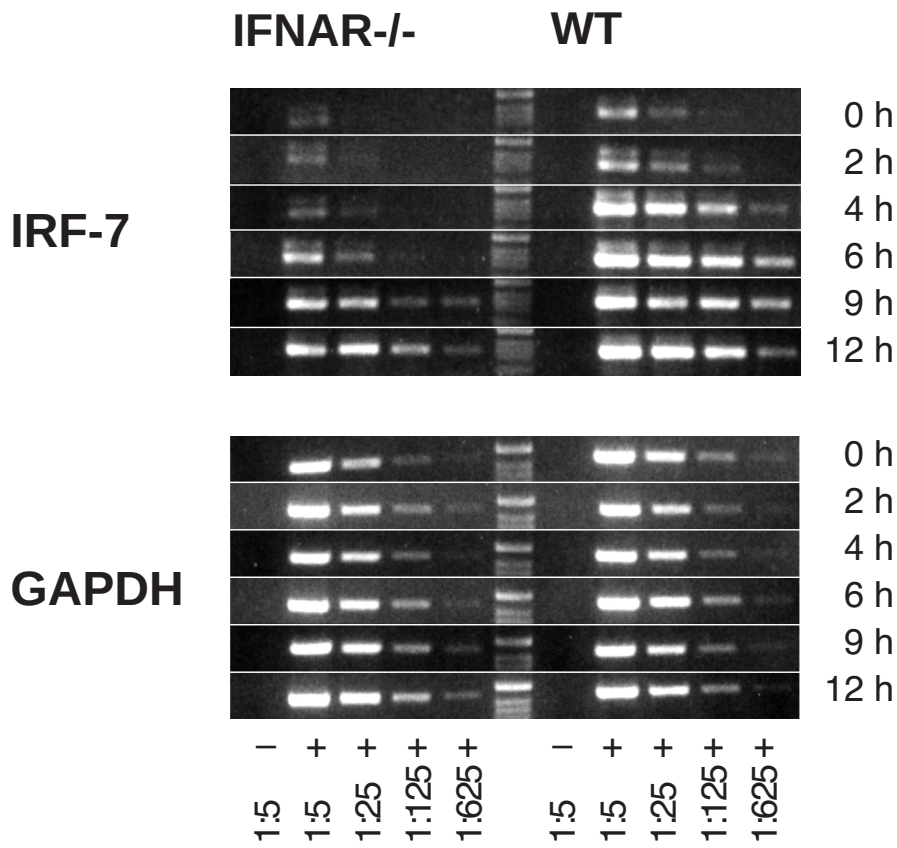

Fig. 3.9 IRF-7 mRNA can be upregulated independent of type I IFN receptor feedback. Total RNA from spleen of IFNAR-/- or WT mice was isolated after i.v. infection with $2 \cdot 10^8$ pfu VSV at the time points indicated. RT-PCR was performed as described in Fig. 3.1.

3.5 Type I IFN response induced by double stranded RNA (poly I:C) *in vivo*

To further study the role of feedback signaling with a non-replicating type I IFN inducer, mice were treated with poly(I:C). Sera of poly(I:C) treated WT and IFNAR-/- mice displayed early peak IFN activity, followed by a rapid decline in the case of IFNAR-/- mice. In WT mice IFN activity was sustained at high level for more than 20 hours. Neutralization of IFN-α and/or IFN-β revealed an abundant contribution of IFN-β to early type I IFN activity in both WT and IFNAR-/- mice. At later time points, strong IFN-α production was observed in WT but not in type I IFN receptor deficient mice (Fig. 3.5 b). Equally, RT-PCR on total RNA of the spleen revealed a strongly impaired IFN-α response in IFNAR-/- mice (Fig. 3.10).
Preferential production of IFN-β upon poly(I:C) treatment - while mainly IFN-α is produced after virus stimulation - indicates that different cell types may be involved in the production of poly(I:C) vs. virus-induced type I IFN. Moreover, these results further support the hypothesis that the sustained production of IFN-α is IFNAR-dependent.

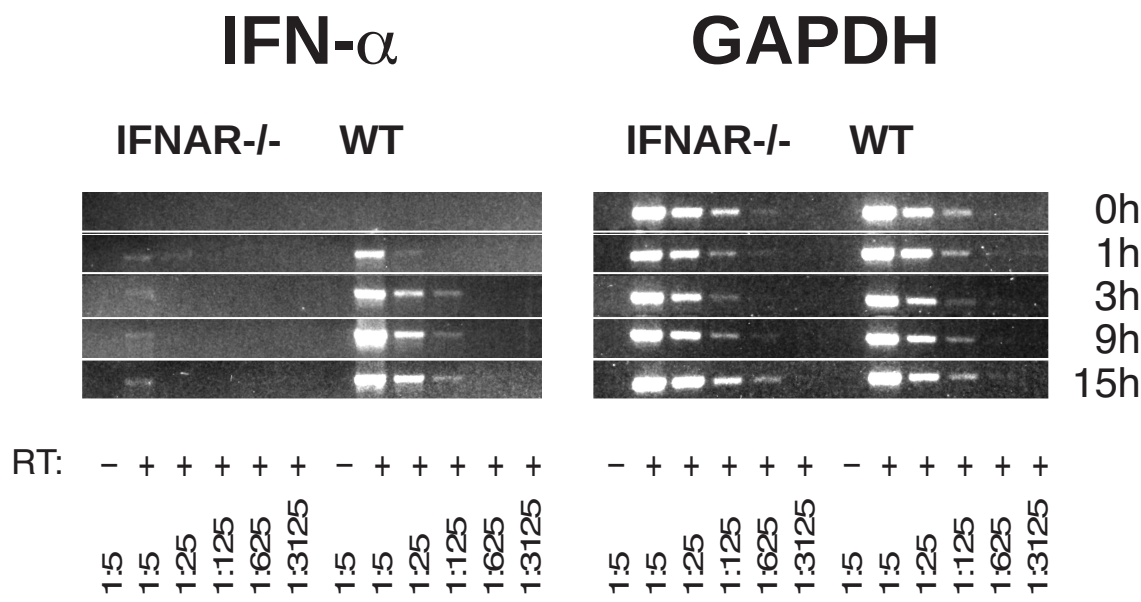

Fig. 3.10 Expression of IFN-α is strongly impaired in the spleens of IFNAR-/- mice stimulated with poly(I:C). Mice were injected intravenously with 140 µg of poly(I:C) at the time points indicated, total RNA of the spleens was prepared. RT-PCR was performed using IFN-α consensus primers as described in Fig. 3.1

3.5.1 Requirement of the primary inducing stimulus for type I IFN production

When stimulated with a non-replicating IFN inducer (UV-HSV or poly(I:C)), type I IFN titers in the sera of IFNAR deficient mice declined rapidly after initial peak expression. To determine whether short lived IFN response observed in IFNAR-/- mice was due to short half life of the inducing stimulus or whether in the absence of receptor feedback the IFN producing cells became generally unable to produce type I IFN, poly(I:C) stimulated mice were restimulated after 24h by a second injection of poly(I:C). The type I IFN serum titers revealed, that also after a second stimulus, peak expression of both WT and IFNAR-/- mice was similar (Fig. 3.11), ruling out a general loss of cells able to produce type I IFNs.

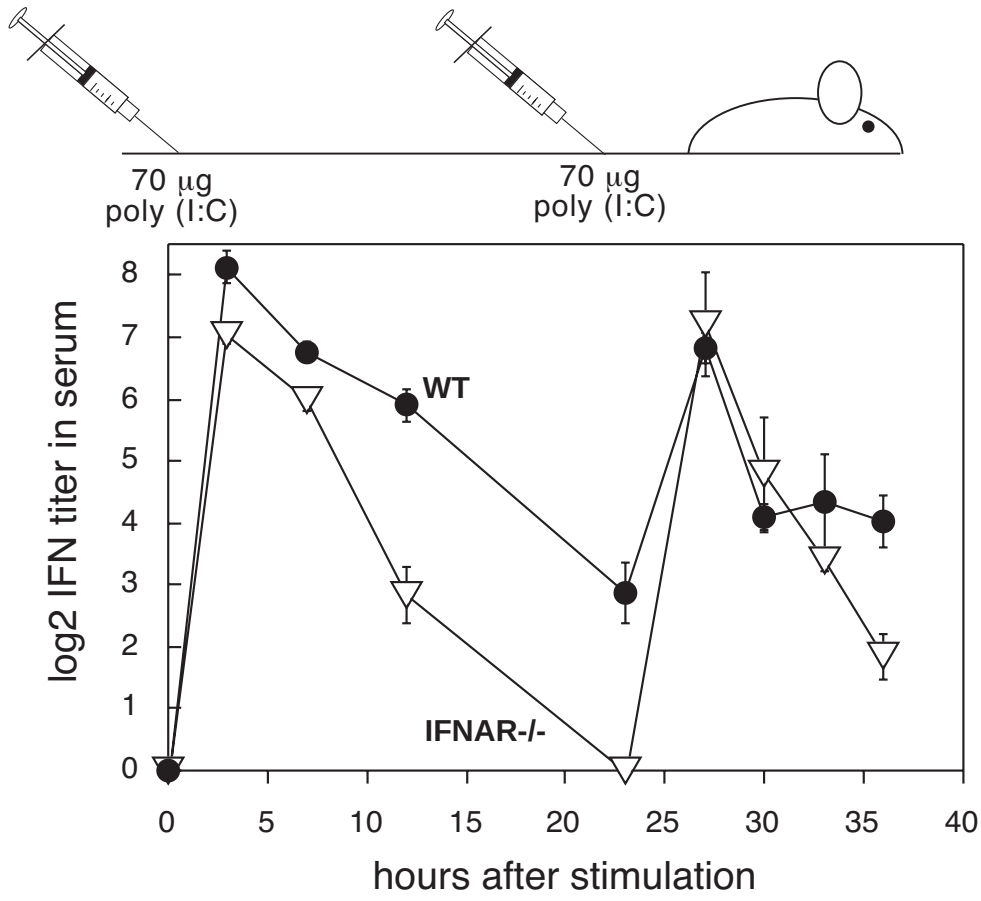

Fig. 3.11 The poly(I:C) induced IFN response may be restimulated and reaches similar peak levels in WT (filled circles) and IFNAR-/- (open triangles) mice. Mice were injected twice at a 24 h interval with 70 µg of poly(I:C). Serum IFN titers were monitored in a CPE protection assay. Data points represent mean IFN titers (±sdev) of the sera of three mice.

Moreover, type I IFN production of IFNAR-/- mice could be sustained by continuous poly(I:C) stimulation, and showed kinetics similar to WT mice after a single injection of poly(I:C) (Fig. 3.12). Interestingly, continued poly(I:C) stimulation had only a minor effect on type I IFN titers in the sera of WT mice.
How long poly(I:C) or UV-HSV remained active *in vivo* cannot be readily determined. However, the kinetics observed in these experiments indicated, that poly(I:C) activity *in vivo* is likely to be short lived and that in the absence of receptor feedback, type I IFN production was strictly dependent on the availability of the primary inducing stimulus. Conversely it can be concluded, that type I IFN receptor feedback *in vivo* constitutes a mechanism to sustain IFN production, even if the inducing stimulus is active only for a short time.

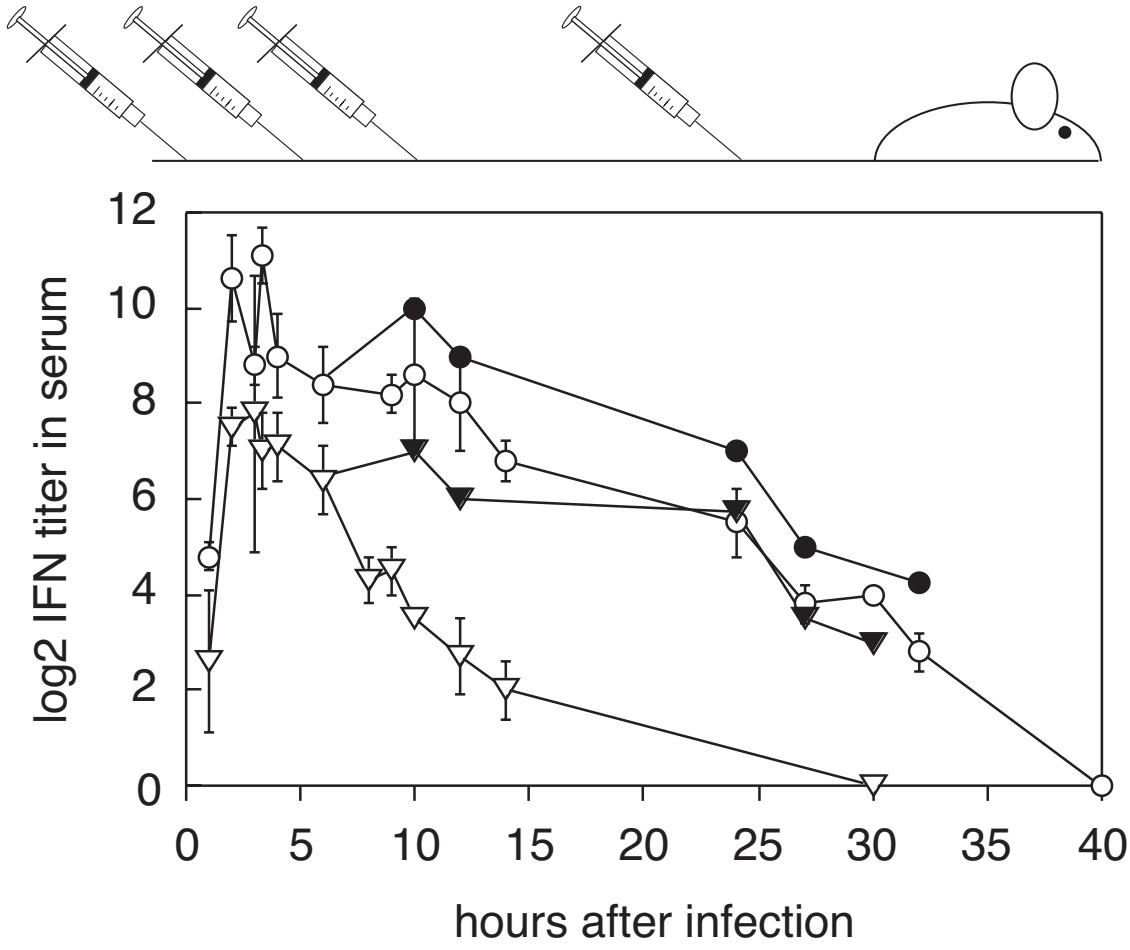

Fig. 3.12 IFN serum titers may be sustained by continued stimulation with poly(I:C). WT (circles) and IFNAR-/- (triangles) mice were injected with 140 µg poly(I:C). Two mice of each group received additional injections of 140 µg poly(I:C) (filled symbols) at 5, 10 and 24 h after the first injection. Type I IFN serum titers were determined by a CPE protection assay. Graph shows the pooled results of two independent experiments**.**

3.6 Site of type I IFN production in vivo

To localize IFN producing cells, mice were infected with VSV and at several time points after infection spleen sections were analyzed immunohistochemically with polyclonal antibody directed against type I IFN. Specific staining became detectable 6 h after infection and decorated a structure surrounding follicles, i.e. the marginal zone. In VSV infected spleens of both WT and IFNAR-/- mice the intensity of type I IFN staining peaked 9h after infection (Fig. 3.13). The observed staining pattern correlates well with maximal IFN titers in the serum of VSV infected mice (Fig. 3.5).

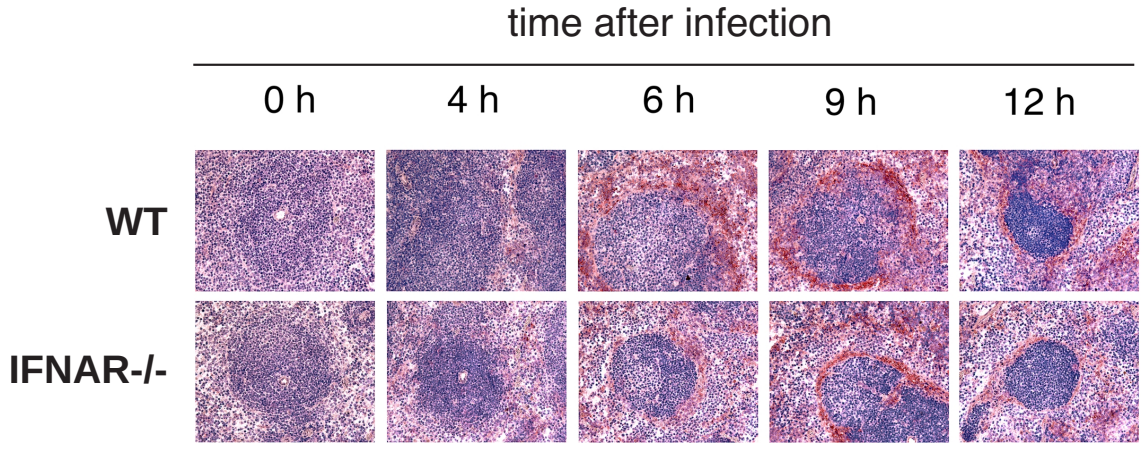

Fig. 3.13 Type IFN production is detected in the marginal zone of the spleens of WT and IFNAR-/- mice and peaks 9 h after VSV infection. WT and IFNAR-/- mice were infected with $2 \cdot 10^8$ pfu VSV. Spleens were snap frozen at the time points indicated and sections were analyzed cryo-histochemically with a polyclonal serum against type I IFN (red). Sections were counterstained with hemalum (blue) to visualize lymph follicles.

In the following experiments WT and IFNAR-/- mice were infected with VSV and 9 h later, consecutive sections were stained with polyclonal antibody directed against type I IFN or with an IFN-α specific monoclonal antibody. While staining with the polyclonal serum appeared more sensitive, stainings with monoclonal antibody revealed distinct type I IFN producing cells scattered in groups within the marginal zone (Fig. 2.14 a and b). After treatment with VSV or UV-HSV, spleens of WT and IFNAR-/- mice showed similar marginal zone stainings with polyclonal antibody, albeit staining of spleens from IFNAR deficient mice was somewhat weaker (Fig. 2.14 c).
In situ hybridization of spleen sections of untreated mice with an IRF-7 probe did not reveal evidence for constitutive IRF-7 expression, neither in few marginal zone cells nor anywhere else in the spleen (data not shown). After VSV infection of WT mice a strong IRF-7 induction was observed all over the spleen. In contrast, no IRF-7 induction was detected in spleens of VSV infected IFNAR-/- mice (Fig. 2.14 d). Together with the above RT-PCR data these observations indicate that virus-induced early IFN-α can be produced independent of IFNAR signaling and IRF-7 upregulation.

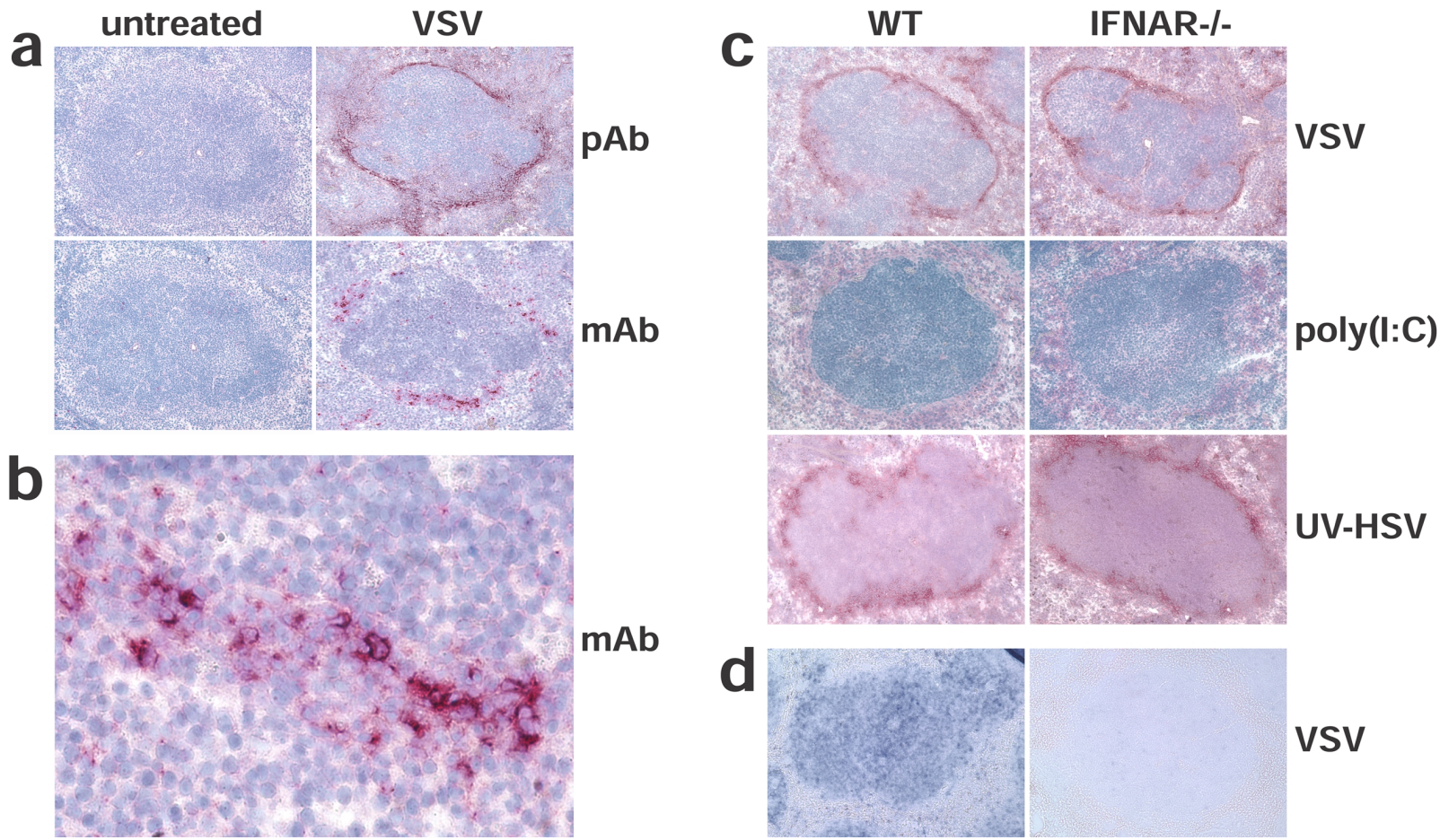

Fig. 3.14 VSV and UV-HSV injection, but not poly(I:C) stimulation, leads to high-level production of type I IFN by cells located in the marginal zone of the spleen. (**a**) WT mice were VSV infected and after 9 h spleens were analyzed histochemically with a polyclonal serum against type I IFN (pAb, upper two panels), or with an IFN-α specific monoclonal antibody (mAb, lower two panels). (**b**) A higher magnification of the marginal zone area of the lower right panel in (a) stained with monoclonal antibody is shown. (**c**) WT and IFNAR-/- mice were VSV, poly (I:C), or UV-HSV injected. After nine hours, and 6 h after UV-HSV stimulation, spleens were analyzed histochemically with a polyclonal serum against type I IFN. Sections in (a-c) were counterstained with hemalum (blue) to visualize lymph follicles. (**d**) In situ hybridization of IRF-7 mRNA (blue) was carried out on paraffin sections of spleen from WT and IFNAR-/- mice prepared 9 h after VSV infection.

Despite substantial IFN levels in the serum, no specific type I IFN staining was detected in the marginal zone of poly(I:C) treated mice (Fig. 2.14 c). Thus, after injection of virus particles, irrespective of whether they were replication competent or not, type I IFN production is located in the marginal zone. The soluble inducer poly(I:C) did not induce high enough type I IFN production in the spleen to be detected by immunohistology. Probably under these conditions type I IFN is produced at low level by numerous cell types and in various tissues.
To test this hypothesis WT mice were stimulated for 6 h with 140 µg poly(I:C), and total RNA prepared from several tissues was tested for IFN-α expression by RT-PCR. Significant levels of IFN-α mRNA were observed in all tissues tested, including the liver, heart, kidneys and lymph nodes of poly(I:C) stimulated mice. In contrast, VSV infected mice showed no or very low IFN-α expression in the heart, kidneys and lungs. However, IFN-α expression in was not exclusively confined to the spleen but was also detected in the liver of VSV infected mice (data not shown). This indicated that IFN produced in organs other than the spleen do contribute to the type I IFN titers measured in the serum after intravenous injection of VSV.

In an attempt to evaluate the contribution of spleen derived IFN vs. IFN produced in other tissues, C57BL/6 mice were spleenectomized and after recovery infected intravenously with VSV. Surprisingly, Serum IFN titers of spleenectomized mice did not diverge significantly from the titers observed in unoperated control animals (Fig. 3.15). This result, together with the observation that after viral infection type I IFN is produced by a defined, rare cell type, makes it important to characterize the interferon producing cell population (IPC) in the mouse, and to determine whether it is present also in organs other than the spleen.

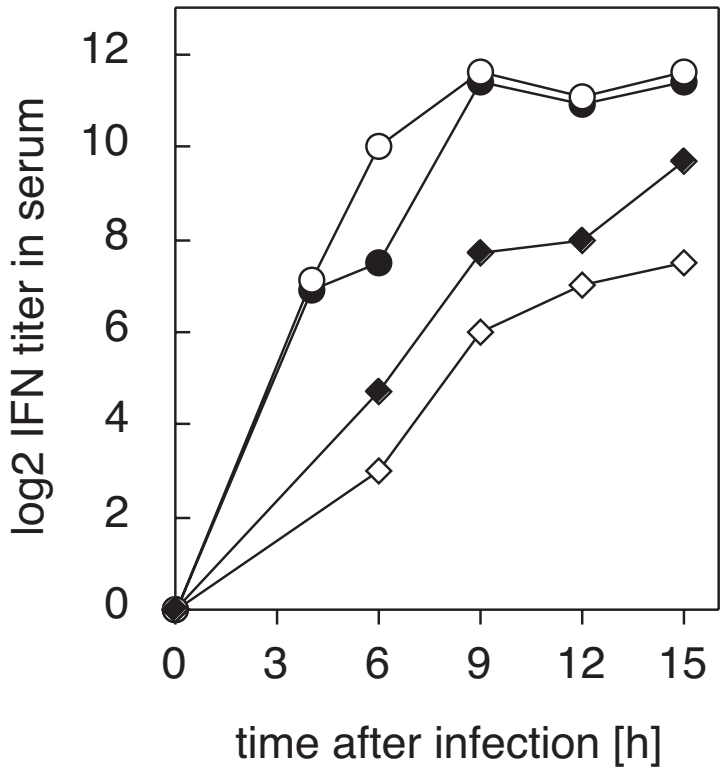

Fig. 3.15 Spleenectomy does not significantly alter the type I IFN response to VSV. C57BL/6 mice were spleenectomized (open symbols) or left untreated (filled symbols). Three days later, mice were infected intravenously with $2 \cdot 10^8$ (circles) or $2 \cdot 10^6$ (diamonds) pfu VSV. Sera were taken at the time points indicated and analyzed in a CPE protection assay. Data points represent mean IFN activity of 2 - 3 sera.

In the following chapters two independent strategies are described to identify type I IFN producing cells and to characterize their tissue distribution and properties in the course of viral infection. The first strategy attempts to visualize IPCs by the transgenic expression of a reporter gene, whereas the second approach aims at the identification of IPCs in WT mice by the means of intracellular and/or surface markers.

3.7 Genetic marking of type I IFN producing cells (IPCs)

In cell culture most any cell type may produce type I IFN in response to a suitable stimulus. It has been known for a long time, however, that after *in vivo* stimulation the majority of type I IFN is produced by few cells producing IFN-α at high level. Mainly due to their rarity and lack of lineage markers, the phenotype of these so-called major IFN producing cells (IPCs) remained elusive. This section describes two strategies to generate transgenic mice expressing a reporter gene in order to identify type I IFN producing cell types. The project aims at genetically marking IPCs exploiting two of their prominent characteristics: High-level expression of IFN-α genes, and - as a more speculative approach - induced/constitutive expression of the transcription factor IRF-7 (Fig. 3.16). As determined by the analysis of IFN-α expression patterns in virus infected spleens (see Fig. 3.4), IFN-α2 is one of the most abundantly expressed IFN-α subtypes *in vivo* and therefore was chosen as target gene.

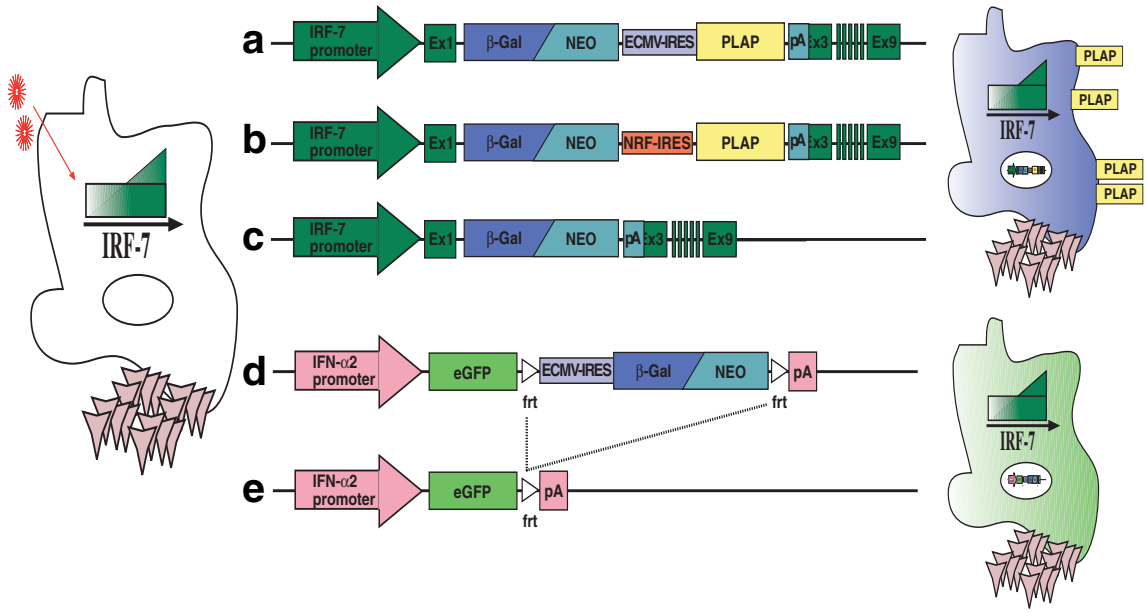

Fig. 3.16 Transgene constructs for the expression of reporter genes under the control of the IRF-7 (a-c) or the IFN-α2 (d,e) promoter. Mouse IFN producing cells (IPCs) may be visualized after introduction of a reporter transgene. (**a**) This construct contains a β-Gal reporter in the beta-Geo/b cassette followed by the EMCV-internal ribosomal entry site (IRES) and a PLAP reporter. β-Galactosidase activity may be visualized by X-Gal staining in histological sections, or in flow cytometry by intracellular staining with the FDG reagent. PLAP may be visualized by surface antibody staining in histology and cytometry. (**b**) This construct is analogous to (a) with the NRF-IRES replacing the EMCV-IRES. (**c**) This construct uses β-Gal as a single reporter gene. (**d**) This construct contains eGFP reporter followed by the EMCV-IRES driving expression of the β-Gal reporter in the beta-GeoK cassette. GFP is a fluorescent protein and can be readily detected by flow cytometry. (**e**) This construct may be derived from (d) after Flp-mediated recombination. It contains eGFP as a single reporter gene. Note that the Kanamycin resistance contained in the beta-GeoK and the beta-Geo/b cassettes functions as a selectable marker in the ET-cloning process (see 3.7.2).

3.7.1 Rationale for the choice of approach

The choice of reporter genes. In general, reporter genes are nucleic acid sequences encoding easily assayed proteins. They are used to replace other coding regions whose protein products are difficult to detect. In the transgene constructs three widely applied reporters in mammals were used. The idea was to utilize different markers for the two constructs that may eventually allow double stainings in doubly transgenic mice.

GFP (green fluorescent protein) is derived from the bioluminescent jellyfish *Aequorea victoria*. GFP is highly fluorescent. GFP shows low toxicity, no interference with normal cellular activities, and is easy to assay. These properties made GFP, especially the ER-targeted variant eGFP, the most commonly used reporter gene. However, because GFP fluorescence is not the result of an enzymatic reaction, the signal is not amplified, as it is the case with β-Gal and PLAP, which may result in lower sensitivity. eGFP was used in the IFN-α2 reporter construct, as it can be readily detected by flow cytometry and requires no further treatment of the cells before the assay.

LacZ as reporter gene, which encodes for β-galactosidase in *E. coli*, is widely used in the analysis of histological sections. Reporter gene expression is usually visualized by x-Gal staining. The recent introduction of the fluorescein di-β-D-galactopyranoside (FDG) reagent and derivatives allowed the use of the β-Gal reporter also for viable cells in flow cytometry (Nolan et al., 1988; Zhang et al., 1991). Besides β-galactosidase, the beta-Geo/b and beta-GeoK cassettes encode Kanamycin resistance and are used here as selectable marker in the ET-cloning approach (see 3.7.2).

Human placental alkaline phosphatase (PLAP) has been used successfully for the identification of transgenic cells within complex *in vivo* systems such as mice (Jacob and Baltimore, 1999). Over-expression of PLAP shows no adverse effects on mouse development or viability (Skynner et al., 1999). PLAP is expressed on the cell surface and alkaline phosphatase activity can readily be assayed in histological sections. Because of endogenous phosphatase activity in some tissues, recognition of PLAP using a monoclonal antibody (Zymed) is favorable and allows for the use of PLAP staining in flow cytometry.

The choice of internal ribosomal entry sites (IRES). IRESs are cis-acting elements that recruit the small ribosomal subunits to an internal initiator codon in the mRNA with the help of cellular trans-acting factors (Martinez-Salas, 1999). In recent years IRES elements have found ample use in molecular biology as they allow bicistronic expression in eucaryotes. Due to stable expression characteristics in many tissues, the EMCV-IRES from encephalomyocarditis virus is the most commonly used element. A recent report established the NF-κB repressing factor (NRF)-IRES as highly efficient ribosomal entry site (Oumard et al., 2000). However, it had not been tested, whether the NRF-IRES would be actively expressed in all tissues. Alongside the EMCV-IRES, the NRF-IRES was chosen in order to allow the first *in vivo* comparison of the expression efficiency of these elements.

The choice of the integration site into the IFN-α2 and IRF-7 genes. All type I IFN genes lack introns. The integration site of the IFN-α2 reporter construct was therefore chosen to

entirely replace the IFN-α2 ORF and leave the 5' and 3' flanking regions untouched. Thereby the reporter construct may use the endogenous IFN-α2 polyadenylation signal (Fig. 3.16d). The reporter construct is however bigger than the IFN-α2 ORF (5.5 kb vs. 920 bp). Flp mediated excision of the EMCV-IRES and the beta-GeoK cassette reduces the integrated reporter to the 800 bp GFP-ORF. This configuration is most likely to faithfully reproduce the expression characteristics of the IFN-α2 gene. The IRF-7 gene is composed of 9 exons. A regulatory sequence important for IRF-7 expression has been reported to reside in the first intron (Sato, Taniguchi 1998). Therefore, integration of a transgene should leave the first intron intact and possibly maintain the spacing of this intron to the IRF-7 promoter. Moreover, the first Exon of IRF-7 only codes for the 5' UTR and 4 $^{2}/_{3}$ amino acids. The integration was therefore targeted to entirely replace the second exon of IRF-7 with exception of the first G. As a consequence, transgene protein synthesis should start at the endogenous ATG, contain the first 5 amino acids of IRF-7 and would then continue with β-galactosidase starting with its second amino acid. In all variants of the IRF-7 construct (Fig. 3.16 a,b,c), the inserted reporter ends with a synthetic polyadenylation site.

The use of BACs. When this project was conceived, the cloned genes for neither IRF-7 nor for any IFN-α subtype were present in the laboratory. Furthermore, sequence information of both the murine genomic IFN locus and the genomic organization of the IRF-7 gene were unavailable in the public domain. We therefore opted for the use of bacterial artificial chromosomes (BACs) that contain our gene of interest. These BACs may be obtained through PCR-based screens on a BAC library of the mouse genome (strain Sv129).
Compared to the classical, smaller transgenes, the use of BAC constructs for the generation of transgenic mice has additional advantages. While small transgene constructs may be integrated into the genome of a transgene founder up to 50 times, BACs as transgenes integrate at a low copy number, i.e. usually only once. This allows for a better control of the gene dose and facilitates the breeding of stable lines of transgene expressing mice.
Because of the size of BAC constructs it is likely that all regulatory sequences required for controlled expression of the transgene are co-introduced. In addition, erroneous transgene expression, known as position effect due to foreign regulatory elements in the neighborhood of the integrated transgene, is reduced. For the generation of the transgene constructs and their homologous integration into bacterial artificial chromosomes (BACs) a novel method for DNA engineering, called ET cloning, was applied. ET-cloning constitutes a convenient way to introduce modifications in large DNA constructs such as BACs (Muyrers et al., 1999), where the use of enzymatic restriction is precluded.

3.7.2 ET-cloning, DNA engineering based on homologous recombination

ET-cloning was developed by Youming Zhang and Joep Muyrers in the group of Francis Stewart at the European Molecular Biology Laboratory in Heidelberg, Germany (Zhang et al., 1998). It is based on DNA exchange by recombination through short regions of homology that is mediated by the Rec**E** and Rec**T** proteins. Recombination occurs *in vivo* between a linear DNA molecule which contains homology arms of 42 nt or more on each of its ends, and a circular DNA target containing the chosen homology arm sequences. Homology arms may be introduced via PCR using long synthetic oligo-nucleotides. In the final recombinant product, the sequence between the homology regions on the circular target DNA is replaced by the sequence present between the homology arms on the linear DNA fragment. Correct recombinants are selected using antibiotic resistance genes introduced by the ET-recombination process (Muyrers et al., 2000). ET recombination has been successfully applied to regular plasmids, large cloning vectors (e.g. cosmids, BACs) and the *E. coli* chromosome. A remarkable development of this methodology was its recent application to direct cloning and subcloning (Zhang et al., 2000). The basic ET cloning variations - as used in this thesis - are schematized in figure Fig. 3.17. The sequence of PCR primers used for the ET-recombination can be found in chapter 2.6.3.

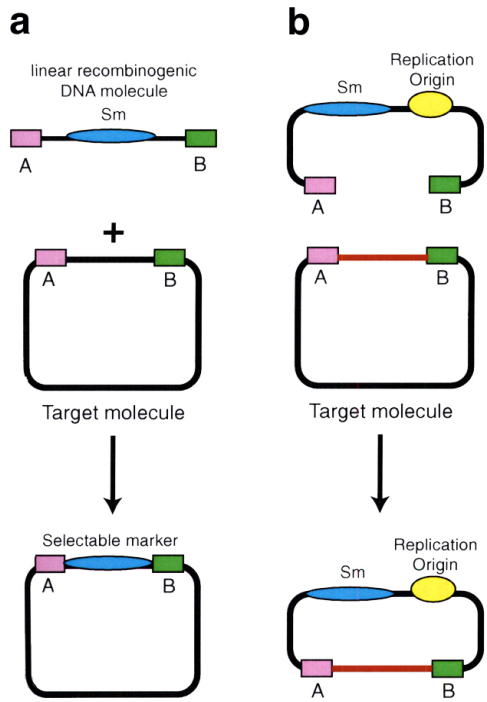

Fig. 3.17 Schematic illustration of the main variations of the ET recombination technology applied to the generation of the targeting constructs described in this thesis. (**a**) ET-cloning: A linear DNA fragment (e.g. a PCR product) is precisely integrated into a target molecule at the location defined by the short homology regions. (**b**) ET-subcloning: A fragment of interest from a donor plasmid (or a BAC) can be subcloned into a more convenient acceptor vector. The acceptor vector is amplified by PCR including the appropriate homology arms in the PCR primers. Note that the target molecule not necessarily needs to be a circular plasmid or BAC but may also be a linear DNA fragment (Original scheme by Giuseppe Testa)**.**

3.7.3 Generation of the IRF-7 reporter constructs

Schematic drawings of the assembly of all plasmids described in the following can be found in Fig. 3.18.

Generation of the pACYC/PLAP plasmid. This plasmid was assembled by ET-subcloning to add a NheI restriction site at both ends of the PLAP ORF (Fig. 3.18 a, right panel). The PCR primers used on pACYC184 template were Plap-sub5 and Plap-sub3. The PCR reaction was performed and then digested with DpnI to destroy residual pACYC184 template. The 2 kb PCR product was purified by gel extraction. The MSCV puro PLAP plasmid (a kind gift of J. Jacob, Atlanta; www.emory.edu/Microbio/jacob; Jacob and Baltimore, 1999) was digested with EcoRI. The ~1.6 kb fragment containing the PLAP-ORF was purified by gel extraction and coelectroporated with the PCR modified pACYC184 fragment into YZ300 cells. Bacteria expressing the recombined plasmid were selected on LB-Cm plates. 8 of 18 minipreps showed the expected fragments after NheI digest. Two selected clones were then tested further with analytic PvuII and SacII digests. The band pattern observed confirmed the expected results.

The NRF-IRES PCR. This proof-reading (cloned Pfu) PCR reaction was performed on pBSRlucNluc plasmid (a kind gift of H. Hauser, GBF, Germany; (Oumard et al., 2000) to endow the NRF-IRES with restriction sites for NheI and PacI at the 3' end and KpnI on both ends (Fig. 3.18 a, left panel). For the PCR reaction the n-ires5 and n-ires3 primer pair was used. The PCR product was purified, KpnI digested and then re-purified (Qiagen).

Generation of the pGK-beta-Geo/b-NRFIRES plasmid. The purified fragment of the NRF-IRES PCR was used as insert for conventional ligation into the KpnI linearized and CIP treated pGK-beta-Geo/b plasmid (a kind gift of Youming Zhang). The beta-Geo/b ORF contains an integrated prokaryotic promoter for the expression of a β-Gal-Neomycin fusion protein. This protein also confers resistance to Kanamycin. Selection was performed on LB-Kan plates. Of 22 minipreps, 13 contained the insert and 7 clones contained the NRF-IRES in the correct orientation as evidenced by analytic DraI digests.

Generation of the pGK-beta-Geo/b-NRFIRES-PLAP(NheI) plasmid. Nhe I digest of the pACYC/PLAP plasmid yielded a 1.6 kb fragment, which was purified by gel extraction. The pGK-beta-Geo/b-NRFIRES plasmid was linearized using the unique NheI site, and then CIP treated. Both fragments were annealed in standard ligation. Selection of transformed bacteria was performed on LB-Kan plates. Of 18 minipreps 13 contained the PLAP insert, and 5 of these in the correct orientation as judged by analytic BamHI and BstEII digests.

Generation of the pGK-beta-Geo/b-NRFIRES-PLAP(PacI) plasmid. This plasmid constitutes a minor modification of the construct described before. Instead of NheI sites, PacI sites were used for the sub-cloning. The insert containing the PLAP ORF was obtained directly from the MSCV puro PLAP plasmid after PacI digest and purification. Of 18 minipreps 9 contained the insert and four contained the PLAP ORF in the correct orientation as determined by BamHI, XbaI and DraI digest.

To verify that the NRF-IRES in the constructs was free of PCR errors, four clones of the pGK-beta-Geo/b-NRFIRES-PLAP(NheI) and one correct clone of the pGK-beta-Geo/b-NRFIRES-PLAP(PacI) were sequenced. In all cases the sequence for the NRF-IRES was error free. The sequencing also evidenced the expected difference in the spacing between the NRFIRES and the start codon of the PLAP ORF in the two constructs. Due to the difference in restriction site used for ligation, the pGK-beta-Geo/b-NRFIRES-PLAP(PacI) plasmid contained an additional 6 bp (i.e. the NheI site).

3.7.4 Introduction of IRF-7 homology arms into 4 variants of the reporter construct by ET-subcloning.

I) Generation of the pACYC-beta-Geo/b-NRFIRES-PLAP(NheI) plasmid. This plasmid was generated to endow the IRF-7 reporter construct with the homology arms required for ET-recombination into exon 2 of the IRF-7 gene (Fig. 3.18 c). The PCR primers used on pACYC184 template were newIRF-7 5'hom and newIRF-7 3'hom. The PCR reaction was performed and then digested with DpnI to destroy residual pACYC184 template. The 2 kb PCR product was purified by gel extraction. The pGK-beta-Geo/b-NRFIRES-PLAP(NheI) plasmid was linearized by XbaI digest. The fragment was desalted by ethanol precipitation and then coelectroporated with the PCR modified pACYC184 fragment into YZ300 cells. Bacteria expressing the recombined plasmid were selected on LB-CmKan plates. 8 out of 14 minipreps showed the correct recombination as revealed by analytic EcoRI and DraI digests. For one positive clone the homology arms to the IRF-7 gene introduced by ET-subcloning were sequenced and confirmed correct.

II) Generation of the pACYC-beta-Geo/b-NRFIRES-PLAP(PacI) plasmid. This plasmid was generated analogous to the (NheI) variant described above. Two out of 6 minipreps showed the desired recombination.

III) Generation of the pACYC-beta-Geo/b-EMCVIRES-PLAP plasmid: This plasmid was generated by ET-cloning, exchanging the NRF-IRES of the pACYC-beta-Geo/b-NRFIRES-PLAP(NheI) plasmid with the EMCV-IRES. The pACYC-beta-Geo/b-NRFIRES-PLAP(NheI) plasmid contains a unique HindIII site inside the NRF-IRES. Hind III linearization 'destroys' the NRF-IRES leaving the beta-Geo/b cassette and the PLAP ORF close to the ends of the linear 8.4 kb fragment. The fragment was purified by gel extraction.
Proof reading PCR (cloned Pfu/Taq 1:1) was performed on the EMCV-IRES contained in the pGK/IRES-beta-GeoK plasmid (obtained from Youming Zhang) using the 5-NRF2EMCV and 3-NRF2EMCVprimers. The PCR reaction was then digested with DpnI to destroy residual plasmid template. The 0.8 kb PCR product containing the EMCV-IRES was purified by gel extraction. The 5' primer contains a homology stretch to the 3' end of the beta-Geo/b cassette and the 3' primer is in part homologous to the 5' end of the PLAP ORF. Therefore ET-recombined plasmid could be generated by coelectroporation of the two purified fragments into competent YZ300 bacteria. The selection was done on LB-Kan plates. Of 9 minipreps 4 showed the correct exchange to the EMCV-IRES and 3 still contained the NRF-IRES as evidenced by analytic XbaI, PstI and Eco RI digests.

IV) Generation of the pACYC-beta-Geo/b plasmid. This plasmid constitutes the most straightforward reporter construct. It contains the β-Gal ORF in the pGK-beta-Geo/b cassette and was generated in a single ET-subcloning step starting from the XbaI linearized pGK-beta-Geo/b plasmid (obtained from Youming Zhang). The fragment was purified by gel extraction and was co-electroporated with the PCR modified pACYC fragment (described in the (Nhe) variant) into competent YZ300 cells. Bacteria expressing the recombined plasmid were selected on LB-CmKan plates. All 8 minipreps yielded the correct recombination as evidenced by analytic PstI and EcoRI digests.

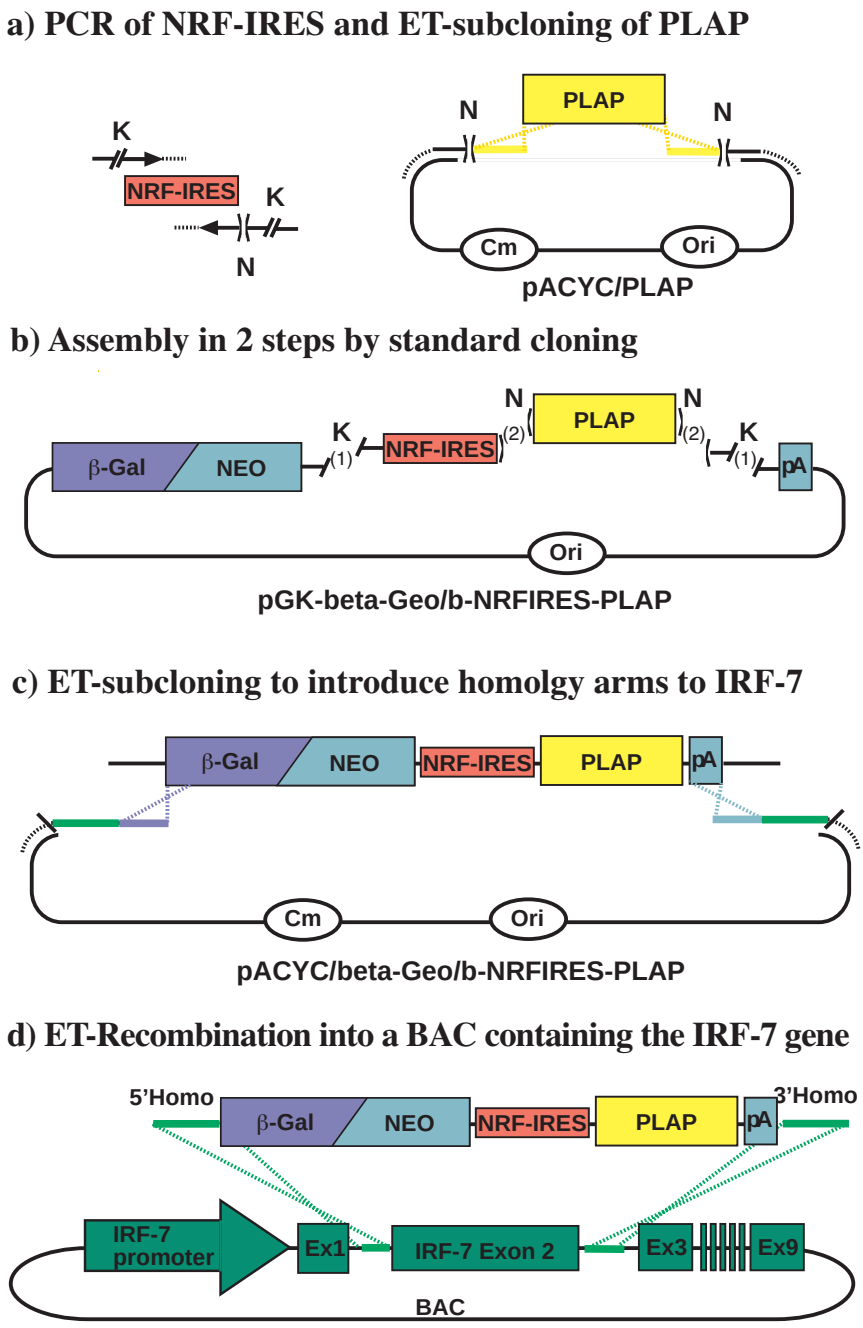

Fig. 3.18 Cloning strategy for the generation of an IRF-7 reporter transgene. (**a**) Proof reading PCR on the NRF-IRES and generation of the pACYC/PLAP plasmid by ET subcloning. (**b**) Two consecutive steps of conventional subcloning led to the generation of the pGK-betaGeo/b-NRFIRES-PLAP plasmid. i) Unique KpnI sites (K) contained in the PCR primers allow the assembly of pGK-betaGeo/b-NRFIRES. ii) This plasmid may be then linearized by NheI digest for the ligation of the ~1.6 kb NheI-PLAP fragment. (**c**) The linearized construct is ET-subcloned into pACYC plasmid backbone, which adds the homology arms required for (**d**) the integration into exon 2 of the IRF-7 BAC. Here the strategy for the generation of one variant of the construct (see Fig. 3.16b) is described. The other variants were generated following a similar strategy. Details on the modifications are described in the text.

3.7.5 Characterization of a BAC clone containing the IRF-7 gene

PCR on genomic DNA with the IRF-7 specific primers used in the RT-PCR experiments (#52 IRF7-up and #53 IRF7-do) yielded a 437 bp product. Subcloning and sequencing of the PCR product revealed two stretches identical with the published IRF-7 cDNA sequence separated by one small intron (87 bp). These primers were then used in a PCR-based screen of a Mouse BAC Library, performed by Research Genetics (Huntsville, Alabama). This screen yielded four positive BAC clones (396G1, 396H1, 443A15, 443B15). Glycerol stocks of the bacteria (strain DH10B) were mailed to our lab. PCR screening and Southern blot using the IRF-7 specific PCR product as probe was performed on several colonies of these clones. These screens revealed that only clone 396G1 contained the IRF-7 gene, all others were negative. Moreover, later it was noted that the original glycerol stock was contaminated with as second, unrelated BAC that did not contain the IRF-7 gene. A fresh glycerol stock containing only clone 396G1 was prepared and was used for further characterization.
Restriction digests of BAC DNA separated by agarose gel electrophoresis yielded a discrete band pattern. In combination with a Southern blot of the same gel, the bands containing parts of the gene of interest can be identified. For the Southern blot shown in Fig. 3.19 the IRF-7 specific PCR product was used as probe. Digestion of the IRF-7 containing BAC with various enzymes also allowed a rough estimate of the size of the BAC, about 110 kb, by summing up the sizes of the DNA bands. A ~3 kb fragment of the EcoRI digest and a 5.5 kb fragment of the HindIII digest were positive in the Southern blot and were isolated and subcloned into the pBluescript (Stratagene) vector. Of 19 minipreps 5 contained the HindIII insert and of 12 minipreps 7 contained the EcoRI insert as de as determined by IRF-7 specific PCR. The plasmids were called pBSIRF-7/HindIII and pBSIRF-7/EcoRI, respectively.

3.7.6 Homologous integration of the IRF-7 reporter constructs into the IRF-7 containing BAC

Several attempt were made to achieve the integration of any of the four versions of the construct into the IRF-7 BAC. However, despite intensive screening, positive recombinants were not obtained. Further attempts to obtain integration were postponed, in favor of the development of the IFN-α2 constructs described in the following, until an improved ET cloning plasmid (developed by Youming Zhang) would be available. The improved plasmid yields highly improved integration frequencies and has been filed for a patent.

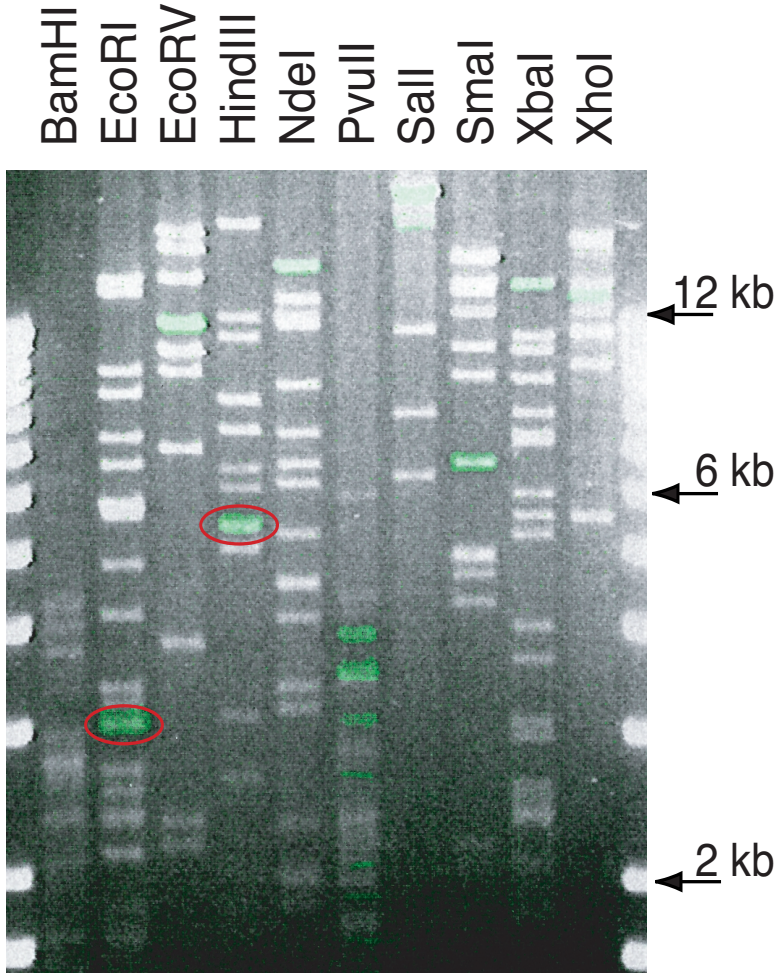

Fig. 3.19 Restriction digest of the IRF-7 BAC. The IRF-7 BAC was digested with the restriction enzymes indicated and bands were separated on a 0.7% agarose gel. The Southern blot (IRF-7 probe) of the same gel is superimposed. For better visibility, the bands of the blot light up in false color (green). Identifying positive bands allows a coarse mapping of the IRF-7 locus. The positive bands of the EcoRI and the HindIII digests (red circles) were isolated from a preparative gel and subcloned in pBluescript for further analysis.

3.7.7 Generation of the IFN-α reporter constructs

Schematic drawings of the assembly of all plasmids described in the following can be found in Fig. 3.20.

Generation of the pYZC/GFP plasmid. This plasmid was generated by ET-subcloning to endow the ORF of eGFP with homology arms required for the integration into the IFN-α2 BAC (Fig. 3.20 a, left panel). The PCR primers used on pACYC184 template were subGFP5 and subGFP3. Besides the homology arms, an additional frt-site followed by a unique BglII site was included in subGFP3. The PCR reaction was performed and then digested with DpnI to destroy residual pACYC184 template. The ~2 kb PCR product was purified by gel extraction. The pEGFP-N1 plasmid (Clontech) was digested with NotI and PstI. The ~800 bp fragment containing the eGFP-ORF was purified by gel extraction and coelectroporated with the PCR modified pACYC184 fragment into YZ300 cells. Bacteria expressing the recombined plasmid were selected on LB-Cm plates. 6 of 8 minipreps showed the expected fragments after Eco RI and XbaI digest.

Generation of the pYZC/IRES-beta-GeoK plasmid. This plasmid was generated by ET-subcloning to add frt site on the 3' end and BglII restriction sites at both ends of the IRES-beta-GeoK cassette (Fig. 3.20 a, right panel). The GeoK cassette contains an ORF that confers Kan-resistance. The PCR primers used on pACYC184 template were subGeoK5 and subGeoK3. The PCR reaction was performed and then digested with DpnI to destroy residual pACYC184 template. The ~2 kb PCR product was purified by gel extraction. The pGK/IRES-beta-GeoK plasmid (obtained from Youming Zhang) was BamHI digested. The ~4.8 kb IRES-beta-GeoK containing fragment was isolated by gel extraction and coelectroporated with the PCR modified pACYC184 fragment into YZ300 cells. Bacteria expressing the recombined plasmid were selected on LB-CmKan plates. Two of 12 minipreps showed the expected fragments after BglII digest.

Generation of the pYZC/GFP-IRES-beta-GeoK plasmid. This plasmid was assembled by standard cloning by ligating the BglII fragment of the pYZC/IRES-beta-GeoK plasmid into the BglII linearized and CIP treated pYZC/GFP plasmid (Fig. 3.20 b). Selection was done on LB-CmKan plates. 7 out of 14 minipreps showed ligation in the correct orientation as evidenced by Eco RI digest. Test digests using AscI and NotI yielded the expected ~5.5 kb fragment of the IFN-α2 reporter construct and a ~2 kb fragment of the pACYC plasmid backbone.

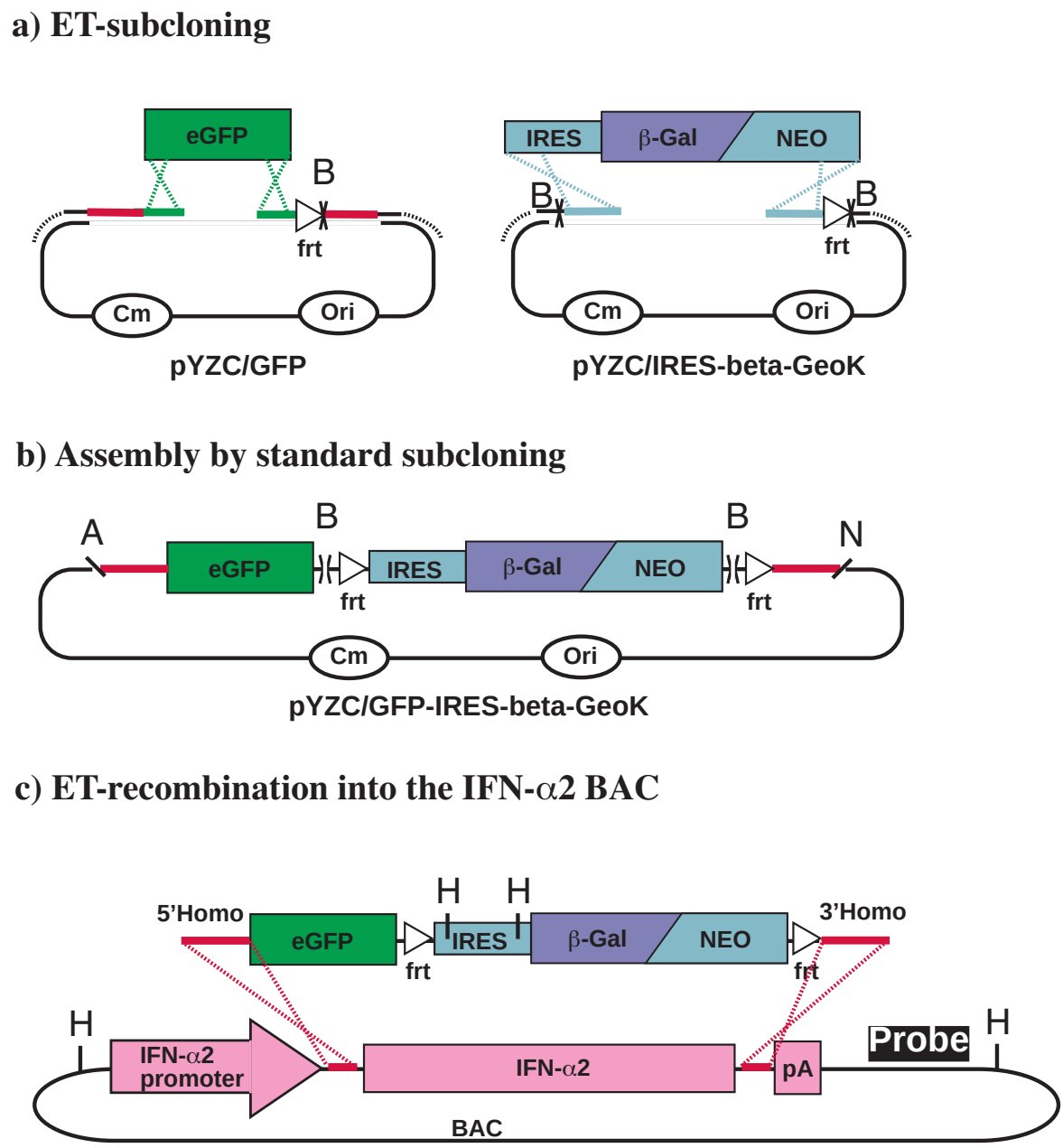

Fig. 3.20 Cloning strategy for the generation of an IFN-α2 reporter transgene. (**a**) Generation of the plasmids pYZC/GFP and pYZC/IRES-beta-GeoK by ET subcloning. Unique BglII sites (B) contained in the PCR primers allow the assembly of the pYZC/GFP-IRES-beta-GeoK plasmid by standard subcloning (**b**). The 5.5 kb fragment containing the reporter construct can be purified after digests with the rare cutting restriction enzymes AscI and NotI (A,N). (**c**) Site specific integration of the reporter construct by ET-recombination, replacing the IFN-α2 ORF in the BAC, can be verified by Southern blot using a 3' flanking probe on a HindIII (H) digest of the BAC.

3.7.8 Characterization of a BAC clone containing the IFN-α2 gene

Sequence alignment of published IFN-α cDNAs revealed that the IFN-α2 cDNA sequence contained unique stretches allowing for the generation of specific RT-PCR primers. Using the primer pair #26 IFNa2up (CTG TGC TTT CCT CGT GAT G) and #27 IFNa2do (CAG ATA CAG GCA TGG ATG TAC) a 729 bp PCR product could be amplified from mouse genomic DNA. Subcloning and sequencing of this PCR product confirmed the identity with the published IFN-α2 sequence. These primers were then used in a PCR-based screen of the BAC Mouse ES-129/SvJ (Rel. I) genomic library, performed by Genome Systems (now Incyte Genomics, St. Louis, Missouri). This screen yielded one positive BAC clone. An LB-agar stab of the bacteria containing this BAC clone (strain DH10B) was mailed to our lab. Confirmation that the BAC clone contained the IFN-α2 gene was obtained by IFN-α2 specific PCR followed by subcloning and sequencing of the PCR product.
For further characterization, DNA of the IFN-α2 BAC was digested with various restriction enzymes. The fragments were separated by agarose gel electrophoresis. Digestion of the IFN-α2 containing BAC with various enzymes allowed a rough estimate of the size of the BAC, about 80 kb, by summing up the sizes of the DNA bands.
Fig. 3.21 shows selected digests with the corresponding Southern blot probed with the IFN-α2 specific PCR product. In most digests 5 fragments were recognized by the probe indicating that up to five regions with high homology to IFN-α2 were contained in the BAC. To determine whether other functional IFN-α subtype genes were contained in the BAC, a PCR using the IFN-α consensus primers (see Fig. 3.4) was performed. The PCR product was subcloned and 24 clones were sequenced. Besides clones containing the IFN-α2 sequence, others containing four different IFN pseudogene sequences were observed. However, no clone of a further functional IFN-α subtype ORF was found.
The DNA bands that tested positive for IFN-α homology in the Southern blot were cut from a preparative gel and purified by gel extraction. IFN-α2 specific PCR on these fragments revealed that in the Eco RI digest a ~6 kb fragment and in the Hind III digest a 3 kb band contained the IFN-α2 ORF. The 3 kb fragment was subcloned in pBluescript (generating pBSIFNa2HindIII) and entirely sequenced by primer walking. The sequence revealed that the complete IFN-α2 ORF (920 bp) was contained in this fragment, preceded by 1.2 kb and followed by 1.4 kb regions. The 3' region contained an EcoRI restriction site. Together with the EcoRI site in the MCS of pBluescript, a 720 bp fragment could be excised and was used as probe in Southern blots. In contrast to the probes covering parts of the IFN-α2 ORF, this probe was specific and thus allowed the identification of fragments containing the IFN-α2 gene. This probe was used in the screens for the homologous integration of the reporter transgene.
Moreover, the subcloned Hind III fragment allowed testing of the IFN-α2 cloning strategy. Functionality of the homology arms of the 5.5 kb IFN-α2 reporter construct was verified by ET-recombination into the pBSIFNa2HindIII plasmid (pBSIFNa2HindIII+construct). To test the functionality of the frt sites, the plasmid containing the whole IFN-α2 reporter construct was transfected into FRT expressing bacteria. In all clones tested the 4.5 kb beta-GeoK cassette was excised as evidenced by analytic restriction digests and the loss of Kanamycin resistance.

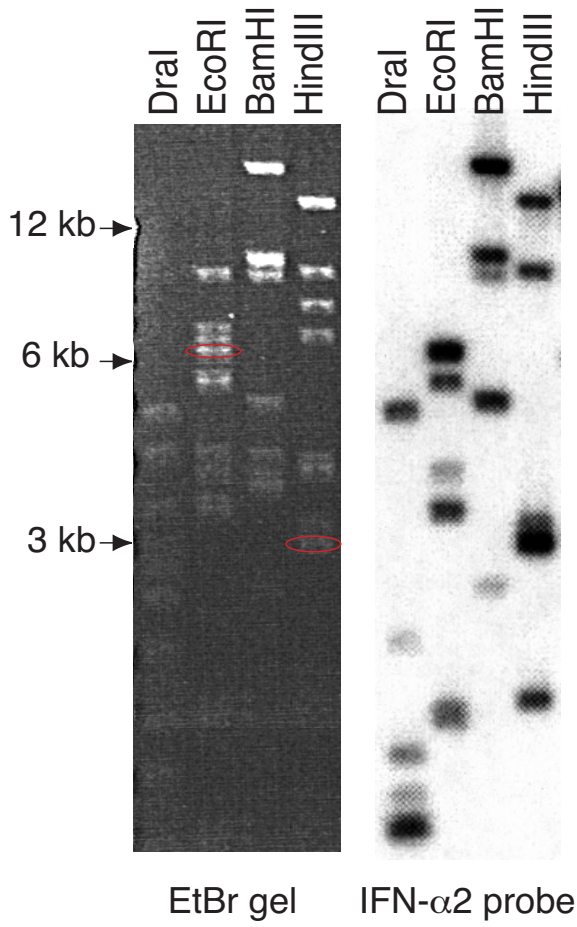

Fig. 3.21 The IFN-α2 BAC contains 5 regions highly homologous to IFN-α2. Southern hybridization of IFN-α2 BAC restriction fragments. A PCR product covering the IFN-α2 ORF was used as a probe. High homology between the IFN-α subtype genes apparently leads to cross hybridization. In most digests 5 fragments showed positive signals, indicating the presence of several genes homologous to IFN-α2 in the BAC. By PCR on gel extracted bands it was shown that the fragments producing the most intense hybridization signal (i.e. a 6 kb Eco RI and a 3 kb Hind III band, red circles) contained the IFN-α2 ORF.

3.7.9 Homologous integration of the IFN-α reporter construct into the IFN-α2 containing BAC

In order to obtain the recombinant IFN-α2 BAC, a ~5.5 kb fragment containing the reporter construct was purified after AscI/NotI double digest of the pYZC/GFP-IRES-beta-GeoK plasmid. This fragment was electroporated in ET-competent DH10B bacteria harboring both the IFN-α2 BAC and the pR6K/BAD/abg/Tet ET-recombination plasmid. Selection was performed on LB-CmKan plates. 43 minipreps were HindIII digested and analyzed on a 0.7% agarose gel. Positive clones were expected to show the characteristic 3 kb band shifted to 5.6 kb (see Fig. 3.22 and Fig. 3.20). 5 clones contained a 5.6 kb band, however, a band at 3 kb was still visible. To test, whether these clones contained the correct integration and whether the residual 3 kb band was an unrelated DNA fragment previously hidden as a

double band, a Southern blot from the same gel was hybridized using the EcoRI fragment 3' of the IFN-α2 gene as a probe. All 5 clones showed the expected band shift in the Southern blot. In the following, all five clones were partially sequenced to verify the integrity of the regions where the ET-recombination had taken place. As BAC DNA can't be readily sequenced, PCRs were performed on the BACs in the regions of interest. PCR products were then directly sequenced. All clones showed the correct DNA sequence.

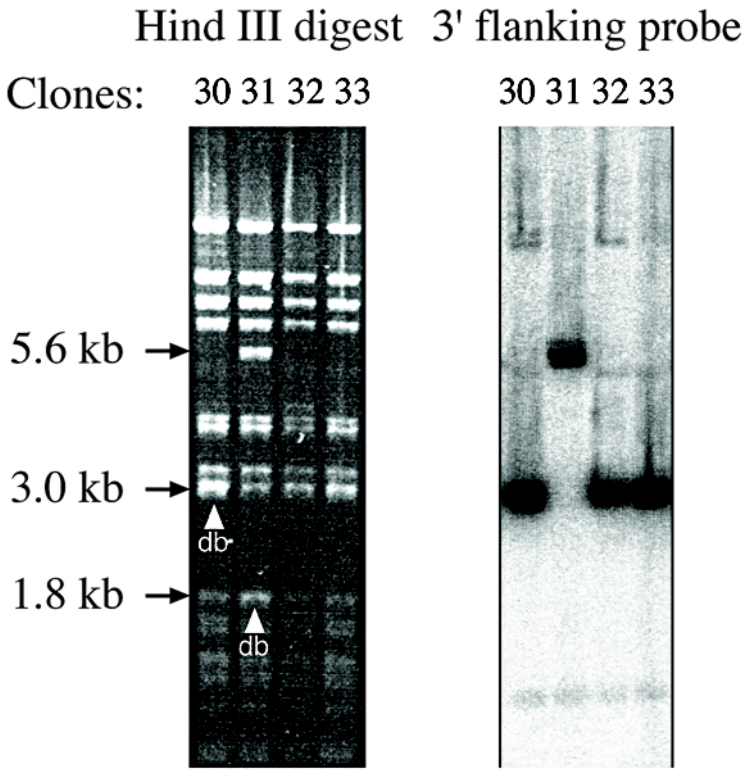

Fig. 3.22 Screening for ET-recombinant IFN-α2 BAC clones. BAC DNA was HindIII digested and fragments were separated on an agarose gel (left panel). Southern blot of the same gel was performed using the EcoRI probe specific for the IFN-α2 3' flanking region (right panel). As expected, recombinant fragments showed a characteristic shift from 3 kb to 5.6 kb (see also Fig. 3.20). In the agarose gel the WT 3 kb and the recombinant 1.8 kb fragments are visible as double bands (db).

To further validate that 5 correct integrations have been obtained and that the recombinant BACs are free of further alterations, a series of restriction digests were performed on these clones and on WT BAC to identify band shifts on agarose gels and in Southern blots. DraI, EcoRI, BamHI and Hind III digests were analyzed and blots were hybridized with the IFN-α2 screening PCR probe. The shifted bands and a correct distribution of the other bands were observed in both the agarose gels and the Southern blots.
DNA of one recombinant IFN-α BAC was then electroporated into Flp expressing bacteria in order to delete the frt-flanked IRES-beta-GeoK cassette. Of 18 minipreparations 3 showed the correct deletion as determined by HindIII digest followed by separation of the fragments on an agarose gel. As expected, these 3 clones also showed a loss of Kanamycin resistance.

Ultrapure maxipreparations of two recombinant IFN-α2 BAC clones and of all three recombinantΔfrt IFN-α2 BAC clones were prepared and reanalyzed after BglI restriction digest on agarose gels and by Southern blot. The EcoRI 3' UTR fragment (Fig. 3.23) and a GFP probe (Table 2.2) were used for hybridisation. All clones showed the correct band pattern. Recombinant BAC clone #42 and clone #12 of the Flp deleted BACs, the two clones yielding the highest DNA content in the maxipreparations, were selected for DNA microinjection into oocytes. These injections were performed using circular BAC DNA. Several attempts for microinjections were made by the Monterotondo transgene facility between February and July 2001, yielding 44 live born offspring. In the screening for transgenic founders at least 3 different transgene specific PCR reactions and appropriate controls were performed on each sample of genomic tail DNA (for details see chapter 2.6.9). However, none of the mice tested so far carried the transgene.

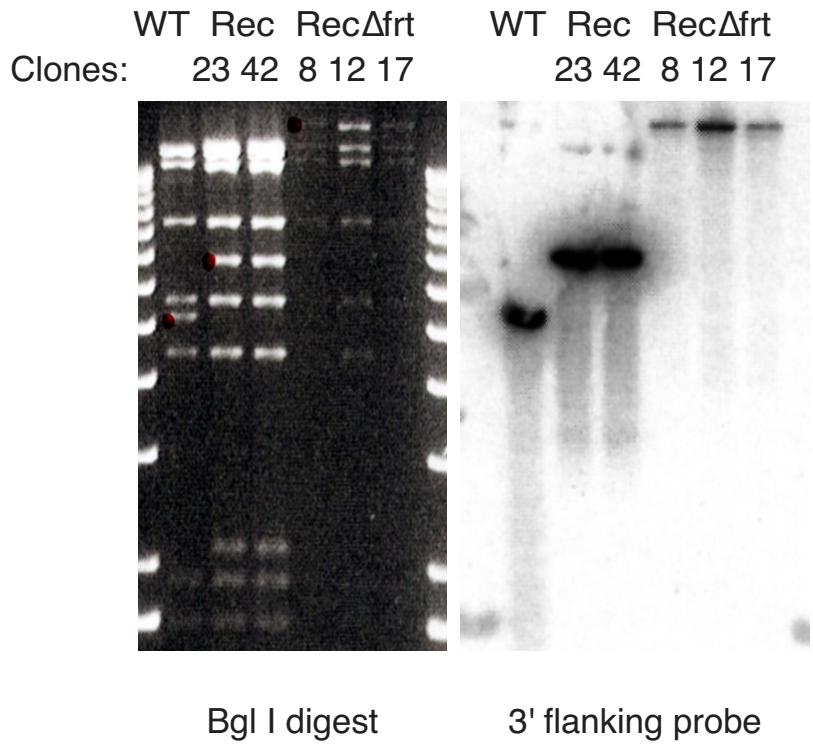

Fig. 3.23 Band shift confirms the integration of the reporter construct and Δfrt deletion of the IRES-beta-GeoK cassette. BAC DNA of WT, recombinant (Rec) and RecΔfrt clones was BglI digested and fragments were separated on an agarose gel (left panel). Southern blot was performed on the same gel and hybridized using the EcoRI probe specific for the IFN-α2 3' flanking region (right panel). Recombination replaced a BglI site in the IFN-α2 ORF, introducing a new BglI site in the betaGeoK cassette. Flp mediated deletion eliminated this BglI site leading to the band shifts observed. Shifted bands are labeled with a red dot.

In order to increase the chances of obtaining transgene positive founders it was decided to prepare NotI linearized BAC fragment (Fig. 3.24). The prepared BAC fragment was micro-injected by the Laboratory of George Kolias, Greece.

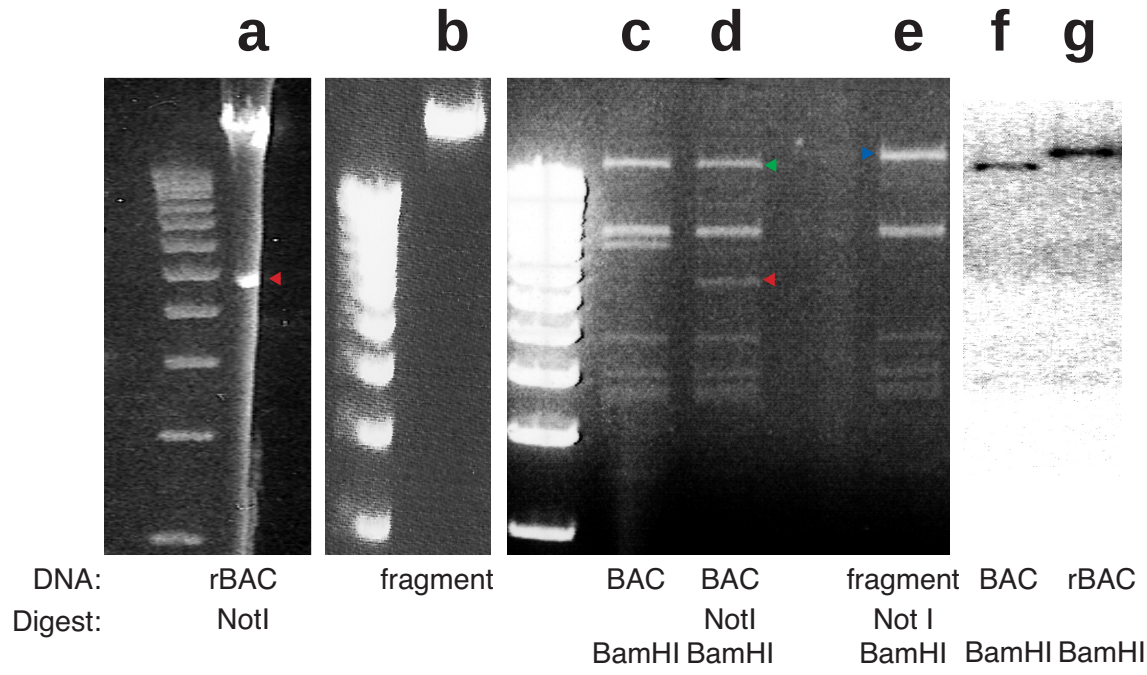

Fig. 3.24 Preparation and verification of recombinant IFN-α2 BAC fragment. (**a**) Preparative Not I digest of the recombinant IFN-α2 BAC (rBAC) clone #42. The lower band (red arrow) comprises the pBeloBAC11 backbone (~7 kb). The upper band contains the IFN-α2 reporter construct (> 70 kb) and was gel purified from an unstained part of the gel. (**b**) Analytic electrophoresis of the purified fragment. (**c,d**) Analytic digests of the 'wild type' IFN-α2 BAC (BAC) to verify that Not I cuts only twice and leaves the fragment containing the IFN-α2 ORF untouched (green arrow). (**e**) Analytic digest of the purified recombinant fragment. Note that the band containing the integration of the reporter construct is slightly shifted (blue arrow). The shift is also evident in a Southern blot comparing Bam HI digests of WT (**f**) and recombinant (**g**) IFN-α2 BAC. The EcoRI probe specific for the IFN-α2 3' flanking region was used for hybridisation.

3.8 Identification of the type I IFN producing cell (IPC) in the mouse

3.8.1 Colocalization of type I IFN with surface markers in histological sections

The phenotype of the major IFN producing cell in VSV pathophysiology is not known. Since the marginal zone is a complex tissue containing specialized macrophages, DCs, endothelial cells and non-recirculating B cells, and probably other cell types, colocalization studies with markers for marginal zone cells could not further resolve the nature of mouse IPCs (Fig. 3.25).

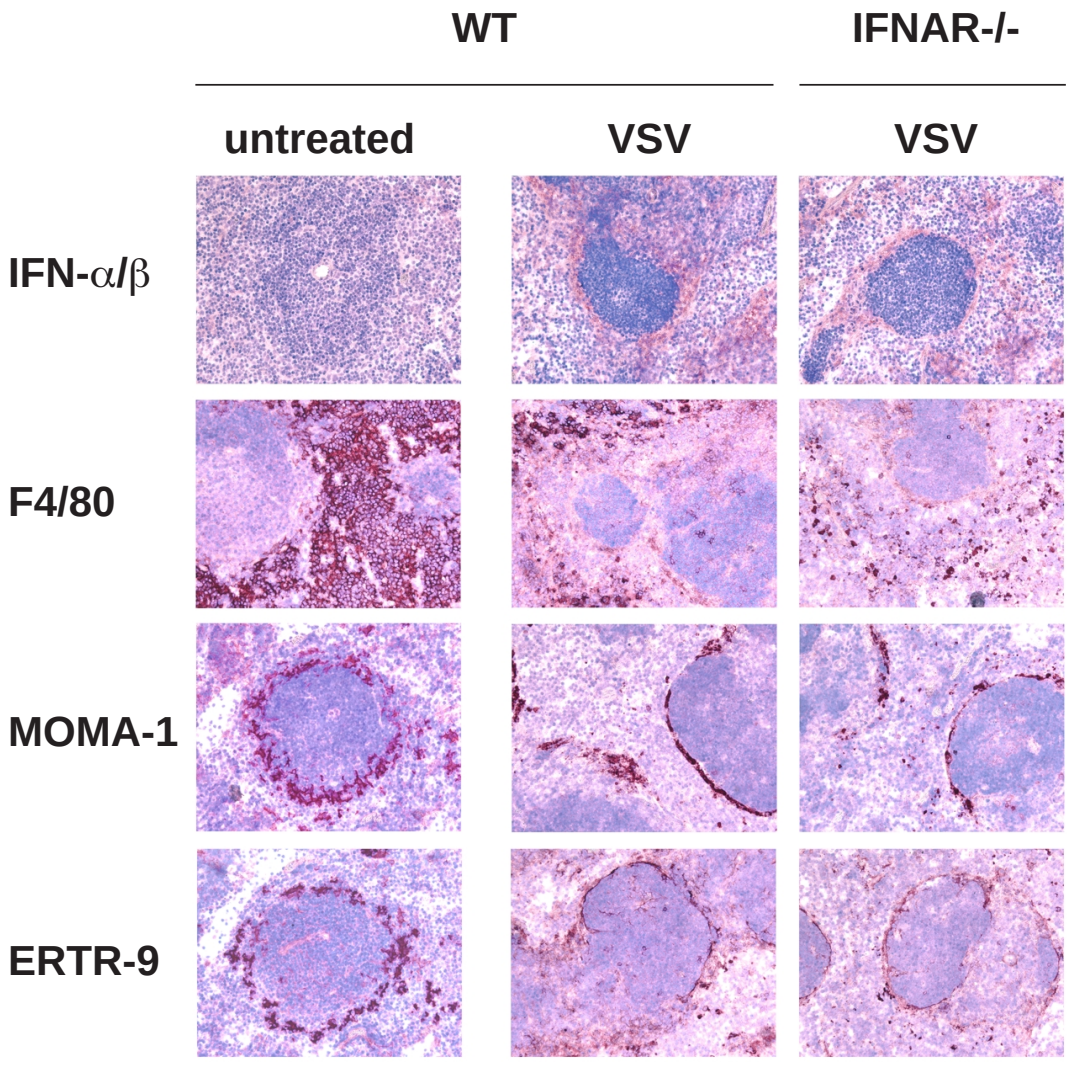

Fig. 3.25 Localization type I IFN production and of Macrophage populations in sections of untreated and VSV infected spleen. WT and IFNAR-/- mice were either left untreated or were infected for 12 h with 2 · 10^8 pfu VSV. Spleens were snap frozen and sections were analyzed cryo-histochemically with polyclonal serum against type I IFN or monoclonal antibodies against F4/80 (red pulp macrophages), MOMA-1 (metallophilic macrophages), and ERTR-9 (marginal zone macrophages). All specific stainings were visualized by the APAAP reaction (red). Sections were counterstained with hemalum (blue) to visualize lymph follicles. Note the dramatic changes of macrophage localization in the course of VSV infection.

3.8.2 By intracellular cytokine staining

In an attempt to directly identify the cells producing IFN-α by flow cytometry, spleens of untreated and VSV infected C57BL/6 mice were stained intracellularly with a monoclonal rat anti-mouse IFN-α antibody. In several experiments a minor population of IFN-α producing cells was identified. The intensity of the IFN staining in these cells was about 5 fold above background. IFN-α positive cells were observed at a frequency of 1/1000 - 1/700 in the spleens of 6h VSV infected mice, but not in spleens of untreated mice. The light scatter characteristics of this cell population showed a forward scatter significantly higher than lymphocytes and a low side scatter (data not shown). A similar FSC/SSC profile has been observed for human IPCs (Svensson et al., 1996).
However, probably due the complex staining protocol requiring an *in vitro* incubation step, the staining intensity was variable. Moreover, due to the fixation of the cells and the harsh washing conditions involving saponin, the staining of several surface markers was strongly reduced and for some surface antibody binding of the epitope was even lost totally.

3.8.3 FACSorting of dendritic cell subsets in the spleen

In a third approach we aimed at identifying the phenotype of the mouse IPC in VSV pathophysiology by FACSorting of cell subtypes classified by differential expression pattern of surface markers. In analogy to the DC origin of human and mouse IPCs (Asselin-Paturel et al., 2001; Cella et al., 1999; Nakano et al., 2001; Siegal et al., 1999) we focused on the analysis of mouse DC subsets. Mice were VSV infected and 9 h later several $CD11c^+$ DC subsets were MACS enriched, FACS-sorted and then analyzed for the IFN-α mRNA content (Fig. 3.26).

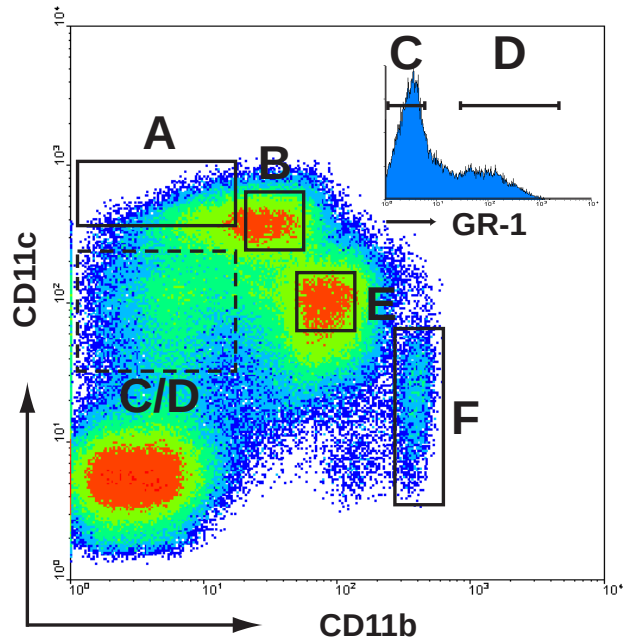

Fig. 3.26 FACSorting scheme of DC fractions. MACS enriched CD11c$^+$ cells were stained with anti-CD11c-Biot./Str.-APC, anti-CD11b-FITC, and anti-GR-1-PE and DC subsets were FACSorted using the indicated gates A-F. Cells from gate C/D were further subdivided by separating GR-1$^-$ (fraction C) and GR-1$^+$ cells (fraction D). DC subsets from the spleen were sorted and total RNA was prepared and analyze by RT-PCR. The RT-PCR results are shown in the following figures.

Surprisingly, only CD11c^{int}CD11b$^-$GR-I$^+$ DCs (fraction D) were strongly positive for IFN-α mRNA, whereas neither lymphoid DCs (CD11c$^+$CD11b$^-$, fraction A), myeloid DCs (CD11c$^+$CD11b$^+$, fraction B), CD11c^{int}CD11b$^+$ DCs (fraction E), nor granulocytes (CD11c$^+$GR-1$^+$, fraction F) showed high IFN-α expression (Fig. 3.27). CD11c^{int}CD11b$^-$ DCs (fraction C) showed slightly enhanced IFN-α mRNA levels (which were at least 125 fold lower than those of fraction D), that might be due to contaminating cells of fraction D. A similar result was obtained from sorted fractions of UV-HSV infected mice. While all other sorted fractions remained negative, and fraction C showed a minor signal, the cells in fraction D strongly expressed IFN-α mRNA (data not shown).

We next asked, whether CD11c^{int}CD11b$^-$GR-I$^+$ cells are producers of IFN-α independent of IFNAR feedback signaling. For this purpose DC subsets were isolated from VSV infected IFNAR-/- mice. Again only CD11c^{int}CD11b$^-$GR-I$^+$ cells showed high-level IFN-α mRNA (Fig. 3.28). These results indicate that although other DC subsets are able to produce IFN-α upon *in vitro* stimulation (Hochrein et al., 2001), they do not play a major role in IFN-α production after VSV infection *in vivo*.

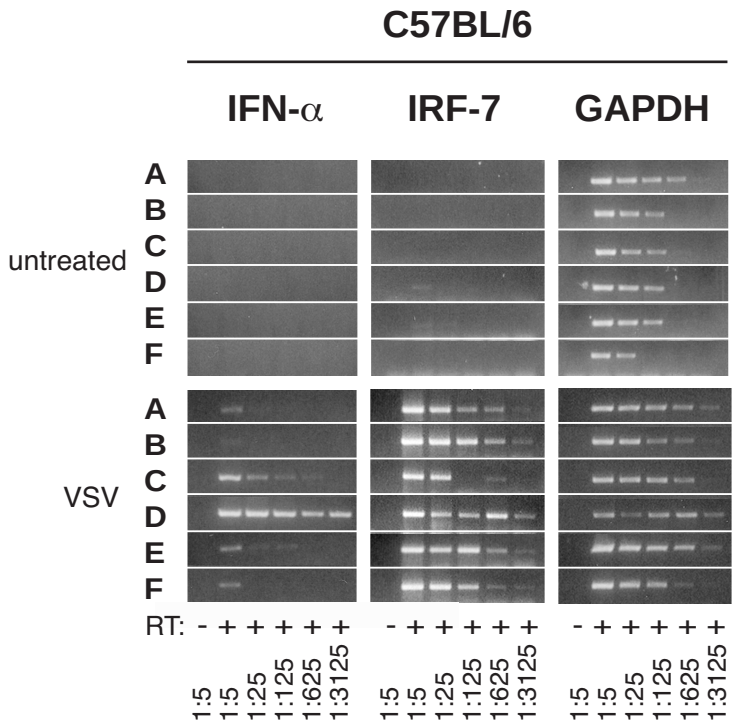

Fig. 3.27 In VSV infected mice CD11c^{int}CD11b^{-}GR-1^{+} DCs express high-level IFN-α. C57BL/6 mice were either left untreated or i.v. infected for 9h with $2 \cdot 10^8$ pfu VSV. Splenic CD11c^{+} cells were enriched by magnetic cell adsorption and fractions A-F were FACSorted as described in Fig. 3.26. Total RNA of about 4-$10 \cdot 10^4$ sorted cells was prepared and analyzed by RT-PCR as described in Fig. 2.1.

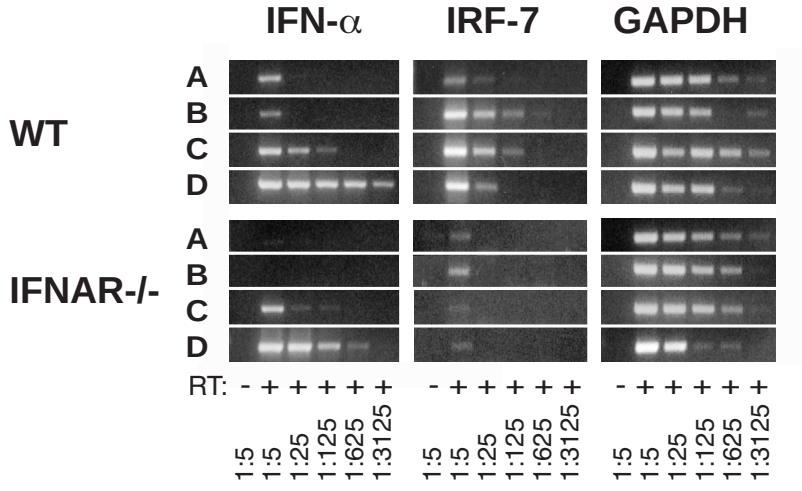

Fig. 3.28 IFN-α production by CD11c^{int}CD11b^{-}GR-1^{+} DCs is independent of IFNAR feedback, Sv129 (WT) and IFNAR-/- mice were i.v. infected for 9h with $2 \cdot 10^8$ pfu VSV. Splenic CD11c^{+} cells were enriched by magnetic cell adsorption and fractions A-D were FACSorted as described in Fig. 3.26. Total RNA of about 4 - $10 \cdot 10^4$ sorted cells was prepared and analyzed by RT-PCR as described in Fig. 2.1.

To determine the pattern of IFN-α subtypes expressed by VSV stimulated WT and IFNAR-/- IPCs, the IFN-α PCR product of $CD11c^{int}CD11b^{-}GR\text{-}1^{+}$ DCs (Fraction D) was subcloned and the DNA sequence of several clones was determined. This analysis revealed that the IPCs of both WT and IFNAR-/- mice expressed a broad spectrum of IFN-α subtypes and that they showed abundant expression of IFN-α2 and IFN-α5. However, compared to WT controls, the expression of several IFN-α subtypes were slightly underrepresented in IPCs isolated from mice incapable of type I IFN receptor feedback.

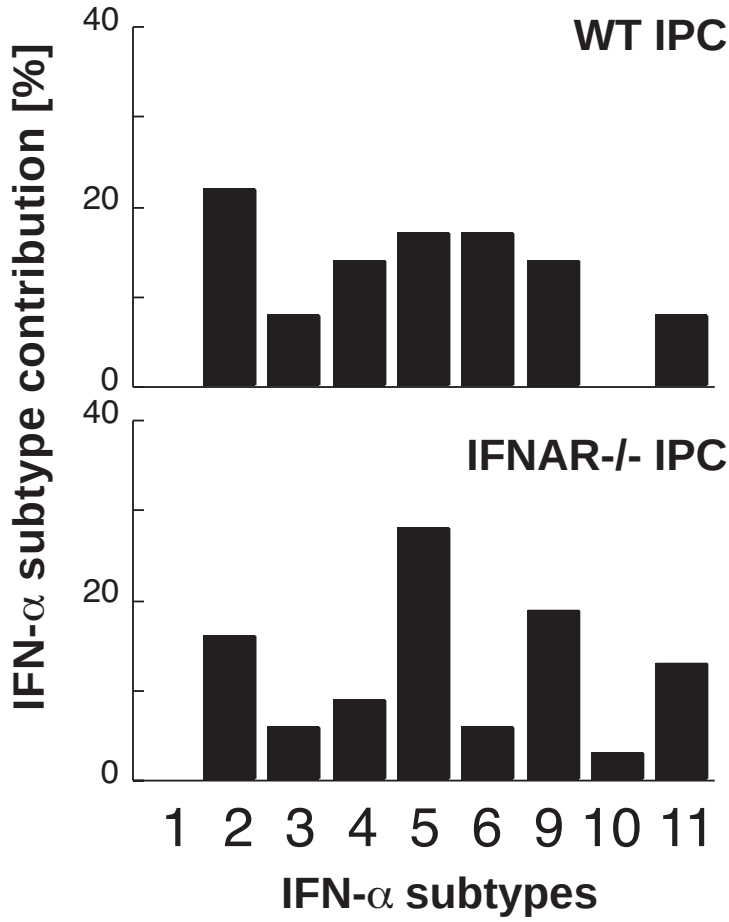

Fig. 3.29 IPCs isolated from VSV infected mice express a broad spectrum of IFN-α subtypes. PCR products of the IFN-α expression analysis 9 h after VSV infection of IPCs sorted from the spleens of WT or IFNAR-/- mice were subcloned. DNA sequence of 36 and 32 single clones was analyzed, respectively. IFN-α sequences were classified according to EMBL database entries. The sequence termed IFN-α10 corresponds to the IFN-αB sequence available on the EMBL database (accession No. L38698).

3.9 Phenotype of the murine IPC

Sorted mouse IPCs rapidly died in cell culture. Less than 20% of the cells survived o.n. culture at 37 °C. Survival could not significantly be enhanced by the addition of cytokines or inducers of maturation such as IL-3, IFN-α, VSV, UV-HSV or poly(I:C) (data not shown). In cytospins, freshly sorted IPCs from the spleens of C57BL/6 mice showed a homogenous morphology, characterized by round shape, smooth surface and eccentric nucleus (Fig. 3.30). These cells were highly similar to human plasmacytoid dendritic cells except that uninduced mouse IPCs only rarely showed dendritic outgrowths. Most recently it has been reported, however that mouse IPCs rapidly develop dendrites after stimulation with CpG DNA (Nakano et al., 2001).

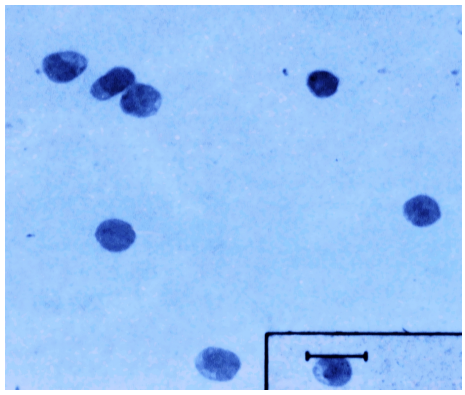

Fig. 3.30 Morphology of sorted mouse IPCs ($CD11c^{int}CD11b^{-}GR\text{-}1^{+}$ DCs). $CD11c^{int}CD11b^{-}GR\text{-}1^{+}$ cells were FACSorted from spleens of C57BL/6 mice as described in Fig. 3.26. Cells were May-Grünwald Giemsa stained and photographed at 40x. Measure indicates 10 µm.

To analyze the surface markers expressed, the IPC population within $CD11c^{+}$ enriched cells could be identified by staining with any two of the fluorescent markers CD11b, CD11c, Ly6C/Gr-1, B220. The gated population, combined with a morphological gate (FSC/SSC), was 75% - 97% pure as assessed by staining with another of the above markers as a third fluorochrome. Best data homogeneity was obtained by screening the $CD11c^{+}$ $Ly6C^{+}$ or the $CD11b^{-}$ $Gr\text{-}1^{+}$ population for expression of B220 as the third fluorochrome (data not shown). The data shown in the following figures were obtained with both marker combinations mentioned above.
To differentiate surface marker expression of the splenic $CD11c^{+}Ly6c^{+}$ IPC and the $CD11c^{+}Ly6c^{-}$ DC population, MACS purified $CD11c^{+}$ cells were stained with a selection of monoclonal antibodies (Fig. 1). Mouse IPCs lacked the expression of lineage markers of B cells (CD19), T cells (CD5), myeloid cells (CD11b) and NK cells (DX5). In contrast to splenic DCs, IPCs stained strongly positive for B220, and > 80% were positive for CD90 and Sca-1. IPCs of the mouse were negative for the expression of IL-3R, F4/80 and CD62L, and showed a characteristic bimodal distribution for CD4 expression. Interestingly, Gr-1 on IPCs could not be costained with Ly6C. Taking the known cross-reactivity of the Gr-1 mAb with the Ly6C antigen into consideration, this suggests that on IPCs both antibodies compete for the same epitope, and that the Ly6C mAb showed the higher binding affinity.

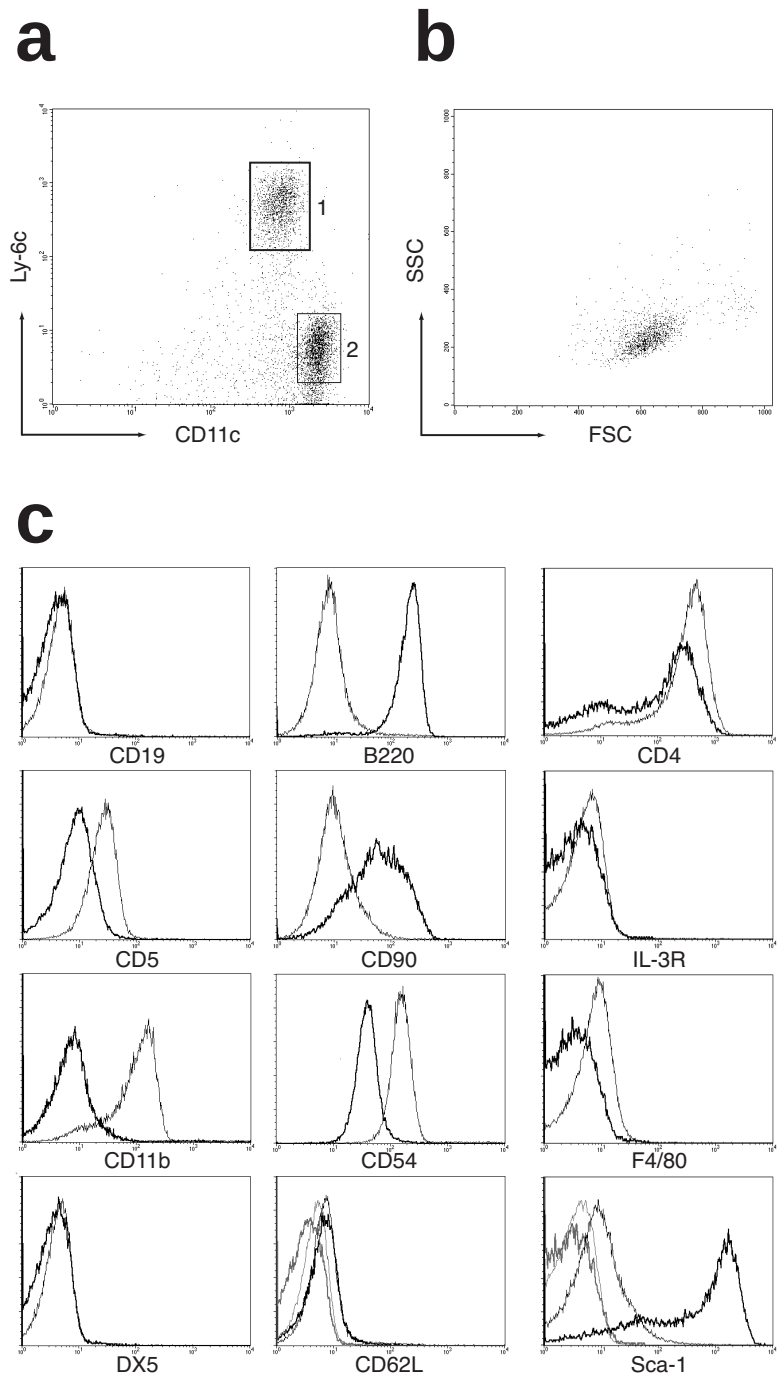

Fig. 3.31 Comparison of surface marker expression on splenic CD11c$^+$ Ly6C$^+$ IPCs and CD11c$^+$ Ly6C$^-$ DCs. CD11c$^+$ spleen cells of Sv129 mice were obtained by MACS sorting and stained with anti CD11c, Ly6C and the mAbs indicated. Numbered squares in (**a**) indicate the gates used in combination with a morphological gate (FSC/SSC) for the subsequent analysis of the IPC (1/bold line) and DC (2/hairline) fraction. Panel (**b**) shows the FSC/SSC distribution of IPC cells from gate 1. Profiles in (**c**) show stainings with FITC-conjugated mAbs (Ly6C-PE) in the left and middle column while the histograms on the right where obtained using PE-conjugated mAbs (Ly6C-FITC). Grey lines represent staining with IgG2a isotype controls. All panels are representative of at least 3 independent analyses.

3.10 Properties of the murine IPC

As described above, sorted IPCs showed poor survival in cell culture *in vitro*. To estimate the IPC half-life *in vivo*, i.e. how quickly the IPC population is renewed in the spleen and the bone marrow, naive Sv129 mice were continuously treated with BrdU. At different time points BrdU incorporation was monitored by FACS analysis of $CD11c^+$ enriched cells and the percentage of BrdU positive cells was determined (Fig. 2). In the spleen more than 75% of $CD11c^+$ $Ly6C^+$ IPC were BrdU positive after 15 days of continuous labeling. In the bone marrow the plateau level of > 75% BrdU positive cells was reached significantly earlier, i.e. already after 6 days. Moreover, BrdU incorporation had a rapid onset in bone marrow IPC, while the splenic IPC population showed a 3 - 5 day lag period before BrdU positive cells accumulated. This suggests an influx of approximately 6 - 7% bone marrow derived IPCs into the spleen per day.

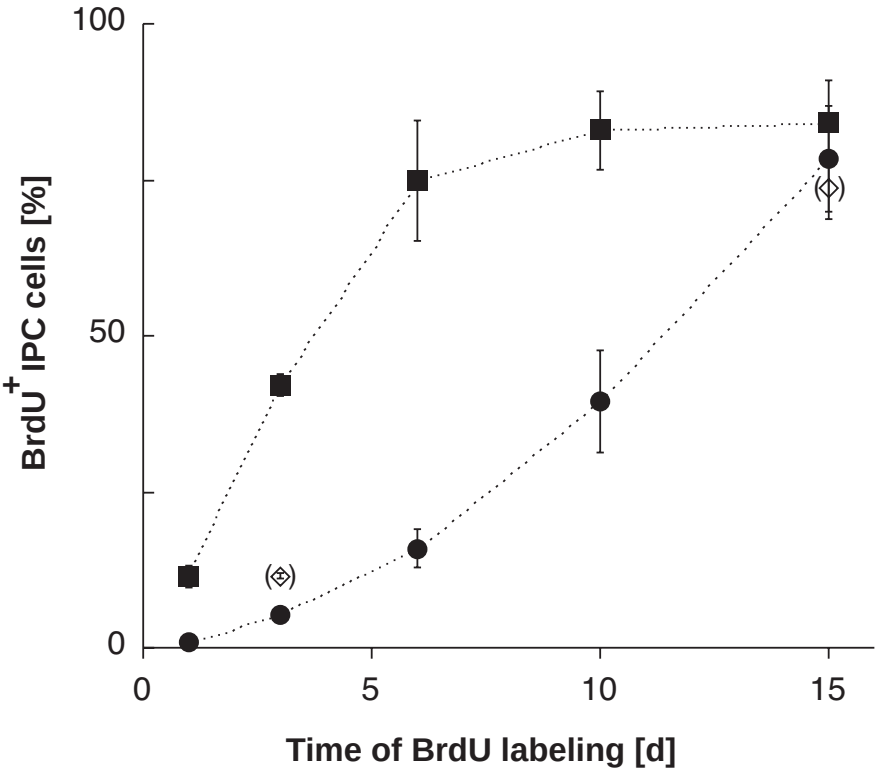

Fig. 3.32 IPC renewal in the bone marrow occurs at a higher rate than in the spleen. For *in vivo* BrdU labeling, Sv129 mice were injected with 1 mg BrdU and subsequently fed with drinking water containing 1 mg/ml BrdU. At the time points indicated MACS sorted $CD11c^+$ spleen or BM cells were fixed and stained with anti-BrdU mAb. IPCs from the spleen (circles) or BM (squares) were identified by CD11c/Ly6C and independently by CD11b/Gr-1 staining. For d3 and d15 the proportion of BrdU positive splenic DCs are shown (in brackets). Each data point represents the mean of 2 analyses and of samples derived from 2-3 mice.

To analyze the properties of IPCs and $CD11c^+$ DCs of the spleen in response to viral infection, we analyzed the expression activation markers and costimulatory molecules involved in APC function 9h after infection with VSV. Expression of the early activation marker CD69 was strongly induced in activated IPCs. Equally, MHC class II and CD 86,

the activation induced costimulatory molecule, were upregulated in both IPCs and DCs. Interestingly, and in contrast to DCs, upregulation of these molecules on IPCs was found to be highly dependent on type I IFN receptor signaling. This hints at differential use of signaling pathways that govern receptor upregulation in DCs and IPCs. After the short term *in vivo* stimulation analyzed here, only minor changes were monitored in stainings for CD40 and CD80 in both IPCs and DCs (data not shown).

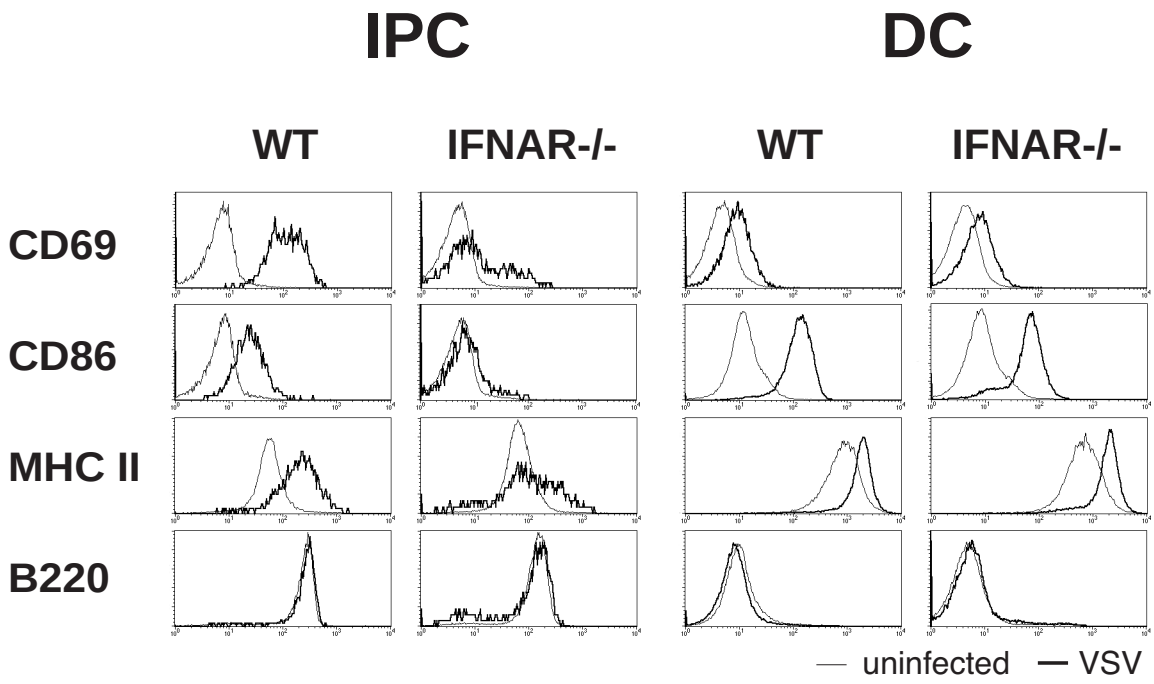

Fig. 3.33 In contrast to classical DCs, upregulation of activation markers on IPCs is IFNAR dependent. WT and IFNAR-/- mice were left untreated (hairline) or injected with $2 \cdot 10^8$ pfu VSV (bold line). Nine hours later, $CD11c^+$ spleen cells were isolated by MACS sorting and the expression of CD69, CD86 and MHCII was analyzed on IPCs or classical DCs. IPCs and DCs were discriminated by anti CD11c/Ly6C(PE) staining, as described in Fig. 3.31. Staining with B220 is used as a control for the purity of the cell fraction analyzed. Results are representative of three independent experiments.

Within the $CD11c^+$ enriched spleen cells, prepared from Sv129 mice at various time points after infection, we observed a highly variable percentage of IPCs ranging from 16% to less than 2% towards later time points after infection (data not shown). To further analyze and quantify the reduced IPC abundance after VSV infection, we developed a protocol to directly determine IPC counts for various tissues of Sv129 mice using two-color immunofluorescence flow cytometry. Freshly prepared single cell suspensions were stained with a mixture of FITC-conjugated antibodies to lineage markers (CD5, CD11b, CD19, DX5) and Ly6C-PE (Fig. 3.34 a). The purity of the gated lineage negative, Ly6C positive IPC population was monitored using CD11c or B220 as a third fluorochrome. Purity was > 80% for most tissues tested (Fig. 3.34 c).

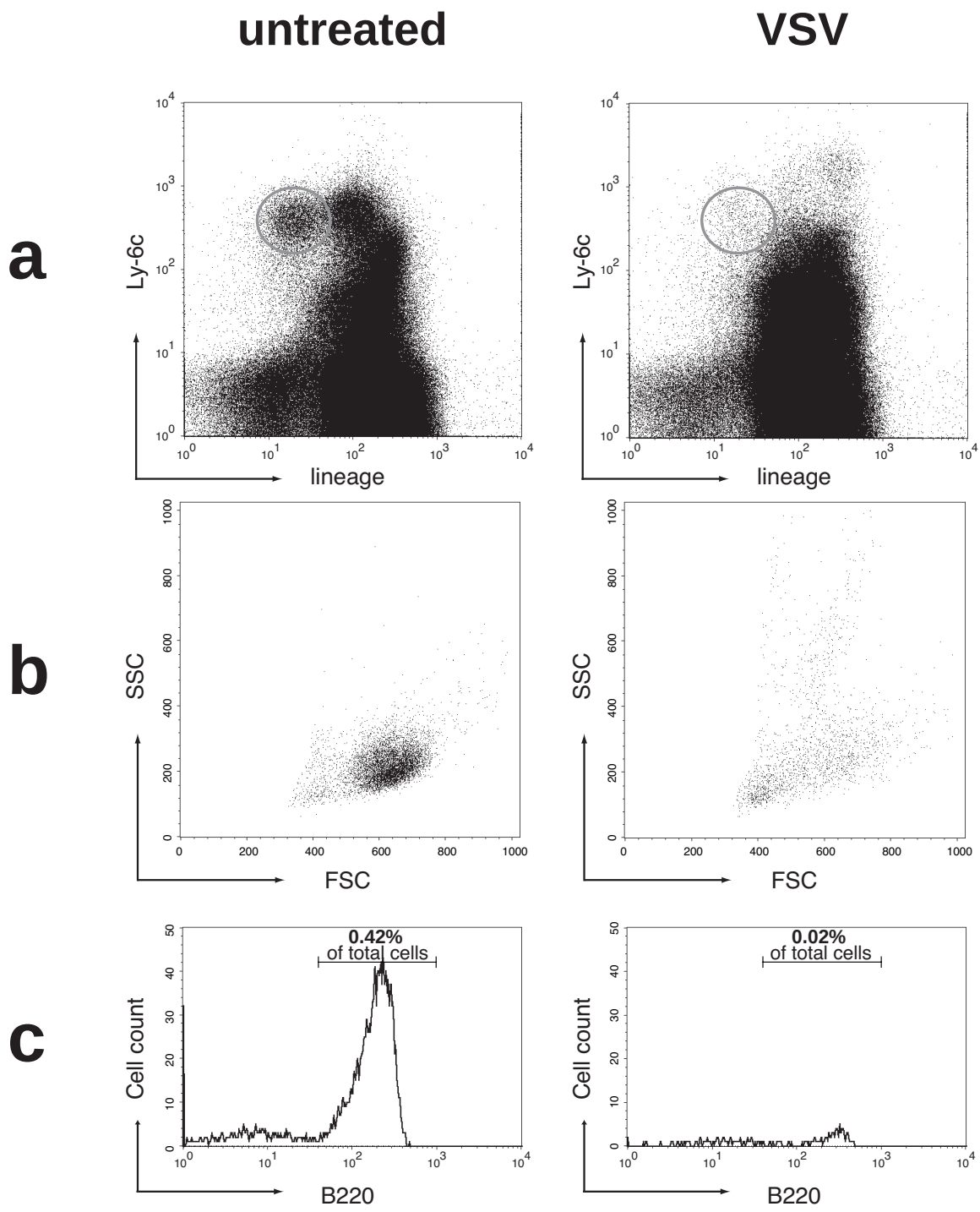

Fig. 3.34 The number of IPCs is drastically reduced in the spleens of acutely VSV infected mice. Sv129 mice were left untreated or infected with $2 \cdot 10^6$ pfu VSV. 18 hours later spleen cell suspensions were prepared and were stained with Ly6C, B220, and FITC-conjugated CD5, CD11b, CD19 and DX-5 mABs (lineage). Panels in (**a**) show 10^6 ungated cells. Thresholds were set to exclude RBCs and cell debris**.** Gated events (grey circle) are shown in (**b**) as FSC/SSC distribution. The proportion of IPCs indicated in (**c**) as % of total cells was determined by gating on lineage nevative $Ly6C^+B220^+$ cells that showed a FSC/SSC distribution characteristic for IPCs.

Relative IPC counts for selected tissues are shown in Fig. 3.35 were determined by gating on lineage negative, $Ly6C^{+}B220^{+}$ cells in combination with a morphological gate (FSC/SSC, Fig. 3.34 b). In uninfected Sv129 mice high IPC counts were found in the liver and bone marrow as well as in the lungs and spleen (0.8% – 0.4% of total cells, respectively). Peripheral LN and similarly mesenteric LN, Peyers patches and kidneys showed IPC frequencies of about 0.2%. IPC counts < 0.1% were monitored in the thymus, PBLs and peritoneal cavity cells (Fig. 3.35 and data not shown). Within 18h after injection of $2 \cdot 10^6$ pfu VSV we observed an up to 10 fold decrease in IPC counts in secondary lymphoid organs, especially in the spleen and peripheral LNs. In other peripheral organs, i.e. the liver and lungs of infected animals, rather a slight increase in IPC counts was observed. IPCs counts in the spleen and LN were similarly reduced in infected IFNAR deficient mice. Of note, however, are the drastically opposite trends of IPC counts in the bone marrow of VSV infected IFNAR-/- mice as compared to Sv129 WT mice. A tentative explanation for the observed phenomenon could be IPC efflux from the bone marrow, as well as from secondary lymphoid tissue, is triggered by an IFNAR independent signal, while IPC differentiation from a bone marrow precursor is induced by IFNAR signaling.

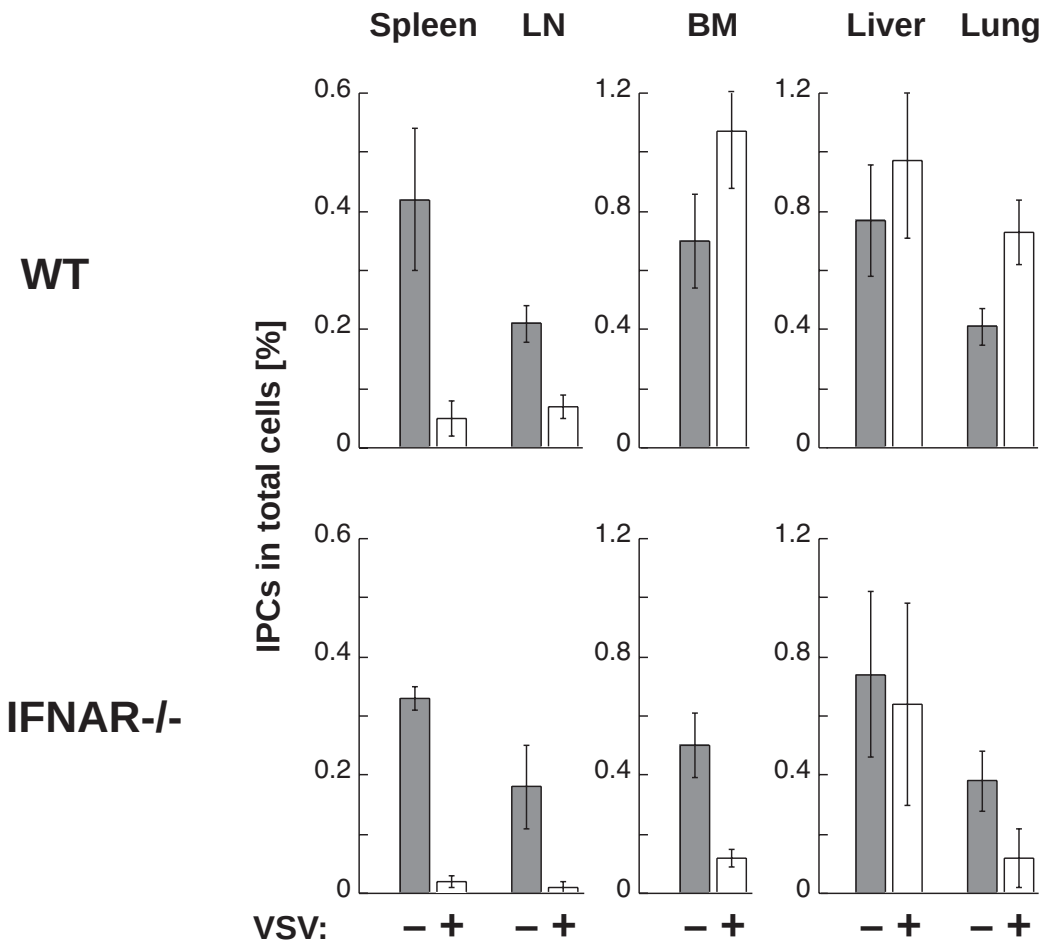

Fig. 3.35 Tissue distribution of IPCs before and after VSV infection. Sv129 and IFNAR-/- mice were left untreated or were infected with $2 \cdot 10^6$ pfu VSV 18 h previously. Cell suspension from the organs indicated was prepared and IPC counts were determined cytometrically as described in Fig. 3.34. Data are means (± sdev) of samples from 3–6 mice.

In order to analyze IPC homeostasis in untreated mice and to study IPC disappearance early after virus infection and the conditions of IPC repopulation at later time points, we monitored the accumulation of BrdU positive IPCs in naïve and VSV infected mice. Compared to untreated mice, the IPC renewal in the bone marrow of VSV infected mice was significantly enhanced (Fig. 3.36), eventually leading to increased IPC counts that were maintained for several days of VSV infection (Fig. 3.35 and data not shown). Following the IPC loss observed in the spleen early after infection, the spleen was gradually repopulated. The IPC population found in the spleen tree days after infection already contained a more than 6 fold increased number of BrdU positive cells as compared to uninfected control mice, suggesting that spleens are repopulated with IPCs from the bone marrow during the recovery phase from acute viral infection.

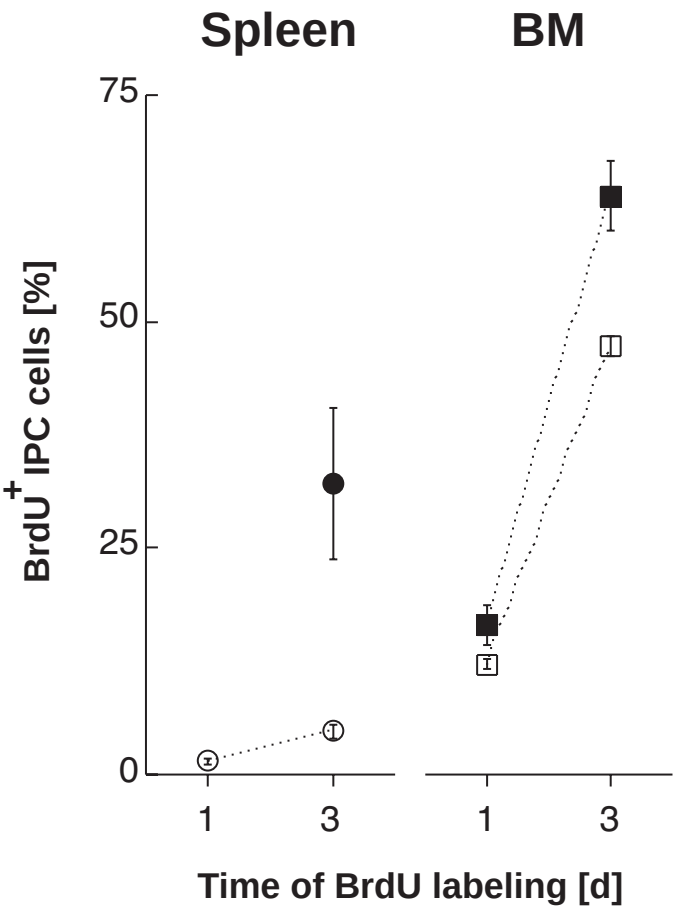

Fig. 3.36 IPC turnover is enhanced in the spleens of mice recovering from acute VSV infection. Sv129 mice were injected i.p. and thereafter fed in the drinking water with BrdU. At the same time the mice were infected with $2 \cdot 10^6$ pfu VSV (filled symbols) or were left uninfected (open symbols). The proportion of BrdU positive IPCs was determined cytometrically as described in Fig. 3.32.

4 Discussion

4.1 Virus induced IFN-α production in the absence of feedback signaling *in vivo*

Despite extensive *in vitro* studies, the role of type I IFN receptor (IFNAR) feedback signaling in viral pathogenesis *in vivo* has not been assessed previously. We show that after viral infection of mice not only IFN-β but also IFN-α is produced immediately and largely independent of IFNAR feedback signaling. This is in contrast to the current model of IFNAR feedback-dependent expression of IFN-α, that was established based on experiments with cultured cells *in vitro*. To reconcile the previous *in vitro* data with our *in vivo* observations, we hypothesized that after viral infection of mice a cell type different from fibroblasts, i.e. the murine IPC, produced the majority of type I IFN, and that in these cells IFN-α expression was regulated differently than in fibroblasts. Indeed, we found that after *in vivo* infection the subset of $CD11c^{int}GR\text{-}1^{+}$ dendritic cells produced IFN-α at high level, and that early IFN-α production by this cell type was largely independent of IFNAR feedback.

The positive feedback regulation of IFN-α genes was first observed in NDV infected MEFs that lack IFN-α expression in the absence of a functional IFN signaling cascade (Harada et al., 1996; Sato et al., 1998). One study showed IFNAR independent IFN-α4 expression in NDV infected MEFs (Marie et al., 1998). Interestingly, IFN-α4 was previously found to dominate IFN-α responses of NDV stimulated L929 fibroblasts (Hoss-Homfeld et al., 1989). However, MEFs infected with VSV (Fig. 3.1, 3.3), or vaccinia virus (Deonarain et al., 2000) showed a strictly IFNAR dependent expression of all IFN-αs. Equally, Sendai virus infected MEFs from IFN-β deficient mice were found unable to produce any IFN-α, unless stimulated by the addition of exogenous IFN-β (Erlandsson et al., 1998).

In contrast to these *in vitro* data, we found that VSV infected mice mount an early IFNAR-independent IFN-α response. Furthermore, IFN-β deficient and IFN-β/IFNAR double-deficient mice treated with UV-HSV still expressed substantial IFN-α levels (Fig. 3.6). While IFN-α production in IFN-β-/- mice could have been promoted by priming with natural type I IFN, produced pathogen-independently (Taniguchi and Takaoka, 2001), IFN-α production in IFN-β/IFNAR double-deficient mice indicated, that IFNAR triggering was not a prerequisite for early IFN-α production. IFN-α levels reached in IFN-β-/- were sufficient to control intravenous VSV infection (data not shown). In contrast, IFN-β deficient mice infected peripherally with vaccinia virus showed a markedly increased susceptibility to lethal disease (Deonarain et al., 2000): following intranasal infection, IFN-β-/- mice showed up to 10^5 fold increased virus titers in the lung as compared to WT mice, and eventually succumbed to the infection. Interestingly, in these experiments virus titers in spleen of WT and IFN-β-/- mice were comparably low, indicating that upon local infection vaccinia virus replication was better controlled in the spleen than in the

peripherally infected organ. Thus, it appears that depending on the route of infection virus may activate IPCs or other susceptible cell types that differ in their requirement of IFNAR feedback for the IFN-α induction.

Apart from the route of infection also the nature of the stimulus may determine the cell type(s) involved in type I IFN production (Levy, 2002). Our histology data show that poly(I:C) does not induce marginal zone IPCs to produce high-level type I IFN, suggesting that the observed IFN titers were contributed mainly by non-IPCs. It is possible that in analogy to the human plasmacytoid DC, mouse IPCs express TLR-9 but not TLR-3 that is involved in poly(I:C) recognition (Alexopoulou et al., 2001; Kadowaki et al., 2001), and thus mouse IPCs are not triggered by poly(I:C). IFN titers in poly(I:C) treated mice showed an early peak of IFN-β expression that only in animals with a functional receptor-feedback was followed by sustained IFN-α expression. This indicated that similar to *in vitro* VSV infected MEFs, IFN-α expression by non-IPCs *in vivo* required IFNAR feedback signaling.

In the current model of positive feedback regulation, IFNAR dependent upregulation of the transcription factor IRF-7 plays a central role. Virus treated mutant MEFs that failed to induce IRF-7 also lacked expression of IFN-α. The IFN-α response could be restored by ectopic expression of IRF-7 (Sato et al., 1998). In IFNAR deficient mice, we observed early IFN-α responses in the absence of detectable IRF-7 upregulation. One possibility is that under these conditions low constitutive IRF-7 levels suffice to drive early IFN-α expression. In this context it is worth noting that in all RT-PCR experiments, unlike other DC subsets, $CD11c^{int}CD11b^{-}GR\text{-}1^{+}$ DCs (fraction D) showed some background IRF-7 expression already in uninfected wild type mice (Fig. 3.27). Alternatively, IPCs might be able to utilize an IRF-7 independent pathway for IFN-α expression, as suggested by the recent finding, that ectopic expression of IRF-5 can substitute for IRF-7 to allow expression of certain IFN-α genes (Barnes et al., 2001). Ultimately, only the generation and analysis of IRF-7 deficient mice can define the role of IRF-7 in the expression of virus-induced IFN-α *in vivo*.

Our immune histological analysis of VSV infected mice revealed that IPCs are predominantly located in the marginal zone. Similarly, we and others have found the same IPC distribution in UV-HSV treated mice (Fig. 3.14, Eloranta and Alm, 1999; Eloranta et al., 1996). The importance of the marginal zone for pathogen surveillance was demonstrated by the scavenger function of marginal zone cells, which can retain microscopically small particles, including pathogens, from the blood (Matsuno et al., 1986). Mice that were experimentally depleted of macrophages in the marginal zone (Seiler et al., 1997), and osteopetrotic (op) mutant mice that are M-CSF deficient and lack the same macrophage populations, showed an increased sensitivity to pathogen infection (Guleria and Pollard, 2001). Thus, in order to be stimulated early in the course of an infection it appears "reasonable" that IPCs are located in the marginal zone. From histological colocalization studies it had been concluded that $MOMA\text{-}1^{+}$ metallophilic and $ERTR\text{-}9^{+}$ marginal zone macrophages might be involved in type I IFN production (Eloranta and Alm, 1999). Since we could not observe a strict correlation of MOMA-1 and ERTR-9 vs. IFN-α/β stainings, and following recent evidence that the human and mouse IPC are plasmacytoid DCs (Asselin-Paturel et al., 2001; Cella et al., 1999; Nakano et al., 2001;

Siegal et al., 1999), we FACS-sorted several DC subsets form spleen of VSV infected and from UV-HSV stimulated mice and analyzed them for IFN-α mRNA expression. These experiments indicated, that the subset of $CD11c^{int}CD11b^{-}GR\text{-}1^{+}$ DCs showed high IFN-α mRNA levels. Interestingly, we did not find increased levels of IFN-α message in myeloid or lymphoid DCs (fractions A and B, respectively) isolated from VSV or UV-HSV treated mice, as could have been expected form recent *in vitro* data (Hochrein et al., 2001).

In conclusion, we suggest to extend the current model of IFNAR feedback dependent expression of IFN-α as follows: i) *In vivo*, local infections may stimulate the production of mainly IFN-β by non-IPCs to protect surrounding tissues in a paracrine fashion. These cells produce IFN-α IFNAR dependently, i.e. only if sufficient autocrine type I IFN stimulation is provided. ii) Systemic infection and acute viremia, that require a generalized anti-viral state, may stimulate IPCs to produce IFN-α early and at high level independent of IFNAR feedback signaling. However, IFNAR feedback defines the magnitude and the duration of sustained IFN-α production, even when the primary inducing stimulus itself is short lived.

To our knowledge, we present the first set of *ex vivo* data defining IPCs in viral pathogenesis. Our results support the concept that highly specialized DCs, located in the marginal zone, produce type I IFN upon pathogen contact. The observation that early IFN-α production of mouse IPCs is largely independent of IFNAR signaling indicates a less stringently regulated IFN-α expression in IPCs as compared to other cell types. Further experiments will reveal, whether - depending on the tissue tropism and the stimulation mechanism - different pathogens may activate discrete cell populations to produce type I IFN, and whether mouse IPCs do play a role in antigen-processing and -presentation.

4.2 Phenotypic and functional characterization of the mouse IPC subset

Originally, we have analyzed rapid upregulation of IFN-α expression after VSV infection for IPC classification, thus identifying a population of $CD11b^{-}CD11c^{int}GR\text{-}1^{+}$ cells. Later it became obvious that the Gr-1 specific antibody cross-reacted at low affinity with the Ly6C antigen. Consequently, binding of anti-Gr-1 antibody was diminished by the competition of high affinity anti-Ly6C antibody. CD11c enriched cells from the spleen could therefore be divided into a $CD11c^{+}Ly6C^{-}$ dendritic cell population and $CD11c^{+}Ly6C^{+}$ IPCs. The latter expressed CD90, Sca-1, and CD54 but not F4/80 or CD62L (Fig. 3.31). The IPC population showed a characteristic low orthogonal light scatter, expressed B-220 in addition to Ly6C, but lacked expression of T-, B-, myeloid and NK- lineage-specific markers (CD5, CD19, CD11b and DX5). These properties allowed the identification of IPCs within unsorted cell suspensions from various organs providing the basis for direct quantitation of IPCs in the absence or presence of acute VSV infection (Fig. 3.34). Most recently, the mouse IPC was identified also by other groups, contributing valuable insight to the initially defined characteristics. The $CD11c^{+}Ly6C^{+}$ IPC subset in the mouse shares many similarities with the human plasmacytoid dendritic cells, including morphology, IPC function, and the expression of sets of TLR (Bruno et al., 2001) and other surface markers. Yet, unlike human plasmacytoid dendritic cells, mouse IPCs do not express the IL-3 receptor, pointing

at possible differences in the requirement for survival stimuli. This is evidenced by the difficulty to culture unstimulated mouse IPCs *in vitro* (Asselin-Paturel et al., 2001).

4.3 Origin of IPCs

Dendritic cells can be derived from proliferating pluripontent precursors in the mouse bone marrow by appropriate cell culture conditions *in vitro* (Metcalf, 1997; Traver et al., 2000). However, the differentiation pathways that generate DCs *in vivo* remain largely unknown (Ardavin et al., 2001)*. In particular, a direct non-proliferating DC precursor has not been defined for myeloid or lymphoid DCs. Like other immune cells, including DCs, mouse IPCs probably derive from a precursor population in the bone marrow. Interestingly, the mouse bone marrow contained a cell type very similar to splenic IPCs. The expression of all surface markers tested was virtually identical on splenic and bone marrow derived IPCs (data not shown). The lack of a bone marrow counterpart of other DC subsets makes the relative abundance of bone marrow cells with IPC phenotype surprising. To analyze the renewal rate of IPCs purified from bone marrow and spleen, BrdU labeling experiments have been performed. The turnover kinetics and the accumulation of BrdU positive IPCs were faster in the bone marrow than in the spleen. These observations suggested that IPCs do reside in the bone marrow and that they can directly populate secondary lymphoid organs.

Yet, direct homing to secondary lymphoid tissues is untypical for immature DC subsets. Classically, immature dendritic cells home to peripheral organs. There they acquire antigen and once activated by a pathogen stimulus they undergo maturation and then migrate to the draining lymph nodes and/or spleen (Cella et al., 1997; Sallusto et al., 1998). Thus, DCs in lymphoid organs have been widely considered to be mature, antigen-presenting cells capable of activating naïve T-cells. However, unlike myeloid and lymphoid dendritic cells found in secondary lymphoid organs, mouse IPCs display immature morphology, lacking the cell protrusions typically found on dendritic cells. In contrast to splenic DCs, IPCs enter lymphoid tissues apparently independent of maturation inducing stimuli. Accordingly, freshly isolated IPCs, in contrast to splenic DCs, were found unable to stimulate proliferation of allogeneic T-cells. IPCs activated and matured by *in vitro* stimulation with CpG-DNA induced weak but evident T-cell proliferation (Asselin-Paturel et al., 2001; Nakano et al., 2001). So far, poor survival in cell culture limited the detailed analysis of the T-cell stimulatory capacity of mouse IPCs. Thus it is still open, whether IPCs may serve as antigen presenting cells capable of initiating an adaptive immune response *in vivo*.

*Note added in proof: A $CD11c^+$ $MHCII^-$ proliferating precursor able to differentiate *in vivo* into all known DC subsets, but not into other myeloid or lymphoid cells, has now been identified in mouse peripheral blood (del Hoyo et al., 2002).

4.4 IPCs in viral pathophysiology

Upon VSV infection of mice, activated IPCs showed upregulation of cell surface molecules, including MHC class II and CD86 costimulatory molecules. Interestingly, upregulation of activation markers by IPCs - but not by other splenic DCs - was dependent on type I IFN receptor signaling. This suggested the use of discrete signaling pathways in DCs and IPCs involved in the induction of cell maturation. Nevertheless, with respect to the evident high-level expression of early inflammatory cytokines, i.e. type I IFNs and IL-12 (Dalod et al., 2002), and the induction of the MHC class II antigen presentation machinery, activated IPCs share many properties with classical DC subsets (Cella et al., 1997).

However, activated IPCs rapidly disappeared from the secondary lymphoid organs of VSV infected animals. One possibility is that the activation stimulus caused a rapid change of IPC morphology as well as surface marker expression. In spleen-cell suspensions from uninfected mice, we could uniquely identify mouse IPCs by the combination of any two of the following surface markers, CD11c, B220, Ly6C and absence of lineage-specific markers (i.e. CD5, CD19, CD11b and DX5), or by combining one of the above criteria with the typical FSC/SSC characteristics. Abrupt and simultaneously altered expression of all 4 surface markers plus a dramatic change in the cell morphology are, however, unlikely to occur, and thus cannot explain the disappearance of activated IPC from spleen. In addition, monitoring activated IPCs over time, we did not observe shifts in cell size or modulation of cell surface marker expression, or 'tailing' in the FACS profiles that would be indicative of altered marker expression and cell shape changes. As a second possibility, stimulated IPCs might be rapidly driven into apoptosis, either due to (over)stimulation or due to the cytopathic effect of VSV. Yet, $2 \cdot 10^5$ viral particles administered intravenously initiate the disappearance of more than a 10 times greater number of IPCs in the spleen alone. The observation that even low viral doses lead to a generalized reduction of IPC counts in lymph nodes and spleen makes a hypothesis involving cell death less likely. IPC loss in secondary lymphoid organs is paralleled by an increase of IPC counts in peripheral organs such as the lung. We therefore favor the possibility that activated IPCs physically leave secondary lymphoid organs and relocate to different organs.

A number of recent studies evidence that the IPC population indeed shows dynamic responses to different kinds of stimuli. Human blood IPC counts are sharply depressed after the administration of corticosteroids and return to normal levels within days after steroid cessation (Shodell and Siegal, 2001). In HIV infected patients long-term survivors showed increased IPC numbers while disease progression was accompanied by markedly reduced IPC levels (Feldman et al., 2001). IPC counts correlated with the viral load found in the corresponding patients (Soumelis et al., 2001). A similar depression in IPC counts has been observed in patients suffering from systemic lupus erythematosus (SLE) (Cederblad et al., 1998). Moreover, in the case of SLE a significant relocation of IPCs to the skin could be demonstrated (Blomberg et al., 2001; Farkas et al., 2001). Migration of IPCs to the site of local inflammation has also been observed in bacterial neuroinfections and in allergic

rhinitis (Pashenkov et al., 2002; Jahnsen et al., 2000). Furthermore, chronically inflamed lymph nodes harbor enlarged quantities of IPCs (Cella et al., 1999).

These observations raise the question of the biological significance of IPC relocation. As discussed earlier, stimulation of high-level IFN-α production by IPCs might be a hallmark of acute viremia that can be better controlled by a generalized antiviral state. It is conceivable, that besides IFN molecules distributed by the blood stream, also IPCs (the cells producing it) may contribute to the amplification of innate immune reactions in peripheral organs. Recently an intriguing connection between type I IFNs, DCs and NK cells has been observed. On its own, IFN-α was almost incapable of inducing DC maturation. In contrast, IFN-α maturation of DCs was potentiated in the presence of NK cells. Similarly, type I IFN mediated activation of NK cells is enhanced in the presence of DCs, suggesting an IFN-α dependent amplification loop that augments the activation of directly interacting DCs and NK cells (Gerosa et al., 2002). In a similar fashion, activated IPCs might function as sentinels that require further stimulation for maturation and possibly differentiation.

In response to an acute inflammatory stimulus (Bruno et al., 2001) or by injection of Flt-3 ligand (Bjorck, 2001) IPC counts in mouse bone marrow, and shortly afterwards in the blood and peripheral organs, were dramatically increased. Also in humans Flt-3 ligand and G-CSF administration have been shown to rapidly elevate IPC numbers in the blood (Arpinati et al., 2000; Pulendran et al., 2000). Thus, the bone marrow may function as a reservoir for IPC homeostasis, allowing prompt IPC recruitment to peripheral tissues upon stimulation. Accordingly IPC numbers in the bone marrow of WT mice were augmented after VSV infection. Yet, VSV infected IFNAR-/- showed sharply decreased IPC counts. The hypothesis of an IPC reservoir in the bone marrow offers a tentative explanation for the observed contrary trends in IFNAR-/- as compared to WT mice: while type I IFNs might directly or indirectly induce the generation of IPCs from a precursor and thus raise IPC levels in the bone marrow, an IFN independent stimulus may trigger the release of IPCs into the periphery.

A non-proliferating $CD11c^{+}Ly6C^{+}CD31^{+}$ cell type from the bone marrow, very similar to the mouse IPCs, has recently been shown to be able to mature *in vitro* into macrophages, lymphoid or myeloid dendritic cells. This reopens the question that has already been formulated for human plasmacytoid dendritic cells (Galibert et al., 2001), i.e. whether IPCs are destined to become a specific dendritic cell type or might serve as a precursor for different maturation routes depending on the stimulus they receive in peripheral tissues.

4.5 Outlook: What is the fate of the IPC *in vivo*?

Several open questions may be addressed by the analysis of the BAC-transgenic IFN-α2 or IRF-7 reporter mice. Firstly, it is not clear whether mouse IPCs constitute the only cell population capable of high-level type I IFN production. Human IPC, as probably their counterpart in the mouse, express a distinct set of TLR (Jarrossay et al., 2001; Kadowaki et al., 2001) making it conceivable that different viral IFN inducers may stimulate bulk IFN

production in different cell subsets. Sendai and lymphocytic choriomeningitis virus (LCMV) for example fail to stimulate high-level IFN production by IPCs (Dalod et al., 2002; Feldman et al., 1994). We obtained similar results for poly(I:C), though it is not clear whether poly(I:C) predominantly stimulates another specific cell type or a broad spectrum of non-IPC cells. A recent example for cellular complementarity in cytokine production has been provided for IL-12, another early cytokine (Dalod et al., 2002). Secondly, also the route of infection might influence the source of type I IFN *in vivo*. Many natural viral infections are acquired through respiratory or mucosal routes. It is therefore intriguing that besides the bone marrow, the lungs of naive mice showed the highest IPC counts (Fig. 3.35) and it will be important to determine whether IPCs of the lung are activated during local pulmonary infections. Thirdly, expression of the reporter gene may help to follow the fate of activated IPCs *in vivo*. The destination of IPC relocation and the cell types that possibly differentiate from activated IPCs could be identified. This may help to resolve the controversial question whether IPCs represent a distinct hematological entity or whether they are a conglomerate of immature cells with distinct differentiation fates.

In summary, the observation that activated IPCs leave secondary lymphoid tissues, and thus behave opposite from maturing dendritic cells, make it unlikely that IPCs play a dominant role in the antigen presentation initiating an adaptive response. The fate of the disappearing IPC cells is, however, not known. It is conceivable that IPCs acquire antigen, mature and differentiate outside secondary lymphoid organs and eventually relocate to the spleen and lymph nodes as antigen presenting cells during later stages of acute viral infections.

Rapid IPC relocation in response to inflammation/infection together with the dynamic increase in IPC output by the bone marrow supports the idea that IPCs might constitute an immature pluripotent precursor, able to differentiate according to stimuli and maturation environment, rather than a distinct lineage of committed cells. Testing this hypothesis will help to determine whether and in what way patients suffering from chronic viral infections such as HIV or Hepatitis C benefit from boosted IPC counts. The therapeutic value of an increased IPC population surely includes but might go well beyond the mere increase in local and generalized IFN-α output. Also non-viral human diseases, such as multiple sclerosis, Behcet's disease and certain cancers have been successfully treated with type I IFNs (Karp et al., 2000; Pitha, 2000; Steis et al., 1987; Walther and Hohlfeld, 1999; Zouboulis and Orfanos, 1998). However, systemic administration of type I IFNs often causes severe side effects that preclude its general use in many cases (ibid.). It is conceivable, that a therapy aimed at activating the patients' endogenous interferon production, i.e. by boosting and/or specifically activating IPCs may be efficient and at the same time may alleviate undesired side effects.

5 References

Agrawal, A., Eastman, Q. M., and Schatz, D. G. (1998). Transposition mediated by RAG1 and RAG2 and its implications for the evolution of the immune system. Nature *394*, 744-51.

Akira, S., Takeda, K., and Kaisho, T. (2001). Toll-like receptors: critical proteins linking innate and acquired immunity. Nat Immunol *2*, 675-80.

Alexopoulou, L., Holt, A. C., Medzhitov, R., and Flavell, R. A. (2001). Recognition of double-stranded RNA and activation of NF-kappaB by Toll-like receptor 3. Nature *413*, 732-8.

Anderson, K. V., Jurgens, G., and Nusslein-Volhard, C. (1985). Establishment of dorsal-ventral polarity in the Drosophila embryo: genetic studies on the role of the Toll gene product. Cell *42*, 779-89.

Ardavin, C., Martinez del Hoyo, G., Martin, P., Anjuere, F., Arias, C. F., Marin, A. R., Ruiz, S., Parrillas, V., and Hernandez, H. (2001). Origin and differentiation of dendritic cells. Trends Immunol *22*, 691-700.

Arpinati, M., Green, C. L., Heimfeld, S., Heuser, J. E., and Anasetti, C. (2000). Granulocyte-colony stimulating factor mobilizes T helper 2-inducing dendritic cells. Blood *95*, 2484-90.

Asai, T., Tena, G., Plotnikova, J., Willmann, M. R., Chiu, W. L., Gomez-Gomez, L., Boller, T., Ausubel, F. M., and Sheen, J. (2002). MAP kinase signalling cascade in Arabidopsis innate immunity. Nature *415*, 977-83.

Asselin-Paturel, C., Boonstra, A., Dalod, M., Durand, I., Yessaad, N., Dezutter-Dambuyant, C., Vicari, A., O'Garra, A., Biron, C., Briere, F., and Trinchieri, G. (2001). Mouse type I IFN-producing cells are immature APCs with plasmacytoid morphology. Nat Immunol *2*, 1144-50.

Bachmann, M. F., Kundig, T. M., Kalberer, C. P., Hengartner, H., and Zinkernagel, R. M. (1994). How many specific B cells are needed to protect against a virus? J. Immunol. *152*, 4235-41.

Barnes, B. J., Moore, P. A., and Pitha, P. M. (2001). Virus-specific Activation of a Novel Interferon Regulatory Factor, IRF-5, Results in the Induction of Distinct Interferon alpha Genes. J. Biol. Chem. *276*, 23382-90.

Basu, S., Binder, R. J., Suto, R., Anderson, K. M., and Srivastava, P. K. (2000). Necrotic but not apoptotic cell death releases heat shock proteins, which deliver a partial maturation signal to dendritic cells and activate the NF-kappa B pathway. Int Immunol *12*, 1539-46.

Bauer, M., Redecke, V., Ellwart, J. W., Scherer, B., Kremer, J. P., Wagner, H., and Lipford, G. B. (2001). Bacterial CpG-DNA triggers activation and maturation of human CD11c-, CD123+ dendritic cells. J. Immunol. *166*, 5000-7.

Birnboim, H. C., and Doly, J. (1979). A rapid alkaline extraction procedure for screening recombinant plasmid DNA. Nucleic Acids Res *7*, 1513-23.

Biron, C. A. (1997). Activation and function of natural killer cell responses during viral infections. Curr Opin Immunol *9*, 24-34.

Biron, C. A. (2001). Interferons alpha and beta as Immune Regulators-A New Look. Immunity *14*, 661-4.

Bjorck, P. (2001). Isolation and characterization of plasmacytoid dendritic cells from Flt3 ligand and granulocyte-macrophage colony-stimulating factor-treated mice. Blood *98*, 3520-6.

Blomberg, S., Eloranta, M. L., Cederblad, B., Nordlin, K., Alm, G. V., and Ronnblom, L. (2001). Presence of cutaneous interferon-alpha producing cells in patients with systemic lupus erythematosus. Lupus *10*, 484-90.

Bobrow, M. N., Harris, T. D., Shaughnessy, K. J., and Litt, G. J. (1989). Catalyzed reporter deposition, a novel method of signal amplification. Application to immunoassays. J Immunol Methods *125*, 279-85.

Boehm, U., Klamp, T., Groot, M., and Howard, J. C. (1997). Cellular responses to interferon-gamma. Annu. Rev. Immunol. *15*, 749-95.

Bogdan, C. (2001). Nitric oxide and the immune response. Nat Immunol *2*, 907-16.

Bouchon, A., Facchetti, F., Weigand, M. A., and Colonna, M. (2001a). TREM-1 amplifies inflammation and is a crucial mediator of septic shock. Nature *410*, 1103-7.

Bouchon, A., Hernandez-Munain, C., Cella, M., and Colonna, M. (2001b). A DAP12-mediated pathway regulates expression of CC chemokine receptor 7 and maturation of human dendritic cells. J Exp Med *194*, 1111-22.

Bruno, L., Seidl, T., and Lanzavecchia, A. (2001). Mouse pre-immunocytes as non-proliferating multipotent precursors of macrophages, interferon-producing cells, CD8alpha(+) and CD8alpha(-) dendritic cells. Eur J Immunol *31*, 3403-12.

Buchholz, F., Angrand, P. O., and Stewart, A. F. (1998). Improved properties of FLP recombinase evolved by cycling mutagenesis. Nat Biotechnol *16*, 657-62.

Burnet, M. (1966). A possible genetic basis for specific pattern in antibody. Nature *210*, 1308-10.

Cederblad, B., Blomberg, S., Vallin, H., Perers, A., Alm, G. V., and Ronnblom, L. (1998). Patients with systemic lupus erythematosus have reduced numbers of circulating natural interferon-alpha-producing cells. J Autoimmun *11*, 465-70.

Cella, M., Engering, A., Pinet, V., Pieters, J., and Lanzavecchia, A. (1997). Inflammatory stimuli induce accumulation of MHC class II complexes on dendritic cells. Nature *388*, 782-7.

Cella, M., Jarrossay, D., Facchetti, F., Alebardi, O., Nakajima, H., Lanzavecchia, A., and Colonna, M. (1999). Plasmacytoid monocytes migrate to inflamed lymph nodes and produce large amounts of type I interferon. Nat. Med. *5*, 919-23.

Cella, M., Salio, M., Sakakibara, Y., Langen, H., Julkunen, I., and Lanzavecchia, A. (1999). Maturation, activation, and protection of dendritic cells induced by double-stranded RNA. J. Exp. Med. *189*, 821-9.

Corey, L. (1998). Principles of Internal Medicine, A. S. Fauci, ed. (Hamburg: MacGraw-Hill), pp. 692-697.

Dalod, M., Salazar-Mather, T. P., Malmgaard, L., Lewis, C., Asselin-Paturel, C., Briere, F., Trinchieri, G., and Biron, C. A. (2002). Interferon [alpha]/[beta] and Interleukin 12 Responses to Viral Infections: Pathways Regulating Dendritic Cell Cytokine Expression In Vivo. J Exp Med *195*, 517-528.

Darnell, J. E., Jr. (1997). STATs and gene regulation. Science *277*, 1630-5.

del Hoyo, G. M., Martin, P., Vargas, H. H., Ruiz, S., Arias, C. F., and Ardavin, C. (2002). Characterization of a common precursor population for dendritic cells. Nature *415*, 1043-7.

Deonarain, R., Alcami, A., Alexiou, M., Dallman, M. J., Gewert, D. R., and Porter, A. C. (2000). Impaired antiviral response and alpha/beta interferon induction in mice lacking beta interferon. J. Virol. *74*, 3404-9.

Diefenbach, A., Schindler, H., Donhauser, N., Lorenz, E., Laskay, T., MacMicking, J., Rollinghoff, M., Gresser, I., and Bogdan, C. (1998). Type 1 interferon (IFNalpha/beta) and type 2 nitric oxide synthase regulate the innate immune response to a protozoan parasite. Immunity *8*, 77-87.

Eloranta, M. L., and Alm, G. V. (1999). Splenic marginal metallophilic macrophages and marginal zone macrophages are the major interferon-alpha/beta producers in mice upon intravenous challenge with herpes simplex virus. Scand. J. Immunol. *49*, 391-4.

Eloranta, M. L., Sandberg, K., and Alm, G. V. (1996). The interferon-alpha/beta responses of mice to herpes simplex virus studied at the blood and tissue level in vitro and in vivo. Scand. J. Immunol. *43*, 356-60.

Erlandsson, L., Blumenthal, R., Eloranta, M. L., Engel, H., Alm, G., Weiss, S., and Leanderson, T. (1998). Interferon-beta is required for interferon-alpha production in mouse fibroblasts. Curr. Biol. *8*, 223-6.

Farkas, L., Beiske, K., Lund-Johansen, F., Brandtzaeg, P., and Jahnsen, F. L. (2001). Plasmacytoid dendritic cells (natural interferon- alpha/beta-producing cells) accumulate in cutaneous lupus erythematosus lesions. Am J Pathol *159*, 237-43.

Feldman, S., Stein, D., Amrute, S., Denny, T., Garcia, Z., Kloser, P., Sun, Y., Megjugorac, N., and Fitzgerald-Bocarsly, P. (2001). Decreased interferon-alpha production in HIV-infected patients correlates with numerical and functional deficiencies in circulating type 2 dendritic cell precursors. Clin Immunol *101*, 201-10.

Feldman, S. B., Ferraro, M., Zheng, H. M., Patel, N., Gould-Fogerite, S., and Fitzgerald-Bocarsly, P. (1994). Viral induction of low frequency interferon-alpha producing cells [published errata appear in Virology 1995 Feb 1;206(2):1159 and 1995 Feb 20;207(1):342]. Virology *204*, 1-7 inhibitory. Thus, exposing normal (but not IFN-IR-/-) T cells to CpG DNA in vivo led to reduced T proliferative responses after TCR ligation in vitro.

Ferbas, J. J., Toso, J. F., Logar, A. J., Navratil, J. S., and Rinaldo, C. R., Jr. (1994). CD4+ blood dendritic cells are potent producers of IFN-alpha in response to in vitro HIV-1 infection. J. Immunol. *152*, 4649-62.

Fujiki, T., and Tanaka, A. (1988). Antibacterial activity of recombinant murine beta interferon. Infect Immun *56*, 548-51.

Galibert, L., Maliszewski, C. R., and Vandenabeele, S. (2001). Plasmacytoid monocytes/T cells: a dendritic cell lineage? Semin Immunol *13*, 283-9.

Gallucci, S., and Matzinger, P. (2001). Danger signals: SOS to the immune system. Curr Opin Immunol *13*, 114-9.

Gerosa, F., Baldani-Guerra, B., Nisii, C., Marchesini, V., Carra, G., and Trinchieri, G. (2002). Reciprocal Activating Interaction between Natural Killer Cells and Dendritic Cells. J Exp Med *195*, 327-333.

Gresser, I., Tovey, M. G., Maury, C., and Bandu, M. T. (1976). Role of interferon in the pathogenesis of virus diseases as demonstrated by the use of anti-interferon serum. II. Studies with herpes simplex, Moloney sarcoma, vesicular stomatitis, Newcastle disease and influenza viruses. J. Exp. Med. *144*, 1316-1323.

Guleria, I., and Pollard, J. W. (2001). Aberrant macrophage and neutrophil population dynamics and impaired Th1 response to Listeria monocytogenes in colony-stimulating factor 1-deficient mice. Infect. Immun. *69*, 1795-807.

Harada, H., Matsumoto, M., Sato, M., Kashiwazaki, Y., Kimura, T., Kitagawa, M., Yokochi, T., Tan, R. S., Takasugi, T., Kadokawa, Y., Schindler, C., Schreiber, R. D., Noguchi, S., and Taniguchi, T. (1996). Regulation of IFN-alpha/beta genes: evidence for a dual function of the transcription factor complex ISGF3 in the production and action of IFN- alpha/beta. Genes Cells *1*, 995-1005.

Havell, E. A. (1993). Listeria monocytogenes-induced interferon-gamma primes the host for production of tumor necrosis factor and interferon-alpha/beta. J Infect Dis *167*, 1364-71.

Hayashi, F., Smith, K. D., Ozinsky, A., Hawn, T. R., Yi, E. C., Goodlett, D. R., Eng, J. K., Akira, S., Underhill, D. M., and Aderem, A. (2001). The innate immune response to bacterial flagellin is mediated by Toll-like receptor 5. Nature *410*, 1099-103.

Hemmi, H., Kaisho, T., Takeuchi, O., Sato, S., Sanjo, H., Hoshino, K., Horiuchi, T., Tomizawa, H., Takeda, K., and Akira, S. (2002). Small anti-viral compounds activate immune cells via the TLR7 MyD88-dependent signaling pathway. Nat Immunol *3*, 196-200.

Hemmi, H., Takeuchi, O., Kawai, T., Kaisho, T., Sato, S., Sanjo, H., Matsumoto, M., Hoshino, K., Wagner, H., Takeda, K., and Akira, S. (2000). A Toll-like receptor recognizes bacterial DNA. Nature *408*, 740-5.

Hiom, K., Melek, M., and Gellert, M. (1998). DNA transposition by the RAG1 and RAG2 proteins: a possible source of oncogenic translocations. Cell *94*, 463-70.

Hochrein, H., Shortman, K., Vremec, D., Scott, B., Hertzog, P., and O'Keeffe, M. (2001). Differential production of IL-12, IFN-alpha, and IFN-gamma by mouse dendritic cell subsets. J. Immunol. *166*, 5448-55.

Hoffmann, J. A., and Reichhart, J. M. (2002). Drosophila innate immunity: an evolutionary perspective. Nat Immunol *3*, 121-6.

Hoss-Homfeld, A., Zwarthoff, E. C., and Zawatzky, R. (1989). Cell type specific expression and regulation of murine interferon alpha and beta genes. Virology *173*, 539-50.

Howell, D. M., Feldman, S. B., Kloser, P., and Fitzgerald-Bocarsly, P. (1994). Decreased frequency of functional natural interferon-producing cells in peripheral blood of patients with the acquired immune deficiency syndrome. Clin. Immunol. Immunopathol. *71*, 223-30.

Hsieh, C. S., Macatonia, S. E., Tripp, C. S., Wolf, S. F., O'Garra, A., and Murphy, K. M. (1993). Development of TH1 CD4+ T cells through IL-12 produced by Listeria-induced macrophages. Science *260*, 547-9.

Isaacs, A., and Lindenmann, J. (1957). Virus interference. I. The interferon. Proc. R. Soc. Lond. (B) *147*, 258-267.

Jacob, J., and Baltimore, D. (1999). Modelling T-cell memory by genetic marking of memory T cells in vivo. Nature *399*, 593-7.

Jahnsen, F. L., Lund-Johansen, F., Dunne, J. F., Farkas, L., Haye, R., and Brandtzaeg, P. (2000). Experimentally induced recruitment of plasmacytoid (CD123high) dendritic cells in human nasal allergy. J Immunol *165*, 4062-8.

Janeway, C. A., Travers, P., Walport, M., and Shlomchik, M. (2001). Immunobiology - The Immune System in Health and Disease, 5 Edition (New York: Garland Publishing).

Jarrossay, D., Napolitani, G., Colonna, M., Sallusto, F., and Lanzavecchia, A. (2001). Specialization and complementarity in microbial molecule recognition by human myeloid and plasmacytoid dendritic cells. Eur J Immunol *31*, 3388-93.

Kabarowski, J. H., Zhu, K., Le, L. Q., Witte, O. N., and Xu, Y. (2001). Lysophosphatidylcholine as a ligand for the immunoregulatory receptor G2A. Science *293*, 702-5.

Kadowaki, N., Antonenko, S., and Liu, Y. J. (2001). Distinct CpG DNA and polyinosinic-polycytidylic acid double-stranded RNA, respectively, stimulate CD11c- type 2 dendritic cell precursors and CD11c+ dendritic cells to produce type I IFN. J. Immunol. *166*, 2291-5.

Kadowaki, N., Ho, S., Antonenko, S., de Waal Malefyt, R., Kastelein, R. A., Bazan, F., and Liu, Y.-J. (2001). Subsets of human dendritic cell precursors express different toll-like receptors and respond to different microbial antigens. J. Exp. Med. *194*, 863-9.

Kadowaki, N., Ho, S., Antonenko, S., Malefyt, R. W., Kastelein, R. A., Bazan, F., and Liu, Y. J. (2001). Subsets of human dendritic cell precursors express different toll-like receptors and respond to different microbial antigens. J Exp Med *194*, 863-9.

Kalinke, U., Bucher, E. M., Ernst, B., Oxenius, A., Roost, H. P., Geley, S., Kofler, R., Zinkernagel, R. M., and Hengartner, H. (1996). The role of somatic mutation in the generation of the protective humoral immune response against vesicular stomatitis virus. Immunity *5*, 639-52.

Karp, C. L., Biron, C. A., and Irani, D. N. (2000). Interferon beta in multiple sclerosis: is IL-12 suppression the key? Immunol Today *21*, 24-8.

Kawai, T., Adachi, O., Ogawa, T., Takeda, K., and Akira, S. (1999). Unresponsiveness of MyD88-deficient mice to endotoxin. Immunity *11*, 115-22.

Kawai, T., Takeuchi, O., Fujita, T., Inoue, J., Muhlradt, P. F., Sato, S., Hoshino, K., and Akira, S. (2001). Lipopolysaccharide stimulates the MyD88-independent pathway and results in activation of IFN-regulatory factor 3 and the expression of a subset of lipopolysaccharide-inducible genes. J Immunol *167*, 5887-94.

Kierszenbaum, F., and Sonnenfeld, G. (1984). Beta-interferon inhibits cell infection by Trypanosoma cruzi. J Immunol *132*, 905-8.

Kurt-Jones, E. A., Popova, L., Kwinn, L., Haynes, L. M., Jones, L. P., Tripp, R. A., Walsh, E. E., Freeman, M. W., Golenbock, D. T., Anderson, L. J., and Finberg, R. W. (2000). Pattern recognition receptors TLR4 and CD14 mediate response to respiratory syncytial virus. Nat Immunol *1*, 398-401.

Lanzavecchia, A., and Sallusto, F. (2001). The instructive role of dendritic cells on T cell responses: lineages, plasticity and kinetics. Curr Opin Immunol *13*, 291-8.

Le Bon, A., Schiavoni, G., D'Agostino, G., Gresser, I., Belardelli, F., and Tough, D. F. (2001). Type I interferons potently enhance humoral immunity and can promote isotype switching by stimulating dendritic cells in vivo. Immunity *14*, 461-70.

Leonard, W. J., and O'Shea, J. J. (1998). Jaks and STATs: biological implications. Annu Rev Immunol *16*, 293-322.

Levy, D. E. (2002). Whence interferon? Variety in the production of interferon in response to viral infection. J Exp Med *195*, F15-8.

Liu, Y. J., Kanzler, H., Soumelis, V., and Gilliet, M. (2001). Dendritic cell lineage, plasticity and cross-regulation. Nat Immunol *2*, 585-9.

Lo, D., Feng, L., Li, L., Carson, M. J., Crowley, M., Pauza, M., Nguyen, A., and Reilly, C. R. (1999). Integrating innate and adaptive immunity in the whole animal. Immunol Rev *169*, 225-39.

Lu, Q., and Lemke, G. (2001). Homeostatic regulation of the immune system by receptor tyrosine kinases of the Tyro 3 family. Science *293*, 306-11.

Luft, T., Pang, K. C., Thomas, E., Hertzog, P., Hart, D. N., Trapani, J., and Cebon, J. (1998). Type I IFNs enhance the terminal differentiation of dendritic cells. J Immunol *161*, 1947-53.

Luster, A. D. (2002). The role of chemokines in linking innate and adaptive immunity. Curr Opin Immunol *14*, 129-35.

Lutfalla, G., and Uze, G. (1994). Structure of the murine interferon alpha/beta receptor-encoding gene: high-frequency rearrangements in the interferon-resistant L1210 cell line. Gene *148*, 343-6.

Lyons, A. B., and Parish, C. R. (1994). Determination of lymphocyte division by flow cytometry. J Immunol Methods *171*, 131-7.

Marie, I., Durbin, J. E., and Levy, D. E. (1998). Differential viral induction of distinct interferon-alpha genes by positive feedback through interferon regulatory factor-7. EMBO J. *17*, 6660-9.

Marrack, P., Kappler, J., and Mitchell, T. (1999). Type I interferons keep activated T cells alive. J Exp Med *189*, 521-30.

Martin, P., del Hoyo, G. M., Anjuere, F., Ruiz, S. R., Arias, C. F., Marin, A. R., and Ardavin, C. (2000). Concept of lymphoid versus myeloid dendritic cell lineages revisited: both CD8alpha(-) and CD8alpha(+) dendritic cells are generated from CD4(low) lymphoid-committed precursors. Blood *96*, 2511-9.

Martinez-Salas, E. (1999). Internal ribosome entry site biology and its use in expression vectors. Curr Opin Biotechnol *10*, 458-64.

Matsuno, K., Fujii, H., and Kotani, M. (1986). Splenic marginal-zone macrophages and marginal metallophils in rats and mice. Cell. Tissue. Res. *246*, 263-9.

Means, T. K., Lien, E., Yoshimura, A., Wang, S., Golenbock, D. T., and Fenton, M. J. (1999). The CD14 ligands lipoarabinomannan and lipopolysaccharide differ in their requirement for Toll-like receptors. J Immunol *163*, 6748-55.

Means, T. K., Wang, S., Lien, E., Yoshimura, A., Golenbock, D. T., and Fenton, M. J. (1999). Human toll-like receptors mediate cellular activation by Mycobacterium tuberculosis. J Immunol *163*, 3920-7.

Medzhitov, R., Preston-Hurlburt, P., and Janeway, C. A., Jr. (1997). A human homologue of the Drosophila Toll protein signals activation of adaptive immunity. Nature *388*, 394-7.

Megyeri, K., Au, W. C., Rosztoczy, I., Raj, N. B., Miller, R. L., Tomai, M. A., and Pitha, P. M. (1995). Stimulation of interferon and cytokine gene expression by imiquimod and stimulation by Sendai virus utilize similar signal transduction pathways. Mol. Cell. Biol. *15*, 2207-18.

Metcalf, D. (1997). Murine hematopoietic stem cells committed to macrophage/dendritic cell formation: stimulation by Flk2-ligand with enhancement by regulators using the gp130 receptor chain. Proc Natl Acad Sci U S A *94*, 11552-6.

Metchinkoff, E. (1905). Immunity in infective diseases. University Press, Cambridge *0*, 591.

Moser, M., and Murphy, K. M. (2000). Dendritic cell regulation of TH1-TH2 development. Nat Immunol *1*, 199-205.

Muller, U., Steinhoff, U., Reis, L. F., Hemmi, S., Pavlovic, J., Zinkernagel, R. M., and Aguet, M. (1994). Functional role of type I and type II interferons in antiviral defense. Science *264*, 1918-21.

Muyrers, J. P., Zhang, Y., and Stewart, A. F. (2000). ET-cloning: think recombination first. Genet Eng (N Y) *22*, 77-98.

Muyrers, J. P., Zhang, Y., Testa, G., and Stewart, A. F. (1999). Rapid modification of bacterial artificial chromosomes by ET-recombination. Nucleic Acids Res *27*, 1555-7.

Nakane, A., and Minagawa, T. (1982). Induction of alpha and beta interferons during the hyporeactive state of gamma interferon by Mycobacterium bovis BCG cell wall fraction in Mycobacterium bovis BCG-sensitized mice. Infect Immun *36*, 966-70.

Nakano, H., Yanagita, M., and Gunn, M. D. (2001). Cd11c(+)b220(+)gr-1(+) cells in mouse lymph nodes and spleen display characteristics of plasmacytoid dendritic cells. J Exp Med *194*, 1171-8.

Neubuser, A., Koseki, H., and Balling, R. (1995). Characterization and developmental expression of Pax9, a paired-box-containing gene related to Pax1. Dev. Biol. *170*, 701-16.

Nolan, G. P., Fiering, S., Nicolas, J. F., and Herzenberg, L. A. (1988). Fluorescence-activated cell analysis and sorting of viable mammalian cells based on beta-D-galactosidase activity after transduction of Escherichia coli lacZ. Proc Natl Acad Sci U S A *85*, 2603-7.

Okamura, Y., Watari, M., Jerud, E. S., Young, D. W., Ishizaka, S. T., Rose, J., Chow, J. C., and Strauss, J. F., 3rd (2001). The extra domain A of fibronectin activates Toll-like receptor 4. J Biol Chem *276*, 10229-33.

Orellana, M. A., Suzuki, Y., Araujo, F., and Remington, J. S. (1991). Role of beta interferon in resistance to Toxoplasma gondii infection. Infect Immun *59*, 3287-90.

Oumard, A., Hennecke, M., Hauser, H., and Nourbakhsh, M. (2000). Translation of NRF mRNA is mediated by highly efficient internal ribosome entry. Mol. Cell. Biol. *20*, 2755-9.

Paquette, R. L., Hsu, N. C., Kiertscher, S. M., Park, A. N., Tran, L., Roth, M. D., and Glaspy, J. A. (1998). Interferon-alpha and granulocyte-macrophage colony-stimulating factor differentiate peripheral blood monocytes into potent antigen-presenting cells. J Leukoc Biol *64*, 358-67.

Pashenkov, M., Teleshova, N., Kouwenhoven, M., Smirnova, T., Jin, Y. P., Kostulas, V., Huang, Y. M., Pinegin, B., Boiko, A., and Link, H. (2002). Recruitment of dendritic cells to the cerebrospinal fluid in bacterial neuroinfections. J Neuroimmunol *122*, 106-16.

Pitha, P. M. (2000). Introduction: interferon's connection to cancer. Semin Cancer Biol *10*, 69-72.

Pulendran, B., Banchereau, J., Burkeholder, S., Kraus, E., Guinet, E., Chalouni, C., Caron, D., Maliszewski, C., Davoust, J., Fay, J., and Palucka, K. (2000). Flt3-ligand and granulocyte colony-stimulating factor mobilize distinct human dendritic cell subsets in vivo. J Immunol *165*, 566-72.

Rajewsky, K. (1996). Clonal selection and learning in the antibody system. Nature *381*, 751-8.

Randolph, G. J., Inaba, K., Robbiani, D. F., Steinman, R. M., and Muller, W. A. (1999). Differentiation of phagocytic monocytes into lymph node dendritic cells in vivo. Immunity *11*, 753-61.

Rincon, M., Anguita, J., Nakamura, T., Fikrig, E., and Flavell, R. A. (1997). Interleukin (IL)-6 directs the differentiation of IL-4-producing CD4+ T cells. J Exp Med *185*, 461-9.

Rolink, A. G., Nutt, S. L., Melchers, F., and Busslinger, M. (1999). Long-term in vivo reconstitution of T-cell development by Pax5-deficient B-cell progenitors. Nature *401*, 603-6.

Roost, H. P., Haag, A., Burkhart, C., Zinkernagel, R. M., and Hengartner, H. (1996). Mapping of the dominant neutralizing antigenic site of a virus using infected cells. J. Immunol. Methods *189*, 233-42.

Sallusto, F., Schaerli, P., Loetscher, P., Schaniel, C., Lenig, D., Mackay, C. R., Qin, S., and Lanzavecchia, A. (1998). Rapid and coordinated switch in chemokine receptor expression during dendritic cell maturation. Eur J Immunol *28*, 2760-9.

Sampson, L. L., Heuser, J., and Brown, E. J. (1991). Cytokine regulation of complement receptor-mediated ingestion by mouse peritoneal macrophages. M-CSF and IL-4 activate phagocytosis by a common mechanism requiring autostimulation by IFN-beta. J Immunol *146*, 1005-13.

Sandberg, K., Eloranta, M. L., Johannisson, A., and Alm, G. V. (1991). Flow cytometric analysis of natural interferon-alpha producing cells. Scand. J. Immunol. *34*, 565-76.

Santini, S. M., Lapenta, C., Logozzi, M., Parlato, S., Spada, M., Di Pucchio, T., and Belardelli, F. (2000). Type I interferon as a powerful adjuvant for monocyte-derived dendritic cell development and activity in vitro and in Hu-PBL-SCID mice. J Exp Med *191*, 1777-88.

Sato, M., Hata, N., Asagiri, M., Nakaya, T., Taniguchi, T., and Tanaka, N. (1998). Positive feedback regulation of type I IFN genes by the IFN-inducible transcription factor IRF-7. FEBS Lett. *441*, 106-10.

Sato, M., Suemori, H., Hata, N., Asagiri, M., Ogasawara, K., Nakao, K., Nakaya, T., Katsuki, M., Noguchi, S., Tanaka, N., and Taniguchi, T. (2000). Distinct and essential roles of transcription factors IRF-3 and IRF-7 in response to viruses for IFN-alpha/beta gene induction. Immunity *13*, 539-48.

Sato, M., Tanaka, N., Hata, N., Oda, E., and Taniguchi, T. (1998). Involvement of the IRF family transcription factor IRF-3 in virus-induced activation of the IFN-beta gene. FEBS Lett. *425*, 112-6.

Schaniel, C., Bruno, L., Melchers, F., and Rolink, A. G. (2002). Multiple hematopoietic cell lineages develop in vivo from transplanted Pax5-deficient pre-B I-cell clones. Blood *99*, 472-8.

Schubert, M., Harmison, G. G., and Meier, E. (1984). Primary structure of the vesicular stomatitis virus polymerase (L) gene: evidence for a high frequency of mutations. J Virol *51*, 505-14.

Seiler, P., Aichele, P., Odermatt, B., Hengartner, H., Zinkernagel, R. M., and Schwendener, R. A. (1997). Crucial role of marginal zone macrophages and marginal zone metallophils in the clearance of lymphocytic choriomeningitis virus infection. Eur. J. Immunol. *27*, 2626-33.

Sen, G. C. (2001). Viruses and interferons. Annu Rev Microbiol *55*, 255-81.

Shodell, M., and Siegal, F. P. (2001). Corticosteroids depress IFN-alpha-producing plasmacytoid dendritic cells in human blood. J Allergy Clin Immunol *108*, 446-8.

Shope, R. E., and Tesh, R. B. (1987). The ecology of rhabdoviruses that infect vertebrates. In The Rhabdoviruses, R. R. Wagner, ed. (New York: Plenum Press), pp. 509-534.

Siegal, F. P., Kadowaki, N., Shodell, M., Fitzgerald-Bocarsly, P. A., Shah, K., Ho, S., Antonenko, S., and Liu, Y. J. (1999). The nature of the principal type 1 interferon-producing cells in human blood. Science *284*, 1835-7.

Silverman, N., and Maniatis, T. (2001). NF-kappaB signaling pathways in mammalian and insect innate immunity. Genes Dev *15*, 2321-42.

Skynner, M. J., Drage, D. J., Dean, W. L., Turner, S., Watt, D. J., and Allen, N. D. (1999). Transgenic mice ubiquitously expressing human placental alkaline phosphatase (PLAP): an additional reporter gene for use in tandem with beta-galactosidase (lacZ). Int J Dev Biol *43*, 85-90.

Soumelis, V., Scott, I., Gheyas, F., Bouhour, D., Cozon, G., Cotte, L., Huang, L., Levy, J. A., and Liu, Y. J. (2001). Depletion of circulating natural type 1 interferon-producing cells in HIV-infected AIDS patients. Blood *98*, 906-12.

Steinhoff, U., Muller, U., Schertler, A., Hengartner, H., Aguet, M., and Zinkernagel, R. M. (1995). Antiviral protection by vesicular stomatitis virus-specific antibodies in alpha/beta interferon receptor-deficient mice. J. Virol. *69*, 2153-8.

Steis, R. G., Foon, K. A., and Longo, D. L. (1987). Current and future uses of recombinant interferon alpha in the treatment of low-grade non-Hodgkin's lymphoma. Cancer *59*, 658-63.

Stevens, J. G. (1989). Human herpesviruses: a consideration of the latent state. Microbiol Rev *53*, 318-32.

Svensson, H., Johannisson, A., Nikkila, T., Alm, G. V., and Cederblad, B. (1996). The cell surface phenotype of human natural interferon-alpha producing cells as determined by flow cytometry. Scand. J. Immunol. *44*, 164-72.

Takeuchi, O., Kawai, T., Muhlradt, P. F., Morr, M., Radolf, J. D., Zychlinsky, A., Takeda, K., and Akira, S. (2001). Discrimination of bacterial lipoproteins by Toll-like receptor 6. Int Immunol *13*, 933-40.

Tanaka, N., Sato, M., Lamphier, M. S., Nozawa, H., Oda, E., Noguchi, S., Schreiber, R. D., Tsujimoto, Y., and Taniguchi, T. (1998). Type I interferons are essential mediators of apoptotic death in virally infected cells. Genes Cells *3*, 29-37.

Taniguchi, T., and Takaoka, A. (2001). A weak signal for strong responses: interferon-alpha/beta revisited. Nat. Rev. Mol. Cell. Biol. *2*, 378-86.

Taylor, J. L., and Grossberg, S. E. (1998). The effects of interferon-alpha on the production and action of other cytokines. Semin Oncol *25*, 23-9.

Tesh, R. B., and Johnson, K. M. (1975). Vesicular stomatitis. In diseases transmitted from animals to man, T. W. Hubbert, M. F. McCullock and R. P. Schnurrenberger, eds. (Springfield, Illinois, pp. 897-910.

Thanos, D., and Maniatis, T. (1995). Virus induction of human IFN beta gene expression requires the assembly of an enhanceosome. Cell *83*, 1091-100.

Thomas, D., Newcomb, W. W., Brown, J. C., Wall, J. S., Hainfeld, J. F., Trus, B. L., and Steven, A. C. (1985). Mass and molecular composition of vesicular stomatitis virus: a scanning transmission electron microscopy analysis. J Virol *54*, 598-607.

Torres, R. M., and Kühn, R. (1997). Laboratory protocols for conditional gene targeting (Oxford, New York, Tokyo: Oxford University Press).

Traver, D., Akashi, K., Manz, M., Merad, M., Miyamoto, T., Engleman, E. G., and Weissman, I. L. (2000). Development of CD8alpha-positive dendritic cells from a common myeloid progenitor. Science *290*, 2152-4.

Underhill, D. M., Ozinsky, A., Smith, K. D., and Aderem, A. (1999). Toll-like receptor-2 mediates mycobacteria-induced proinflammatory signaling in macrophages. Proc Natl Acad Sci U S A *96*, 14459-63.

Uze, G., Lutfalla, G., and Gresser, I. (1990). Genetic transfer of a functional human interferon alpha receptor into mouse cells: cloning and expression of its cDNA. Cell *60*, 225-34.

van Vliet, E., Melis, M., and van Ewijk, W. (1985). Marginal zone macrophages in the mouse spleen identified by a monoclonal antibody. Anatomical correlation with a B cell subpopulation. J Histochem Cytochem *33*, 40-4.

Wagner, R. R. (1987). The Rhabdoviruses (New York, London: Plenum Press).

Walther, E. U., and Hohlfeld, R. (1999). Multiple sclerosis: side effects of interferon beta therapy and their management. Neurology *53*, 1622-7.

Wathelet, M. G., Lin, C. H., Parekh, B. S., Ronco, L. V., Howley, P. M., and Maniatis, T. (1998). Virus infection induces the assembly of coordinately activated transcription factors on the IFN-beta enhancer in vivo. Mol. Cell. *1*, 507-18.

Yeow, W. S., Au, W. C., Juang, Y. T., Fields, C. D., Dent, C. L., Gewert, D. R., and Pitha, P. M. (2000). Reconstitution of virus-mediated expression of interferon alpha genes in human fibroblast cells by ectopic interferon regulatory factor-7. J. Biol. Chem. *275*, 6313-20.

Yie, J., Merika, M., Munshi, N., Chen, G., and Thanos, D. (1999). The role of HMG I(Y) in the assembly and function of the IFN-beta enhanceosome. Embo J *18*, 3074-89.

Yoneyama, M., Suhara, W., Fukuhara, Y., Sato, M., Ozato, K., and Fujita, T. (1996). Autocrine amplification of type I interferon gene expression mediated by interferon stimulated gene factor 3 (ISGF3). J Biochem (Tokyo) *120*, 160-9.

Zhang, X., Sun, S., Hwang, I., Tough, D. F., and Sprent, J. (1998). Potent and selective stimulation of memory-phenotype CD8+ T cells in vivo by IL-15. Immunity *8*, 591-9.

Zhang, Y., Buchholz, F., Muyrers, J. P., and Stewart, A. F. (1998). A new logic for DNA engineering using recombination in Escherichia coli. Nat. Genet. *20*, 123-8.

Zhang, Y., Muyrers, J. P., Testa, G., and Stewart, A. F. (2000). DNA cloning by homologous recombination in Escherichia coli. Nat Biotechnol *18*, 1314-7.

Zhang, Y. Z., Naleway, J. J., Larison, K. D., Huang, Z. J., and Haugland, R. P. (1991). Detecting lacZ gene expression in living cells with new lipophilic, fluorogenic beta-galactosidase substrates. Faseb J *5*, 3108-13.

Zhou, A., Paranjape, J. M., Der, S. D., Williams, B. R., and Silverman, R. H. (1999). Interferon action in triply deficient mice reveals the existence of alternative antiviral pathways. Virology *258*, 435-40.

Zinkernagel, R. M., Bachmann, M. F., Kundig, T. M., Oehen, S., Pircher, H., and Hengartner, H. (1996). On immunological memory. Annu Rev Immunol *14*, 333-67.

Zouboulis, C. C., and Orfanos, C. E. (1998). Treatment of Adamantiades-Behcet disease with systemic interferon alfa. Arch Dermatol *134*, 1010-6.

6 Abbreviations

Ab(s)	antibody(ies); mAb monoclonal antibody, pAb polyclonal serum
Ag	antigen
APC	antigen presenting cell
BAC	bacterial artificial chromosome
BCR	B cell receptor
BM	bone marrow
bp	base pair
BSA	bovine serum albumin
β-Gal	beta galactosidase
CD	cluster of differentiation
cDNA	complementary DNA
CPE	cytopathic effect
CpG	prokaryotic DNA motif
CTL	cytotoxic T lymphocyte
DC	dendritic cell
DMEM	Dulbecco's Modified Eagle's Medium
DMSO	dimethylsulfoxide
DNA	deoxyribonucleic acid
DNAse	deoxyribonuclease
dNTP	2' deoxyribonucleosidetriphosphate
DTT	dithiothreitol
EDTA	ethylene-diaminetetraacetic acid
ELISA	enzyme-linked immunosorbent assay
EMCV	encephalomyocarditis virus
ES	cells embryonic stem cells
ET-Cloning	homologous recombination in bacteria expressing RecE and RecT
FACS	fluorescence activated cell sorting
FCS	fetal calf serum
FDG	fluorescein di-β-D-galactopyranoside
FITC	fluorescein isothiocyanate
FSC	forward scatter
GFP	green fluorescent protein
GM-CSF	granulocytes macrophage colony stimulating factor
HIV	human immunodeficiency virus
HSV	type I herpes simplex virus
i.p.	intraperitoneal
i.v.	intravenous
IFN	interferon
IFNAR	type I IFN receptor
Ig	immunoglobulin
IL	interleukin
IPC	professional IFN producing cell
IRES	internal ribosomal entry site
IRF	interferon regulatory factor
kb	kilobase pairs
LB	Luria Bertrami medium
LCMV	lymphocytic choriomeningitis virus
LN	lymph node

LPS	lipopolysaccharide
MACS	magnetic adsorption cell sorting
MEF	mouse embryonic fibroblast
MHC	major histocompatibility complex
moi	multiplicity of infection
mRNA	messenger RNA
MZ	marginal zone
NDV	Newcastle disease virus
NEO	neomycin resistance
NK	natural killer cell
NRF	NF-kB repressing factor
OD	optical density
PAMP	pathogen associated molecular pattern
PBS	phosphate buffered saline
PC	peritoneal cavity
PCR	polymerase chain reaction
PE	phycoerythrin
pfu	plaque forming units
PKR	double stranded RNA-dependent protein kinase R
PLAP	human placental alkaline phosphatase
poly(I:C)	synthetic double stranded RNA
PRR	pattern recognition receptor
RAG	recombination activating gene
RNA	ribonucleic acid
rpm	revolutions per minute
RPMI	Rosewell-Park-Memorial-Institute cell culture medium
RSS	recombination signal sequences
RT	room temperature
RT-PCR	reverse transcription PCR
SA	streptavidin
SDS	sodium dodecyl sulfate
SPF	specific pathogen free
SSC	side scatter
TCR	T cell receptor
tg	transgene
TLR	Toll-like receptor
Tris	Tris(hydroxymethyl)aminoethane
UV	ultraviolet
UV-HSV	UV-inactivated herpes simplex virus
VSV	Vesicular stomatitis virus
WT	wild type
YZ300	ET-recombination competent strain of $RecA^+$ bacteria

7 Erklärung

Ich versichere, daß ich die von mir vorgelegte Dissertation selbständig angefertigt, die benutzten Quellen und Hilfsmittel vollständig angegeben und die Stellen der Arbeit - einschließlich Tabellen, Karten und Abbildungen -, die anderen Werken im Wortlaut oder dem Sinn nach entnommen sind, in jedem Einzelfall als Entlehnung kenntlich gemacht habe; daß diese Dissertation noch keiner anderen Fakultät oder Universität zur Prüfung vorgelegen hat; daß sie - abgesehen von unten angegebenen Teilpublikationen - noch nicht veröffentlicht worden ist sowie, daß ich eine solche Veröffentlichung vor Abschluß des Promotionsverfahrens nicht vornehmen werde. Die Bestimmungen dieser Promotionsordnung sind mir bekannt. Die von mir vorgelegte Dissertation ist von Prof. Dr. Klaus Rajewsky betreut worden.

Köln, den 28. Februar 2001 Winfried Barchet

Teilpublikationen:

Winfried Barchet, Marina Cella, Bernhard Odermatt, Carine Asselin-Paturel, Marco Colonna and Ulrich Kalinke *"Virus-induced Interferon α Production by a Dendritic Cell Subset in the Absence of Feedback Signaling In Vivo "*

Journal of Experimental Medicine (2002), 195:507-516

Reprint siehe Appendix Seite 116*f.*

8 Zusammenfassung

Bei verschiedenen Virusinfektionen ist die Induktion einer wirkungsvollen Typ I Interferonantwort (IFN-α/β) entscheidend wichtig für das Überleben des Wirtsorganismus. *In vivo* wird der größte Teil des Typ I Interferons von einem seltenen Zelltyp produziert, der als professionelle Interferon-produzierende Zelle (IPC) bezeichnet wird. Der Phänotyp von IPCs in der viralen Pathogenese in der Maus und die molekularen Mechanismen der Typ I Interferon Produktion durch IPCs sind bisher nicht untersucht worden.

Durch Experimente an mit Newcastle disease Virus (NDV) infizierten Fibroblasten (MEFs) in der Zellkultur, wurde das Modell der autokrinen Rückkopplungsregulation der Typ I Interferonproduktion etabliert. Gemäß diesem Modell ist die Transkription der IFN-α Gene – mit der Ausnahme von IFN-α4 – sowohl von der Aktivierung des Typ I IFN Rezeptors (IFNAR), als auch von der Aktivierung der Transkription von Interferon Regulations Faktor (IRF)-7 abhängig. In einem akut infizierten Wirtsorganismus wird jedoch der größte Teil Typ I Interferon wahrscheinlich nicht von Fibroblasten produziert. Deshalb haben wir die Rolle der Rückkopplungsregulation für die Typ I Interferonproduktion in der viralen Pathogenese *in vivo* untersucht. Überraschenderweise waren mit vesikulärem Stomatitis Virus (VSV) oder mit UV-inaktiviertem Herpes Simplex Virus (UV-HSV) behandelte Mäuse in der Lage umgehend IFN-α herzustellen, und dies weit gehend unabhängig von IFNAR Aktivierung und der Transkription von IRF-7. Typ I Interferon wurde in großer Menge von wenigen Zellen produziert, die sich in der Marginalzone (MZ) der Milz befanden. Im Gegensatz dazu konnte in mit synthetischer Doppelstrang-RNA (poly(I:C)) behandelten Mäusen keine Interferonproduktion durch Zellen in der MZ festgestellt werden. Darüber hinaus war die Produktion von IFN-α in poly(I:C) behandelten Mäusen IFNAR abhängig. Diese Ergebnisse werden im Rahmen eines erweiterten Modells der IFN-α Produktion diskutiert, in dem Unterschiede der Regulation der Typ I Interferon-produktion in unterschiedlichen Zelltypen berücksichtigt wurden.

Um die professionelle IFN produzierende Zelle in der Maus zu ermitteln, wurden Reportergene unter die Kontrolle der Promotoren der Gene für IFN-α2 oder IRF-7 gestellt. Diese Transgenkonstukte wurden durch homologe Rekombination (ET-cloning) in künstlichen bakteriellen Chromosomen (BACs) integriert. Derzeit werden transgene Mäuse generiert, die diese BAC Reporterkonstrukte exprimieren. Die Analyse dieser Mäuse kann es ermöglichen, die Reifung und Differenzierung von IPCs *in vivo* zu verfolgen, und Erkenntnisse darüber zu gewinnen, ob aktivierte IPCs als Antigen präsentierende Zellen fungieren können.

In einem zweiten Ansatz zur Identifizierung von IPCs der Maus, wurden zahlreiche Zellpopulationen von CD11c positiven dendritischen Zellen (DC) aus VSV infizierten Mäusen isoliert und auf die Transkription von IFN-α mRNA untersucht. Im Gegensatz zu allen anderen untersuchten Populationen, produzierten $CD11c^{int}CD11b^{-}GR\text{-}1^{+}$ dendritische Zellen große Mengen IFN-α. Dieser Zelltyp wies eine den plasmazytoiden dendritischen Zellen des Menschen ähnliche Morphologie auf. Interessanterweise produzierten IPCs der Maus IFN-α unabhängig davon, ob sie aus VSV infizierten Mäusen mit funktionellem oder defektem IFNAR isoliert worden waren. Demnach aktiviert VSV vorrangig einen darauf spezialisierten DC Zelltyp – die IPC der Maus – welcher in der Folge große Mengen von IFN-α weitgehend unabhängig von IFNAR Rückkopplungsregulation produziert. Die Infektion mit VSV führte auf IPCs der Maus umgehend zur Aufregulation von MHC Klasse II und CD86 Molekülen, ein Charaktermerkmal von dendritischen Zellen. Im Gegensatz zu DCs verschwanden IPCs jedoch rasch aus sekundär lymphatischem Gewebe akut infizierter Mäuse. Gleichzeitig nahm die Zahl der IPCs im Knochenmark stark zu und ein leichter Anstieg der Zellzahl wurde auch in einigen der peripheren Organe beobachtet. Eine Wiederbesiedlung der Milz mit IPC Zellen fand während des Abklingens der akuten Virusinfektion statt.

Somit ist der hier beschriebene IPC Zelltyp in der Lage sofort nach viraler Aktivierung IFN-α zu produzieren und weist einige Eigenschaften von dendritischen Zellen auf. Da aktivierte IPCs jedoch die sekundären lymphatischen Organen verlassen, ist es unwahrscheinlich, dass Ihnen eine bedeutende Rolle während der Antigenpräsentation in der Anfangsphase einer adaptiven Immunantwort zukommt.

9 Kurzzusammenfassung

Eine wirkungsvolle Typ I Interferonantwort (IFN-α/β) ist entscheidend wichtig für die Kontrolle von viralen Infekten. In dieser Studie zeigen wir, dass die Produktion von IFN-α in Fibroblasten (MEFs) die mit vesikulärem Stomatitis Virus (VSV) infiziert sind, abhängig von der Aktivierung des Typ I IFN Rezeptors (IFNAR) ist. Im Gegensatz dazu ist in infizierten Mäusen eine frühe IFN-α Antwort IFNAR unabhängig. In VSV infizierten Mäusen wurde Typ I IFN von wenigen Zellen produziert, die sich in der Marginalzone (MZ) der Milz befanden. Im Gegensatz zu anderen dendritischen Zelltypen (DCs), produzieren $CD11c^{int}CD11b^{-}GR\text{-}1^{+}$ DCs große Mengen IFN-α, unabhängig davon, ob sie aus VSV infizierten Mäusen mit funktionellem oder defektem IFNAR isoliert wurden. Dieser dendritische Zelltyp wies eine den menschlichen professionellen Interferon-produzierenden Zellen (IPC) ähnliche Morphologie auf. Die VSV Infektion führte auf IPCs der Maus umgehend zur Aufregulation von MHC Klasse II und CD86 Molekülen, ein Charaktermerkmal von dendritischen Zellen. Im Gegensatz zu DCs verschwanden IPCs jedoch rasch aus sekundär lymphatischem Gewebe akut infizierter Mäuse. Demnach aktiviert VSV vorrangig IPCs zur Produktion von großen Mengen IFN-α und dies weit gehend unabhängig von der IFNAR Rückkopplungsregulation. Da aktivierte IPCs jedoch die sekundären lymphatischen Organen verlassen, ist es unwahrscheinlich, dass Ihnen eine bedeutende Rolle während der Antigenpräsentation in der Anfangsphase einer adaptiven Immunantwort zukommt.

10 Abstract

An effective type I interferon (IFN-α/β) response is critical for the control of many viral infections. Here we show that in vesicular stomatitis virus (VSV) infected mouse embryonic fibroblasts (MEFs) the production of IFN-α is dependent on type I IFN receptor (IFNAR) triggering, whereas in infected mice early IFN-α production is IFNAR-independent. In VSV infected mice type I IFN is produced by few cells located in the marginal zone of the spleen. Unlike other dendritic cell subsets (DCs), FACS-sorted $CD11c^{int}CD11b^{-}GR\text{-}1^{+}$ DCs show high IFN-α expression, irrespective of whether they were isolated from VSV infected IFNAR competent or deficient mice. This DC subset showed a morphology reminding plasmacytoid dendritic cells and similar to the human professional IFN producing cell (IPC) and was therefore termed mouse IPC. On mouse IPCs, VSV infection leads to a prompt upregulation of MHC class II and CD86 molecules, a hallmark of DC maturation. However, in contrast to DCs, IPCs rapidly disappeared from secondary lymphoid tissues of acutely virus-infected mice. Thus, VSV preferentially activates mouse IPCs to produce high-level IFN-α largely independent of IFNAR feedback signaling. Because activated IPCs apparently leave secondary lymphoid tissues, they are unlikely to constitute a major antigen presenting cell during the initial activation of the adaptive immune response.

Winfried Barchet
Jakob-Degen-Str. 14
D-73614 Schorndorf

Lebenslauf

Name	Winfried Hubertus Gerhard B a r c h e t
Geburtsdatum	15. Mai 1973
Geburtsort	Stuttgart
Familienstand	ledig
Schulbesuch	September 1979 - Juli 1983 Grundschule Schorndorf September 1983 - Mai 1992 Max-Planck-Gymnasium Schorndorf
Schulabschluß	19. Mai 1992 Allgemeines Abitur
Wehrdienst	Juli 1992 - Juni 1993 3./ Gebirgssanitätsbataillon 8 Kempten, Allgäu
Grundstudium	Oktober 1993 - September 1995 Freie Universität Berlin Fachbereich Chemie Studienfach: Biochemie
Hauptstudium	Oktober 1995 - Mai 1998 Eidgenössische Technische Hochschule Zürich, Schweiz Studienrichtung XAe: Biochemie
Diplomarbeit	Januar 1997 - Juli 1997 Institut für Experimentelle Immunologie Prof. Dr. Hans Hengartner und Prof. Dr. Rolf M. Zinkernagel
Diplom	04. Mai 1998 Diplom der ETH-Zürich mit Auszeichnung Prüfungsfächer: Biochemie, Molekular- biologie, Gen- und Enzymtechnologie, Pharmakologie, Immunologie
Praktikum	Juni 1998 - August 1998 Centers for Disease Control and Prevention (CDC), Atlanta, Georgia Prof. Dr. Don Brenner
Doktorarbeit	September 1998 - Mai 2002 PhD-fellowship des European Molecular Biology Laboratory (EMBL) für das EMBL Mouse Biology Programme, Monterotondo (Rom), Italien Dr. Ulrich Kalinke und Prof. Dr. Klaus Rajewsky

12 Acknowledgments

I would like to thank all of the people in Monterotondo, Cologne, Zürich, Heidelberg and Basel whose vital support made the work for this thesis a stimulating, multi-centered experience. In particular:

First and foremost, Ulrich Kalinke, for introducing me to the fascinating field of innate immunity while it wasn't yet fashionable, for his patience and for always taking the time to evaluate the next steps while reminding me to keep in mind the 'big picture'.

Klaus Rajewsky for his genuine interest in my progress, the vivid discussions in the 'MR–clubs' and for his role as the *Doktorvater* of this thesis.

Marion Huth for being the lively hub of the lab, for manifold assistance including sequencing and managing our SPF breedings.

Walter Witke and Liliana Minichiello for their advice, resolving my many questions of the day.

Antonella Viola and Manolis Pasparakis for our necessarily infrequent, but for me seminal discussions.

Hans Hengartner for offering his mentoring support for this thesis. Bernhard Odermatt and Lenka Vlk for their extensive collaborative effort and for sharing insights in their expertise.

Francis Stewart and the people in his laboratory for their inclusive atmosphere while I was visiting, and especially Youming Zhang and Giuseppe Testa for teaching me how to 'think recombination first'.

Marco Colonna and Marina Cella for being great teachers and for making it possible to experience the vibrant environment of the Basel Institute for Immunology. Hubertus Kohler and Tracy Hayden for expert cell sorting and Axel Bouchon for sharing the 'internal' information, which originally sparked this collaboration.

George Kolias and Jakki Kelly-Barett for microinjections of BAC-DNA, Emerald Perlas for establishing the IRF-7 in situ hybridisations, and Sandra Gessani and Patrizia Puddu for introducing me to the IFN-γ assay.

Udo Ringeisen, Daniel Browne, Russ Hodge, Maj Britt Hansen, Norbert Wey and Richard 'excelit' Butler for their patience and their help to navigate the technical quicksands.

The members of my thesis advisory committee, Fotis C. Kafatos and Gareth Griffiths for their thoughtful recommendations, gratefully extended to Jacomine Krijnse-Locker and Iain Mattaj.

Christian Bogdan for critically reading the thesis manuscript.

Rosaria, Sandra, Aga, Chryssa, Laura, Cagla, Jens, Tobias and Valeria for being friends.

My mum, my brother and the extended family for their constant support.

Lodovica for being Lodo and most everything else.

Appendix - Reprint

Virus-induced Interferon α Production by a Dendritic Cell Subset in the Absence of Feedback Signaling In Vivo

Winfried Barchet,[1] Marina Cella,[2] Bernhard Odermatt,[3] Carine Asselin-Paturel,[4] Marco Colonna,[2] and Ulrich Kalinke[1]

[1]*Mouse Biology Programme, EMBL-Monterotondo, I-00016 Monterotondo-Scalo (Roma), Italy*
[2]*Basel Institute for Immunology, CH-4005 Basel, Switzerland*
[3]*Department of Pathology, University of Zürich, CH-8091 Zürich, Switzerland*
[4]*Schering-Plough, Laboratory for Immunological Research, Dardilly T-69570, France*

Abstract

An effective type I interferon (IFN-α/β) response is critical for the control of many viral infections. Here we show that in vesicular stomatitis virus (VSV)-infected mouse embryonic fibroblasts (MEFs) the production of IFN-α is dependent on type I IFN receptor (IFNAR) triggering, whereas in infected mice early IFN-α production is IFNAR independent. In VSV-infected mice type I IFN is produced by few cells located in the marginal zone of the spleen. Unlike other dendritic cell (DC) subsets, FACS®-sorted $CD11c^{int}CD11b^{-}GR\text{-}1^{+}$ DCs show high IFN-α expression, irrespective of whether they were isolated from VSV-infected IFNAR-competent or -deficient mice. Thus, VSV preferentially activates a specialized DC subset presumably located in the marginal zone to produce high-level IFN-α largely independent of IFNAR feedback signaling.

Key words: IFN type I • virus infection • dendritic cell subsets • IFN regulatory factor 7 • type I IFN receptor

Introduction

Type I IFNs (IFN-α/β) constitute a family of cytokines comprising in the mouse at least 11 IFN-α isoforms and one IFN-β, which were identified by their ability to protect cells against viral infection (1). For a broad spectrum of viruses a functional type I IFN response is critical for the survival of the infected host (2, 3). Beyond the direct antipathogenic activity, type I IFNs synergize with other proinflammatory stimuli to activate innate effectors such as NK cells, macrophages, and dendritic cells (DCs)* (4) and may modulate antigen presentation and the adaptive immune response (5).

The biologic activity of all IFN-α subtypes and of IFN-β is mediated by binding to the common type I IFN receptor (IFNAR), a heterodimer consisting of the α-chain (IFNAR-1) and the β-chain (IFNAR-2, references 6 and 7). IFNAR signaling activates a multitude of IFN-inducible genes whose products may drastically alter cell homeostasis; in order to impede viral replication, cell proliferation is halted and both transcription and translation are strongly reduced. High-level expression of type I IFN, that can be detrimental to the host (8, 9), is tightly regulated (10) and usually restricted to the state of acute viremia.

The molecular mechanism of type I IFN induction was intensively investigated by analyzing virus-stimulated mouse embryonic fibroblasts (MEFs) derived from gene-targeted mice deficient of factors involved in the type I IFN signaling cascade. MEFs from mice lacking IFN-β, IFNAR-1, signal transducer and activator of transcription 1, or IFN regulatory factor (IRF)-9 showed a defective IFN-α response (11–14). This suggested that after the production of early IFN-β, and possibly IFN-α4, expression of other IFN-α genes was dependent on IFNAR feedback signaling. Two members of the IRF family, IRF-3 and IRF-7, have been shown to play a key role in the sequential induction of type I IFN genes. Virus-mediated serine phosphorylation leads to IRF-3 activation and translocation to the nucleus (15). There, IRF-3 is part of an enhanceosome complex promoting the expression of IFN-β, and presumably of IFN-α4. Early type I IFN is secreted and triggers IFNAR signaling in an autocrine fashion. Among

Address correspondence to Ulrich Kalinke, Dept. of Immunology, Paul-Ehrlich-Institute, Paul-Ehrlich-Str. 51-59, D-3225 Langen, Germany. Phone: 49-6103-77-2002/3; Fax: 49-6103-77-1253; E-mail: kalul@pei.de

**Abbreviations used in this paper:* CPE, cytopathic effect; CpG, prokaryotic DNA motif; DC, dendritic cell; HSV, type I herpes simplex virus; IFNAR, type I IFN receptor; IPC, IFN-producing cell; IRF, IFN regulatory factor; MEF, mouse embryonic fibroblast; MOI, multiplicity of infection; NDV, Newcastle disease virus; poly(I:C), synthetic double-stranded RNA; SPF, specific pathogen free; TLR, Toll-like receptor; VSV, vesicular stomatitis virus; WT, wild-type.

other type I IFN–induced genes, IFNAR signaling strongly upregulates IRF-7 expression (12, 13). Virus infection leads to IRF-7 activation by phosphorylation that drives the expression of the majority of IFN-α subtypes, and hence amplifies the type I IFN response. It is not known, however, which serine kinase(s) is/are responsible for the activation of IRF-3 and IRF-7. It appears that several pathways may lead to IRF-3 and IRF-7 activation. Some viruses, such as type I herpes simplex virus (HSV), induce an IFN response independent of viral replication whereas others, e.g., vesicular stomatitis virus (VSV), lose the ability to induce type I IFN upon inactivation. Furthermore, a variety of nonviral IFN inducers has been described, including prokaryotic DNA motifs (CpG-DNA), synthetic double-stranded RNA (poly[I:C]), lipopolysaccharide, and imiquimod derivatives (16, 17).

In cell culture, virtually any cell type can produce type I IFN in response to appropriate stimulation, yet, depending on the expression of pattern recognition receptors distinct cell types are stimulated by different IFN inducers. For example CpG-DNA but not poly(I:C)–treated human $CD11c^-$ DCs produce type I IFN, whereas a reverse correlation was found for $CD11c^+$ DCs (17, 18). Accordingly, $CD11c^-$ DCs express the Toll-like receptor (TLR)-9 and $CD11c^+$ DCs express TLR-3 (17, 19), which have been shown to be involved in the recognition of CpG or poly(I:C), respectively (20, 21). So far, the major IFN-producing cell (IPC) has not been defined in the context of infection with specific pathogens. Several studies addressed the nature of the human IPC (22–24), which eventually was defined as the subset of $CD11c^-$ plasmacytoid DCs (25, 26). There are indications that upon stimulation of mice certain macrophages (27) or DC subsets can produce type I IFN (28–30).

Considering the above information, in an acutely infected host fibroblasts presumably do not produce the majority of type I IFN. Therefore, we investigated whether the positive feedback regulation of type I IFN induction, as identified in MEFs, also plays a role in viral pathogenesis in vivo. Surprisingly, VSV- and UV-HSV–treated mice mount early IFN-α responses largely independent of IFNAR feedback signaling. We provide evidence that unlike fibroblasts, mouse IPCs can produce early IFN-α independent of IFNAR signaling. These data are discussed in the context of an extended model of IFN-α induction based on the cell type involved in the production of IFN-α.

Materials and Methods

Mice and Viruses. IFNAR-deficient mice ($IFNAR^{-/-}$) on the SV129 background (3) and IFN-$\beta^{-/-}$ mice on the Balb/c background (14) were bred under specific pathogen free (SPF) conditions. Unmutated SV129 mice (referred to as wild-type [WT]) were obtained from the SPF-breeding colony of the European Mutant Mouse Archive (EMMA), Monterotondo, Italy. C57BL/6 mice were purchased at IFFA-Credo. Experimental mouse work was done under SPF conditions in compliance with regulations of the Ministerio della Sanità, Rome, Italy (decreto ministeriale n° 15/2001-b, 3/3.1). VSV-IND (Mudd-Summers isolate) was originally obtained from D. Kolakofsky, University of Geneva, Geneva, Switzerland. VSV was grown on BHK-21 cells (31) and plaqued on Vero cells. Stocks were maintained in MEM containing 2% heat-inactivated FCS. HSV strain F originally obtained by American Type Culture Collection was grown on Vero cells. HSV was purified from cell culture supernatant by PEG 40.000 (Serva) precipitation. After several pelleting steps for 1 h at 43,000 *g* virus was resuspended in PBS and titrated on Vero cells. After UV irradiation (1.2 Joule/cm^2) HSV inactivation was verified by plaquing on Vero cells.

Cell Culture. WT and $IFNAR^{-/-}$ MEFs were derived from day 13 embryos (32) and maintained in DMEM supplemented with 10% FCS. Cell monolayers were infected with VSV at a multiplicity of infection (MOI) of 10. After 1 h of incubation at 37°C the virus suspension was replaced by DMEM 10% FCS.

Expression Analysis. Preparation of total RNA was performed using the TRIZOL reagent (GIBCO BRL) according to the manufacturer's instructions. Tissue samples were snap-frozen and homogenized in Trizol using a Polytron (Kinematica). On cultured cell monolayers and FACS®-sorted cells Trizol was applied directly. To eliminate possible DNA contamination total RNA was incubated for 15 min at 37°C with 10 U of DNase (Boehringer Mannheim). cDNA was prepared using Superscript II (GIBCO BRL) according to the manufacturer's instructions. To estimate relative amounts of specific mRNAs, PCRs were performed with serially fivefold diluted cDNA using published primers for IFN-α (consensus primers annealing with all IFN-α subtypes) and IRF-7 (13). The mRNA content was normalized by RT-PCR analysis with GAPDH-specific primers from the same publication. The absence of contaminating DNA was verified by PCR analysis of RNA preparations not treated with reverse transcriptase.

Quantification of IFN Activity. The IFN bioassay was based on the protection of L929 cells from the cytopathic effect (CPE) of VSV (CPE inhibition assay). To inactivate potential viral contamination, 1:5 prediluted serum samples from VSV-infected mice were UV-irradiated with 1.2 Joule/cm^2. Duplicates of serially twofold diluted sera were transferred to 24 h preincubated semiconfluent monolayers of L929 cells in 96-well plates. After 24 h incubation at 37°C supernatants were removed and VSV was added at a MOI of 0.05. After 48 h incubation at 37°C, supernatants were taken away and protected cells were stained with 0.5% crystal violet in 5% formaldehyde, 50% ethanol, and 0.8% sodium chloride. After extensive washing with water and air drying, the dye was extracted from stained cells with 100 μl/well 0.1 M sodium citrate in 50% ethanol, pH 4.2, and the crystal violet content was determined on an ELISA reader at 570 nm. In the CPE inhibition assay an international mouse IFN-α/β reference standard of 100 IU/ml (Gu02–901–511; NIAID Repository) and recombinant IFN-αA standards (PBL Biomedical Laboratories) of 100, 500, 2,500, and 10,000 IU/ml were included. For IFN quantification the 50% protective serum dilution was indicative. A $\log_2 5$ titer corresponded to 1,000 IU IFN-αA. The contribution of IFN-β or IFN-α to the total type I IFN activity was determined by preincubating sera for 1 h with excess amounts of neutralizing anti–IFN-α (clone 4E-A1; Yamasa Shoyu) or anti-IFN-β (clone 7F-D3; Yamasa Shoyu) mAbs. Protection from CPE due to IFN-γ was formally excluded by an IFN-γ Elisa (Promega) indicating that the IFN-γ content of all samples tested was below the detection threshold of the assay.

Immunohistochemistry. Freshly removed organs were immersed in HBSS and snapped frozen in liquid nitrogen. Tissue

sections of 5-μm thickness were cut in a cryostat, placed on siliconized glass slides, air dried, fixed with acetone for 10 min, and stored at –70°C. IFN was stained using a polyclonal sheep anti–mouse IFN-α/β antiserum (PBL Biomedical Labs) or monoclonal rat anti–mouse IFN-α antibody (Serotec). The primary sheep antibody was detected with affinity purified biotinylated donkey anti–sheep Ig antibodies (Jackson ImmunoResearch Laboratories) and alkaline phosphatase labeled avidin/biotin complexes (ABC/AP Dako). The primary rat mAb was detected with affinity purified peroxidase labeled goat anti–rat Ig antibody. For signal amplification by catalyzed reporter deposition, biotinylated thyramine (33) and 3% H_2O_2 was added for 7 min, and covalently bound biotin was revealed by ABC/AP. Alkaline phosphatase was visualized using naphthol AS-BI (6-bromo-2-hydroxy-3-naphtholic acid-2-methoxy anilide) phosphate and new fuchsin as substrate. Endogenous alkaline phosphatase was blocked by levamisole. The dilutions of secondary antibodies were made in TBS containing 5% normal mouse serum. Incubations were done at room temperature for 30 min; TBS was used for all washing steps. Color reactions were performed at room temperature for 15 min with reagents from Sigma-Aldrich. Sections were counterstained with hemalum and coverslips mounted with glycerol and gelatin.

In Situ Hybridization of IRF-7 mRNA. Spleens were fixed overnight in 4% paraformaldehyde in PBS and then embedded in paraffin wax. Sections were cut at 5–7-μm and mounted onto Superfrost-Plus slides (BDH). The IRF-7 riboprobe was generated by cloning a 351 bp RT-PCR product into pBluescript followed by Digoxygenin-11-UTP-labeling using the Boehringer RNA labeling kit. In situ hybridization was performed as described previously (34).

DC Subset Isolation by FACS® Sorting. Single cell suspension of 3–5 spleens was prepared and $CD11c^+$ cells were enriched by magnetic adsorption cell sorting (MACS®; Miltenyi Biotec). Three-color stainings were made using anti-CD11c–biotin–, anti-CD11b–FITC–, and anti-GR-1–PE–conjugated mAbs followed by streptavidin-APC (all from BD PharMingen). 4–10 × 10^4 cells of each subset were sorted from ~10^7 cells on a MoFlo cytometer (Cytomation).

Results

Feedback Signaling Is Required for the Expression of IFN-α mRNA in VSV-infected MEFs but not in VSV-infected Mice. Tissue culture experiments have shown previously that the expression of all IFN-α genes, except IFN-α4, was dependent on IFNAR feedback signaling in Newcastle disease virus (NDV)-stimulated MEFs (12, 13). To validate this finding under conditions of a productive virus infection, IFNAR competent (WT) and IFNAR-deficient ($IFNAR^{-/-}$) MEFs were VSV-infected and IFN-α mRNA expression was monitored by RT-PCR analysis. WT fibroblasts showed elevated IFN-α mRNA levels beginning 4 h after VSV infection and peak expression between 9 h and 12 h (Fig. 1 a). Similar to NDV-stimulated MEFs, VSV-infected MEFs predominantly expressed IFN-α4 as determined by subcloning of RT-PCR products and sequence analysis of random clones (Fig. 2 a). In contrast, IFN-α upregulation was not observed in VSV-infected MEFs lacking the IFNAR (Fig. 1 a). Thus, in VSV-infected MEFs the IFN-α production is strictly dependent on IFNAR feedback signaling.

To next examine IFN responses in vivo, IFN-α gene expression was analyzed in spleen from WT and $IFNAR^{-/-}$ mice infected with VSV. Surprisingly, IFN-α mRNA was induced rapidly and to a similar extent in spleen of WT and $IFNAR^{-/-}$ mice. At later time points, IFN-α expression in spleen of $IFNAR^{-/-}$ mice decreased slightly, whereas spleen from WT mice showed a further increase in IFN-α expression (Fig. 1 b). The IFN-α subtype analysis revealed that both VSV-infected IFNAR-competent and -deficient

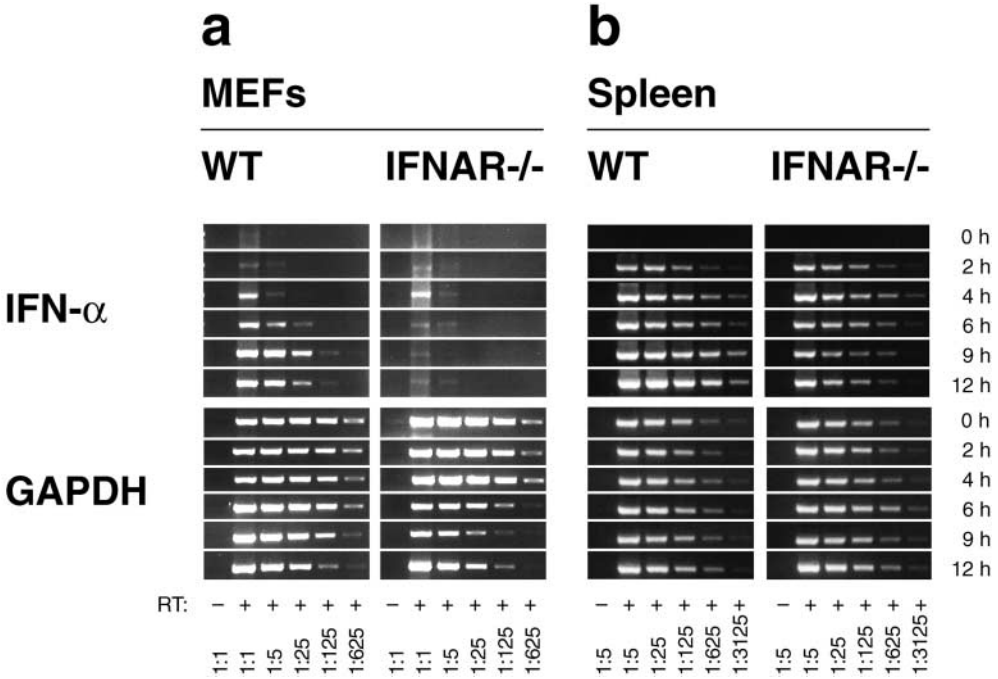

Figure 1. VSV infection stimulates IFNAR-independent production of IFN-α in mice, but not in MEFs. (a) MEFs derived from WT or IFNAR-deficient mice ($IFNAR^{-/-}$) were infected with VSV at a MOI of 10 and (b) WT and $IFNAR^{-/-}$ mice were intravenously injected with 2 × 10^8 PFU VSV. Total RNA of 10^6 cultured MEFs or of spleen tissue was extracted, and the mRNA content of different samples was normalized by a GAPDH-specific RT-PCR. The expression of IFN-α mRNA was monitored using consensus primers amplifying all IFN-α subtypes. The analysis was performed with serially fivefold diluted cDNA samples starting with undiluted material; spleen derived samples were fivefold prediluted.

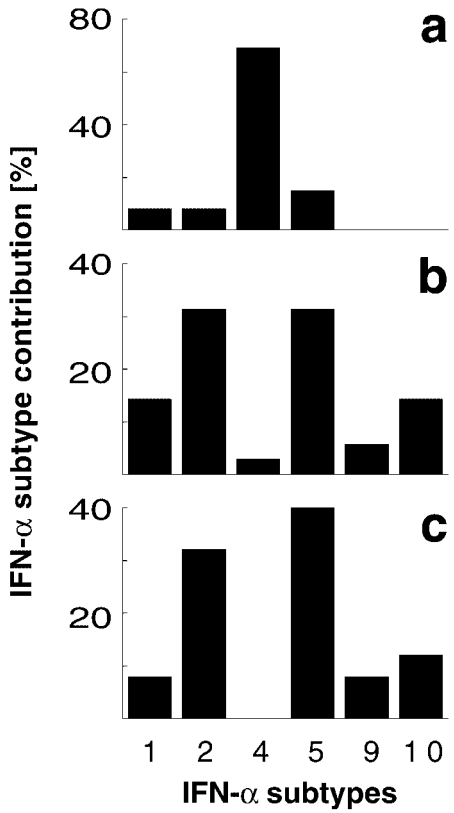

Figure 2. Differential IFN-α expression profiles of VSV infected MEFs and mice. PCR products of the IFN-α expression analysis 6 h after VSV infection of (a) WT MEFs, (b) spleen of WT mice, or (c) spleen of IFNAR$^{-/-}$ mice were subcloned and DNA sequence of 13, 35, and 25 single clones was analyzed, respectively. IFN-α sequences were classified according to EMBL database entries. The sequence termed IFN-α10 corresponds to the IFN-α/β sequence available on the EMBL database (GenBank/EMBL/DDBJ accession no. L38698).

mice showed abundant expression of IFN-α2 and 5, whereas IFN-α4 was found only rarely (Fig. 2 b and c). Thus, different IFN-α patterns found after VSV infection of MEFs and mice suggested that in vivo the majority of IFN-α is produced by a cell type different from fibroblasts. Moreover, similar IFN-α patterns found in WT and IFNAR$^{-/-}$ mice indicated a largely feedback-independent production of early IFN-α in VSV-infected mice.

Early IFNAR-independent and Late IFNAR-dependent IFN-α Expression in VSV- and UV-HSV–treated Mice. To correlate IFN-α mRNA levels and IFN serum activities, blood serum of VSV-infected mice was taken and analyzed in a CPE inhibition assay. As early as 4 h after VSV infection IFN activity was found in the serum of both WT and IFNAR$^{-/-}$ animals. Specific inhibition of IFN-α and/or IFN-β by neutralizing mAbs in the CPE inhibition assay revealed a major contribution of IFN-α to the serum IFN activity, irrespective of whether IFNAR signaling was functional or not. Serum IFN titers of WT animals increased more rapidly than IFNAR$^{-/-}$ mice eventually leading to ~30-fold higher IFN titers in WT animals than in IFNAR$^{-/-}$ mice (Fig. 3 a).

Since VSV replication is not controlled in IFNAR-deficient mice, a highly elevated virus load and increased cell death could have interfered with cytokine production in IFNAR$^{-/-}$ mice. Thus, we next analyzed type I IFN responses after stimulation with nonreplicating virus. Since UV-inactivated VSV does not induce type I IFN responses (data not shown), mice were injected with UV-inactivated HSV. 2 h after the treatment, WT and IFNAR$^{-/-}$ mice showed similar peak IFN activity with ~50 and 35% IFN-α contribution, respectively. While the IFN response was short-lived in IFNAR$^{-/-}$ mice, IFN titers in WT mice were sustained for several hours, and a switch to a more pronounced IFN-α expression was found (Fig. 3 c). To verify the induction of early IFN-α in the absence of IFNAR-feedback signaling, mice deficient of the IFNAR or IFN-β were intercrossed and IFNAR$^{-/-}$ IFN-β$^{-/-}$ double-knockout mice and IFNAR$^{+/-}$ IFN-β$^{-/-}$ littermates were stimulated with UV-HSV. Even in the absence of IFN-β initial IFN-α titers showed the same magnitude in receptor deficient and competent mice. At later time points IFN-α production was sustained and further enhanced in IFN receptor competent mice as compared with IFNAR$^{-/-}$ mice (Fig. 4). Thus, upon treatment with live VSV- or UV-inactivated HSV early IFNAR-independent IFN-α production is observed. Yet, at later time points IFNAR-feedback signaling is critical to sustain the production of IFN-α.

Early IFN-α Production in the Absence of IRF-7 Induction. The transcription factor IRF-7 has been shown to be upregulated upon IFNAR triggering (12, 13) and was proposed to be critically required for the expression of IFN-α subtype genes (12, 35). Therefore, we asked whether early IFNAR-independent IFN-α was produced in the absence of IRF-7 induction. The RT-PCR analysis of IRF-7 mRNA levels in VSV-infected WT and IFNAR$^{-/-}$ mice revealed a prompt IRF-7 upregulation only in WT mice but not in IFNAR-deficient mice (Fig. 5). These experiments indicated that in VSV-infected mice early IFN-α was induced in the absence of detectable IRF-7 upregulation. At later time points IFNAR-independent IRF-7 upregulation was observed (data not shown) which, however, did not suffice to promote a sustained production of IFN-α in IFNAR$^{-/-}$ mice.

Poly(I:C) Treatment of Mice Induces Late IFN-α Production. To further study the role of feedback signaling with a nonreplicating type I IFN inducer, mice were treated with poly(I:C). Sera of poly(I:C)–treated WT and IFNAR$^{-/-}$ mice displayed early peak IFN activity, followed by a rapid decline in the case of IFNAR$^{-/-}$ mice. In WT mice IFN activity was sustained at a high level for >20 h. Neutralization of IFN-α and/or IFN-β revealed an abundant contribution of IFN-β to early type I IFN activity in both WT and IFNAR$^{-/-}$ mice. At later time points, strong IFN-α production was observed in WT but not in IFNAR-deficient mice (Fig. 3 b).

Preferential production of IFN-β after poly(I:C) treatment, while mainly IFN-α is produced after virus stimulation, indicates that different cell types may be involved in the

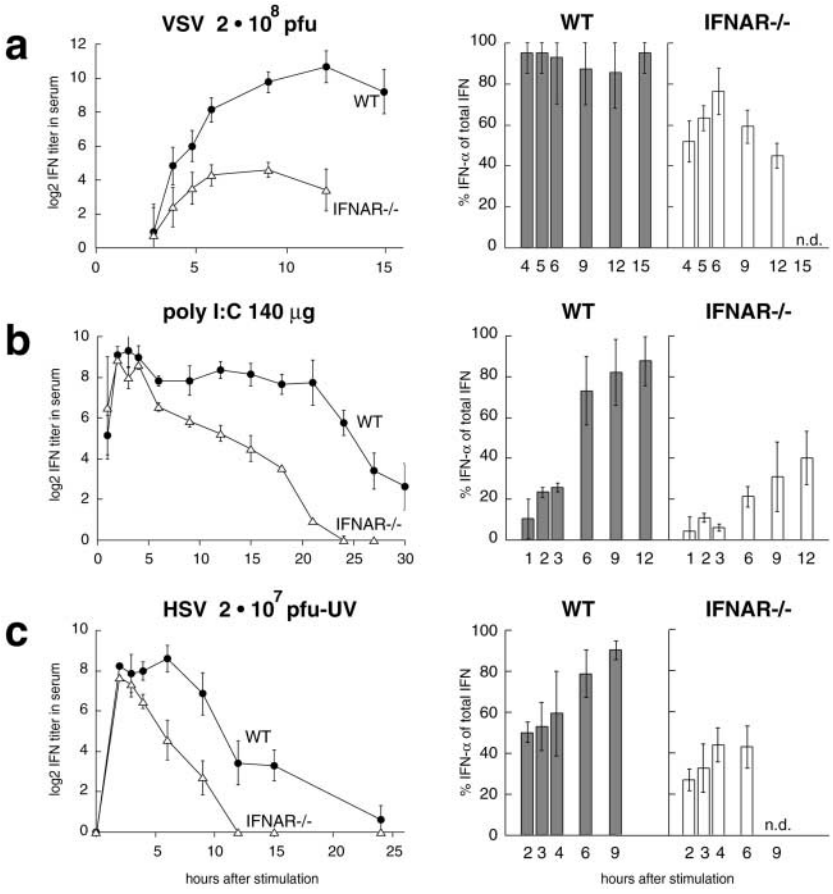

Figure 3. Type I IFN activity in the serum of mice treated with VSV, poly(I:C), or UV-HSV. WT mice (black circles) and IFNAR$^{-/-}$ (white triangles) mice were intravenously stimulated with (a) 2×10^8 PFU VSV, (b) 100 μg poly(I:C), or (c) 2×10^7 PFU UV-HSV. Mice were bled at the indicated time points and serum IFN titers were determined in a CPE protection assay. A $\log_2$ of 5 corresponds to 1,000 IU of IFN-α. The contribution of IFN-α or IFN-β to the total IFN activity was determined by specific inhibition with mAbs.

production of poly(I:C)– versus virus-induced type I IFN. Moreover, these results further support the hypothesis that the sustained production of IFN-α is IFNAR dependent.

VSV Infection but not Poly(I:C) Treatment Stimulates High-Level Type I IFN Production in Cells Located in the Marginal Zone of the Spleen. To localize IPCs, mice were infected with VSV and 9 h later, spleens were analyzed immunohistochemically with type I IFN-specific antibodies. Consecutive sections were stained with polyclonal antibody directed against type I IFN or with an IFN-α–specific mAb. While staining with the polyclonal serum appeared more sensitive and decorated a structure surrounding follicles, i.e., the marginal zone, stainings with mAb revealed distinct type I IPCs scattered in groups within the marginal zone (Fig. 6 a and b). After treatment with VSV or UV-HSV, spleens of WT and IFNAR$^{-/-}$ mice showed similar marginal zone stainings with polyclonal antibody, albeit staining of spleens from IFNAR-deficient mice was somewhat weaker (Fig. 6 c). Despite comparable IFN levels in the serum, no specific type I IFN staining was detected in the marginal zone of poly(I:C)–treated mice (Fig. 6 c). Thus, after injection of virus particles, irrespective of whether they are replicative or not, type I IFN production is localized to the marginal zone. The soluble inducer poly(I:C) did not induce high enough type I IFN produc-

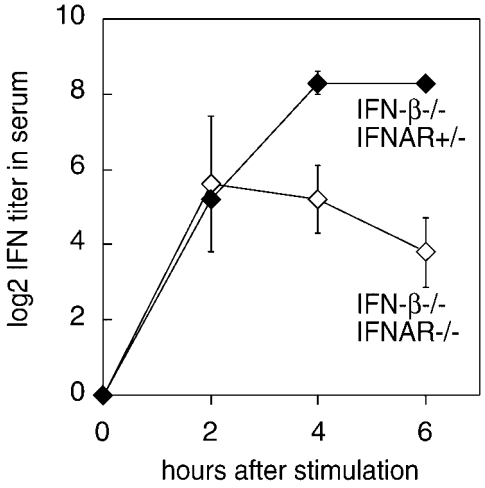

Figure 4. IFN-α is produced in mice deficient of IFN-β and IFNAR. IFN-β–deficient mice (black diamonds) and double-deficient mice lacking IFN-β and IFNAR (white diamonds) were intravenously injected with 2×10^7 PFU UV-HSV. Sera were taken at indicated time points and analyzed in a CPE protection assay. Mean IFN activity of three mice per time point is indicated. Results are shown of one out of two independent experiments. Note that the indicated IFN serum activities exclusively derived form IFN-α because the analyzed mice were IFN-β deficient.

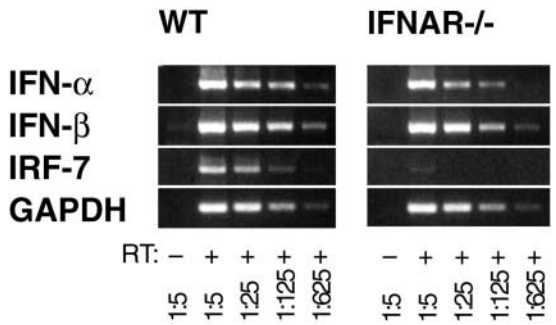

Figure 5. VSV infected IFNAR$^{-/-}$ mice show an early induction of IFN-α before the onset of IRF-7 expression. Total RNA from spleen of IFNAR$^{-/-}$ or WT mice was isolated 3 h after intravenous infection with 2×10^8 PFU VSV. RT-PCR was performed as described in Fig. 1.

tion in the spleen to be detected by immunohistology. Probably under these conditions type I IFN is produced at a low level by numerous cell types and in various tissues.

In situ hybridization of spleen sections of untreated mice, with an IRF-7 probe, did not reveal evidence for constitutive IRF-7 expression, neither in few marginal zone cells nor anywhere else in the spleen (data not shown). After VSV infection of WT mice a strong IRF-7 induction was observed all over the spleen. In contrast, no IRF-7 induction was detected in spleens of VSV-infected IFNAR$^{-/-}$ mice (Fig. 6 d). Together with the above RT-PCR data these observations indicate that virus-induced early IFN-α can be produced independent of IFNAR signaling and IRF-7 upregulation.

Identification of the Major IPC. The phenotype of the major IPC in VSV pathophysiology is not known. Since the marginal zone is a complex tissue containing specialized macrophages, DCs, endothelial cells, and nonrecirculating B cells, colocalization studies with markers for marginal zone cells could not further resolve the nature of mouse IPCs (data not shown). In analogy to the DC origin of human and mouse IPCs (25, 26, 29, 30) we aimed for the analysis of mouse DC subsets. Mice were VSV-infected and, 9 h later, several CD11c$^+$ DC subsets were FACS®-sorted and analyzed for the IFN-α mRNA content (Fig. 7 a). Surprisingly, only CD11c^{int}CD11b$^-$GR-I$^+$ DCs (fraction D) were strongly positive for IFN-α mRNA, whereas neither lymphoid DCs (CD11c$^+$CD11b$^-$, fraction A), myeloid DCs (CD11c$^+$CD11b$^+$, fraction B), CD11c^{int} CD11b$^+$ DCs (fraction E), nor granulocytes (CD11c$^+$GR-1$^+$, fraction F) showed high IFN-α expression (Fig. 7 b). CD11c^{int}

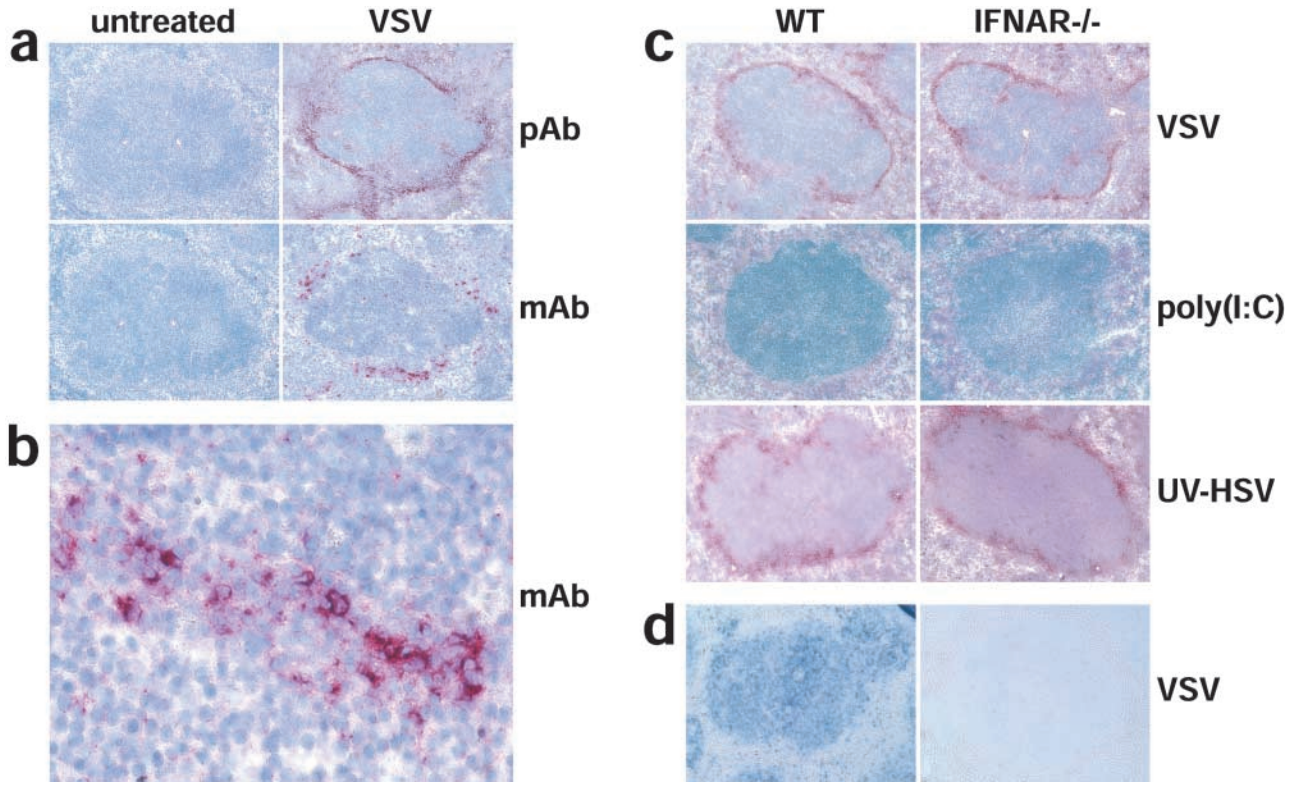

Figure 6. VSV and UV-HSV injection, but not poly(I:C) stimulation, leads to high-level production of type I IFN by cells located in the marginal zone of the spleen. (a) WT mice were VSV infected and after 9 h spleens were analyzed immunohistochemically with a polyclonal serum against type I IFN (pAb, top two panels) or with an IFN-α–specific mAb (mAb, bottom two panels). (b) A higher magnification of the marginal zone area of the bottom right panel in (a) stained with mAb is shown. (c) WT and IFNAR$^{-/-}$ mice were VSV, poly (I:C), or UV-HSV injected. After 9 h and 6 h after UV-HSV stimulation, spleens were analyzed immunohistochemically with a polyclonal serum against type I IFN. Sections in (a–c) were counterstained with hemalum (blue) to visualize lymph follicles. (d) In situ hybridization of IRF-7 mRNA (blue) was performed on paraffin sections of spleen from WT and IFNAR$^{-/-}$ mice prepared 9 h after VSV infection.

$CD11b^-$ DCs (fraction C) showed slightly enhanced IFN-α mRNA levels (which were at least 125-fold lower than fraction D), that might be due to contaminating cells of fraction D. We next asked whether $CD11c^{int}CD11b^-GR\text{-}I^+$ cells are producers of IFN-α independent of IFNAR feedback signaling. For this purpose DC subsets were isolated from VSV-infected $IFNAR^{-/-}$ mice. Again only $CD11c^{int}$ $CD11b^-GR\text{-}I^+$ cells showed high-level IFN-α mRNA (Fig. 7 c). These results indicate that although other DC subsets are able to produce IFN-α upon in vitro stimulation (28), they do not play a major role in IFN-α production after VSV infection in vivo.

Discussion

Here we show that after viral infection of mice not only IFN-β but also IFN-α is produced immediately and largely independent of IFNAR feedback signaling. This is in contrast to the current model of IFNAR feedback-dependent expression of IFN-α, that was established based on in vitro data. To reconcile the previous in vitro data with our in vivo observations, we hypothesized that after viral infection of mice a cell type different from fibroblasts, i.e., the murine IPC, produced the majority of type I IFN, and that in these cells IFN-α expression was regulated differently than in fibroblasts. Indeed, we found that after in vivo infection the subset of $CD11c^{int.}GR\text{-}1^+$ DCs produced IFN-α at high level, and that early IFN-α production by this cell type was largely independent of IFNAR feedback.

The positive feedback regulation of IFN-α genes was first observed in NDV-infected MEFs that lack IFN-α expression in the absence of a functional IFN signaling cascade (11, 12). One study showed IFNAR-independent IFN-α4 expression in NDV-infected MEFs (13). Interestingly, IFN-α4 was previously found to dominate IFN-α responses of NDV-stimulated L929 fibroblasts (36). However, MEFs infected with VSV (Fig. 1), or vaccinia virus (37) showed a strictly IFNAR-dependent expression of all IFN-αs. Equally, Sendai virus-infected MEFs from IFN-β–deficient mice were found unable to produce any IFN-α, unless stimulated by the addition of exogenous IFN-β (14).

In contrast to these in vitro data, we found that VSV-infected mice mount an early IFNAR-independent IFN-α response. Furthermore, IFN-β–deficient and IFN-β/IFNAR double-deficient mice treated with UV-HSV still expressed substantial IFN-α levels (Fig. 4). While IFN-α production in $IFN\text{-}\beta^{-/-}$ mice could have been promoted by priming with natural type I IFN, produced pathogen independently (38), IFN-α production in IFN-β/IFNAR double-deficient mice indicated that IFNAR triggering was not a prerequisite for early IFN-α production. IFN-α levels reached in $IFN\text{-}\beta^{-/-}$ were sufficient to control intravenous VSV infection (data not shown). In contrast, IFN-β–deficient mice infected peripherally with vaccinia virus showed a markedly increased susceptibility to lethal disease (37): after intranasal infection, $IFN\text{-}\beta^{-/-}$ mice showed up to 10^5-fold increased virus titers in the lung as compared

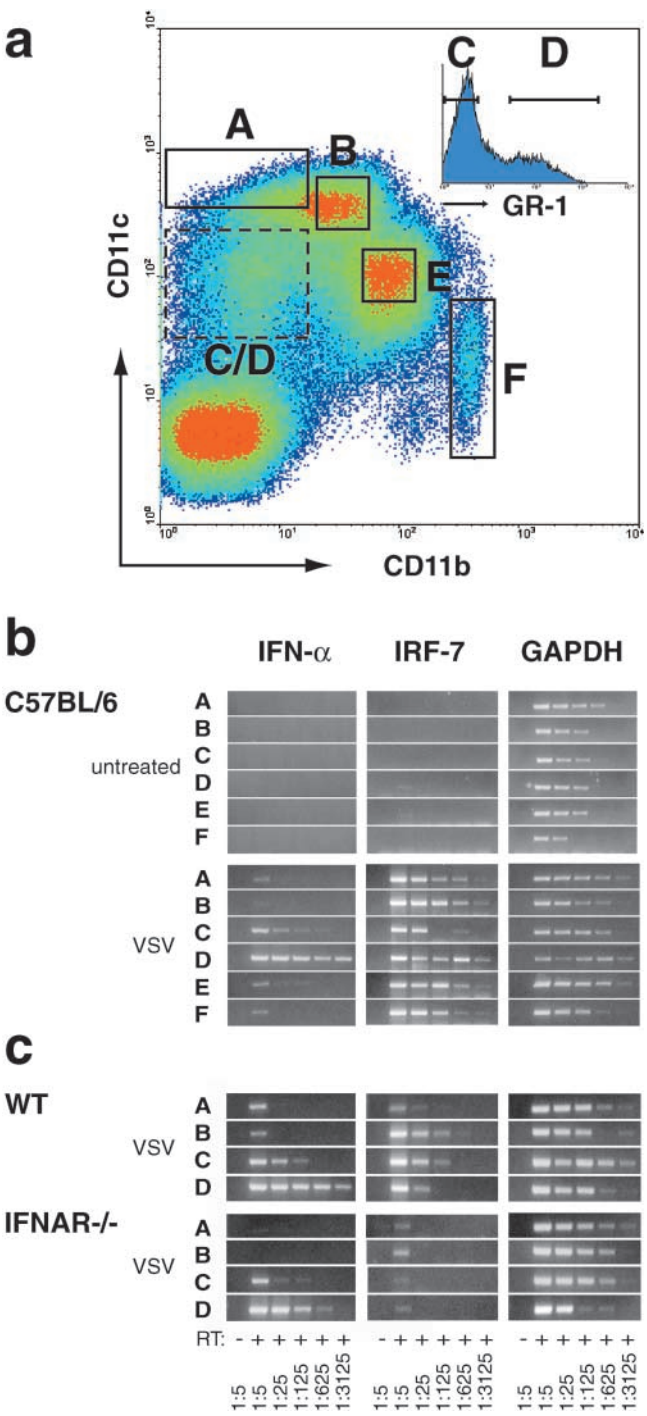

Figure 7. In VSV-infected mice $CD11c^{int}CD11b^-GR\text{-}1^+$ DCs express high-level IFN-α. (a) Mice were intravenously infected with 2×10^8 PFU VSV and 9 h later spleens were removed to prepare single cell suspensions. MACS®-enriched $CD11c^+$ cells were stained with anti-CD11c-Biot./Str.-APC, anti-CD11b-FITC, and anti-GR-1-PE, and DC subsets were FACS®-sorted using the indicated gates A–F. Cells from gate C/D were further subdivided by separating $GR\text{-}1^-$ (fraction C) and $GR\text{-}1^+$ cells (fraction D). Sorted fractions were derived from spleen of (b) VSV infected or untreated C57BL/6 mice, and of (c) VSV-infected Sv129 (WT) and $IFNAR^{-/-}$ mice. Total RNA of ~4–10 × 10^4 sorted cells was prepared and analyzed by RT-PCR as described in Fig. 1.

with WT mice, and eventually succumbed to the infection. Interestingly, in these experiments virus titers in spleen of WT and IFN-$\beta^{-/-}$ mice were comparably low, indicating that upon local infection vaccinia virus replication was better controlled in the spleen than in the peripherally infected organ. Thus, it appears that depending on the route of infection virus may activate IPCs or other susceptible cell types that differ in their requirement of IFNAR feedback for the IFN-α induction.

Apart from the route of infection also the nature of the stimulus may determine the cell type(s) involved in type I IFN production. Our histology data show that poly(I:C) does not induce marginal zone IPCs to produce high-level type I IFN, suggesting that the observed IFN titers were contributed mainly by nonIPCs. It is possible that in analogy to the human plasmacytoid DCs, mouse IPCs express TLR-9 but not TLR-3 that is involved in poly(I:C) recognition (19, 21), and thus mouse IPCs are not triggered by poly(I:C). IFN titers in poly(I:C)–treated mice showed an early peak of IFN-β expression that only in animals with a functional receptor feedback was followed by sustained IFN-α expression. This indicated that similar to in vitro VSV-infected MEFs, IFN-α expression by nonIPCs in vivo required IFNAR feedback signaling.

In the current model of positive feedback regulation, IFNAR-dependent upregulation of the transcription factor IRF-7 plays a central role. Virus-treated mutant MEFs that failed to induce IRF-7 also lacked expression of IFN-α. The IFN-α response could be restored by ectopic expression of IRF-7 (12). In IFNAR-deficient mice, we observed early IFN-α responses in the absence of detectable IRF-7 upregulation. One possibility is that under these conditions low constitutive IRF-7 levels suffice to drive early IFN-α expression. In this context it is worth noting that in all RT-PCR experiments, unlike other DC subsets, $CD11c^{int}CD11b^{-}GR\text{-}1^{+}$ DCs (fraction D) showed some background IRF-7 expression already in uninfected WT mice (Fig. 7 b). Alternatively, IPCs might be able to utilize an IRF-7–independent pathway for IFN-α expression, as suggested by the recent finding, that ectopic expression of IRF-5 can substitute for IRF-7 to allow expression of certain IFN-α genes (39). Ultimately, only the generation and analysis of IRF-7–deficient mice can define the role of IRF-7 in the expression of virus-induced IFN-α in vivo.

Our immune histological analysis of VSV-infected mice revealed that IPCs are predominantly located in the marginal zone. Similarly, we and others have found the same IPC distribution in UV-HSV–treated mice (27, 40). The importance of the marginal zone for pathogen surveillance was demonstrated by the scavenger function of marginal zone cells, which can retain microscopically small particles, including pathogens, from the blood (41). Mice that were experimentally depleted of macrophages in the marginal zone (42), and osteopetrotic (op) mutant mice that are M-CSF deficient and lack the same macrophage populations, showed an increased sensitivity to pathogen infection (43). Thus, in order to be stimulated early in the course of an infection it appears "reasonable" that IPCs are located in the marginal zone. From histological colocalization studies it had been concluded that $MOMA\text{-}1^{+}$ metallophilic and $ERTR\text{-}9^{+}$ marginal zone macrophages might be involved in type I IFN production (27). Since we could not observe a strict correlation of MOMA-1 and ERTR-9 versus IFN-α/β stainings, and after recent evidence that the human and mouse IPC are plasmacytoid DCs (25, 26, 29, 30), we FACS®-sorted several DC subsets from spleen of VSV-infected mice and analyzed them for IFN-α mRNA expression. These experiments indicated that the subset of $CD11c^{int}CD11b^{-}GR\text{-}1^{+}$ DCs showed high IFN-α mRNA levels. Interestingly, we did not find increased levels of IFN-α message in myeloid or lymphoid DCs (fractions A and B, respectively) isolated from VSV-infected mice, as could have been expected form recent in vitro data (28).

In conclusion, we suggest to extend the current model of IFNAR feedback dependent expression of IFN-α as follows. (i) In vivo, local infections may stimulate the production of mainly IFN-β by nonIPCs to protect surrounding tissues in a paracrine fashion. These cells produce IFN-α IFNAR dependently, i.e., only if sufficient autocrine type I IFN stimulation is provided. (ii) Systemic infection and acute viremia that require a generalized antiviral state may stimulate IPCs to produce IFN-α early and at high-level independent of IFNAR feedback signaling; however, IFNAR feedback defines the magnitude and duration of sustained IFN-α production.

To our knowledge, we present the first set of ex vivo data defining IPCs in viral pathogenesis. Our results support the concept that highly specialized DCs, located in the marginal zone, produce type I IFN upon pathogen contact. The observation that early IFN-α production of mouse IPCs is largely independent of IFNAR signaling indicates a less stringently regulated IFN-α expression in IPCs as compared with other cell types. Further experiments will reveal, whether, depending on the tissue tropism and the stimulation mechanism, different pathogens may activate discrete cell populations to produce type I IFN, and whether mouse IPCs do play a role in antigen processing and presentation. A better understanding of the role of IPCs in viral pathophysiology can have important diagnostic and therapeutic implications, as exemplified by publications showing reduced IPC counts in HIV-infected AIDS patients (44, 45).

Submitted: 2 October 2001
Revised: 30 November 2001
Accepted: 7 December 2001

We thank M. Huth, L. Vlk, N. Wey, and E. Perlas for technical assistance, T. Hayden and H. Kohler for expert cell sorting, S. Weiss for providing IFN-β–deficient mice, G. Schönrich and M. Raftery for providing HSV, M. Ferrantini and F. Belardelli for showing us the method of the CPE inhibition assay, K. Rajewsky for helpful suggestions, and P. Seiler and P. Aichele for critical comments on the manuscript.

This work was supported in part by the Max Planck Research Award to K. Rajewsky. The Basel Institute for Immunology was

founded and supported by F. Hoffmann-La Roche AG, Basel, Switzerland.

References

1. Isaacs, A., and J. Lindenmann. 1957. Virus interference. I. The interferon. *Proc. R. Soc. Lond.* 147:258–267.
2. Gresser, I., M.G. Tovey, C. Maury, and M.T. Bandu. 1976. Role of interferon in the pathogenesis of virus diseases as demonstrated by the use of anti-interferon serum. II. Studies with herpes simplex, Moloney sarcoma, vesicular stomatitis, Newcastle disease, and influenza viruses. *J. Exp. Med.* 144: 1316–1323.
3. Muller, U., U. Steinhoff, L.F. Reis, S. Hemmi, J. Pavlovic, R.M. Zinkernagel, and M. Aguet. 1994. Functional role of type I and type II interferons in antiviral defense. *Science.* 264: 1918–1921.
4. Cella, M., M. Salio, Y. Sakakibara, H. Langen, I. Julkunen, and A. Lanzavecchia. 1999. Maturation, activation, and protection of dendritic cells induced by double-stranded RNA. *J. Exp. Med.* 189:821–829.
5. Le Bon, A., G. Schiavoni, G. D'Agostino, I. Gresser, F. Belardelli, and D.F. Tough. 2001. Type I interferons potently enhance humoral immunity and can promote isotype switching by stimulating dendritic cells in vivo. *Immunity.* 14:461–470.
6. Uze, G., G. Lutfalla, and I. Gresser. 1990. Genetic transfer of a functional human interferon α receptor into mouse cells: cloning and expression of its cDNA. *Cell.* 60:225–234.
7. Lutfalla, G., and G. Uze. 1994. Structure of the murine interferon α/β receptor-encoding gene: high-frequency rearrangements in the interferon-resistant L1210 cell line. *Gene.* 148:343–346.
8. Akwa, Y., D.E. Hassett, M.L. Eloranta, K. Sandberg, E. Masliah, H. Powell, J.L. Whitton, F.E. Bloom, and I.L. Campbell. 1998. Transgenic expression of IFN-α in the central nervous system of mice protects against lethal neurotropic viral infection but induces inflammation and neurodegeneration. *J. Immunol.* 161:5016–5026.
9. Gresser, I. 1997. Wherefore interferon? *J. Leukoc. Biol.* 61: 567–574.
10. Wathelet, M.G., C.H. Lin, B.S. Parekh, L.V. Ronco, P.M. Howley, and T. Maniatis. 1998. Virus infection induces the assembly of coordinately activated transcription factors on the IFN-β enhancer in vivo. *Mol. Cell.* 1:507–518.
11. Harada, H., M. Matsumoto, M. Sato, Y. Kashiwazaki, T. Kimura, M. Kitagawa, T. Yokochi, R.S. Tan, T. Takasugi, Y. Kadokawa, et al. 1996. Regulation of IFN-α/β genes: evidence for a dual function of the transcription factor complex ISGF3 in the production and action of IFN-α/β. *Genes Cells.* 1:995–1005.
12. Sato, M., N. Hata, M. Asagiri, T. Nakaya, T. Taniguchi, and N. Tanaka. 1998. Positive feedback regulation of type I IFN genes by the IFN-inducible transcription factor IRF-7. *FEBS Lett.* 441:106–110.
13. Marie, I., J.E. Durbin, and D.E. Levy. 1998. Differential viral induction of distinct interferon-α genes by positive feedback through interferon regulatory factor-7. *EMBO J.* 17:6660–6669.
14. Erlandsson, L., R. Blumenthal, M.L. Eloranta, H. Engel, G. Alm, S. Weiss, and T. Leanderson. 1998. Interferon-β is required for interferon-α production in mouse fibroblasts. *Curr. Biol.* 8:223–226.
15. Sato, M., N. Tanaka, N. Hata, E. Oda, and T. Taniguchi. 1998. Involvement of the IRF family transcription factor IRF-3 in virus-induced activation of the IFN-β gene. *FEBS Lett.* 425:112–116.
16. Megyeri, K., W.C. Au, I. Rosztoczy, N.B. Raj, R.L. Miller, M.A. Tomai, and P.M. Pitha. 1995. Stimulation of interferon and cytokine gene expression by imiquimod and stimulation by Sendai virus utilize similar signal transduction pathways. *Mol. Cell. Biol.* 15:2207–2218.
17. Bauer, M., V. Redecke, J.W. Ellwart, B. Scherer, J.P. Kremer, H. Wagner, and G.B. Lipford. 2001. Bacterial CpG-DNA triggers activation and maturation of human $CD11c^-$, $CD123^+$ dendritic cells. *J. Immunol.* 166:5000–5007.
18. Kadowaki, N., S. Antonenko, and Y.J. Liu. 2001. Distinct CpG DNA and polyinosinic-polycytidylic acid double-stranded RNA, respectively, stimulate CD11c- type 2 dendritic cell precursors and $CD11c^+$ dendritic cells to produce type I IFN. *J. Immunol.* 166:2291–2295.
19. Kadowaki, N., S. Ho, S. Antonenko, R. de Waal Malefyt, R.A. Kastelein, F. Bazan, and Y.-J. Liu. 2001. Subsets of human dendritic cell precursors express different toll-like receptors and respond to different microbial antigens. *J. Exp. Med.* 194:863–869.
20. Hemmi, H., O. Takeuchi, T. Kawai, T. Kaisho, S. Sato, H. Sanjo, M. Matsumoto, K. Hoshino, H. Wagner, K. Takeda, and S. Akira. 2000. A Toll-like receptor recognizes bacterial DNA. *Nature.* 408:740–745.
21. Alexopoulou, L., A.C. Holt, R. Medzhitov, and R.A. Flavell. 2001. Recognition of double-stranded RNA and activation of NF-κB by Toll-like receptor 3. *Nature.* 413:732–738.
22. Sandberg, K., M.L. Eloranta, A. Johannisson, and G.V. Alm. 1991. Flow cytometric analysis of natural interferon-α producing cells. *Scand. J. Immunol.* 34:565–576.
23. Ferbas, J.J., J.F. Toso, A.J. Logar, J.S. Navratil, and C.R. Rinaldo, Jr. 1994. $CD4^+$ blood dendritic cells are potent producers of IFN-α in response to in vitro HIV-1 infection. *J. Immunol.* 152:4649–4662.
24. Svensson, H., A. Johannisson, T. Nikkila, G.V. Alm, and B. Cederblad. 1996. The cell surface phenotype of human natural interferon-α producing cells as determined by flow cytometry. *Scand. J. Immunol.* 44:164–172.
25. Siegal, F.P., N. Kadowaki, M. Shodell, P.A. Fitzgerald-Bocarsly, K. Shah, S. Ho, S. Antonenko, and Y.J. Liu. 1999. The nature of the principal type 1 interferon-producing cells in human blood. *Science.* 284:1835–1837.
26. Cella, M., D. Jarrossay, F. Facchetti, O. Alebardi, H. Nakajima, A. Lanzavecchia, and M. Colonna. 1999. Plasmacytoid monocytes migrate to inflamed lymph nodes and produce large amounts of type I interferon. *Nat. Med.* 5:919–923.
27. Eloranta, M.L., and G.V. Alm. 1999. Splenic marginal metallophilic macrophages and marginal zone macrophages are the major interferon-α/β producers in mice upon intravenous challenge with herpes simplex virus. *Scand. J. Immunol.* 49: 391–394.
28. Hochrein, H., K. Shortman, D. Vremec, B. Scott, P. Hertzog, and M. O'Keeffe. 2001. Differential production of IL-12, IFN-α, and IFN-γ by mouse dendritic cell subsets. *J. Immunol.* 166:5448–5455.
29. Nakano, H., M. Yanagita, and M.D. Gunn. 2001. $Cd11c^+b220^+gr\text{-}1^+$ cells in mouse lymph nodes and spleen display characteristics of plasmacytoid dendritic cells. *J. Exp. Med.* 194:1171–1178.
30. Asselin-Paturel, C., A. Boonstra, M. Dalod, I. Durand, N.

Yessaad, C. Dezutter-Dambuyant, A. Vicari, A. O'Garra, C. Biron, F. Briere, and G. Trinchieri. 2001. Mouse type I IFN-producing cells are immature APCs with plasmacytoid morphology. *Nat. Imm.* 2:1144–1150
31. McCaren, L.C., J.J. Holland, and J.T. Syverton. 1959. The mammalian cell-virus relationship. I. Attachment of poliovirus to cultivated cells of primate and non-primate origin. *J. Exp. Med.* 109:475–485.
32. Torres, R.M., and R. Kühn. 1997. Laboratory protocols for conditional gene targeting. Oxford University Press, Oxford. pp. 1–167.
33. Bobrow, M.N., T.D. Harris, K.J. Shaughnessy, and G.J. Litt. 1989. Catalyzed reporter deposition, a novel method of signal amplification. Application to immunoassays. *J. Immunol. Methods.* 125:279–285.
34. Neubuser, A., H. Koseki, and R. Balling. 1995. Characterization and developmental expression of Pax9, a paired-box-containing gene related to Pax1. *Dev. Biol.* 170:701–716.
35. Yeow, W.S., W.C. Au, Y.T. Juang, C.D. Fields, C.L. Dent, D.R. Gewert, and P.M. Pitha. 2000. Reconstitution of virus-mediated expression of interferon α genes in human fibroblast cells by ectopic interferon regulatory factor-7. *J. Biol. Chem.* 275:6313–6320.
36. Hoss-Homfeld, A., E.C. Zwarthoff, and R. Zawatzky. 1989. Cell type specific expression and regulation of murine interferon α and β genes. *Virology.* 173:539–550.
37. Deonarain, R., A. Alcami, M. Alexiou, M.J. Dallman, D.R. Gewert, and A.C. Porter. 2000. Impaired antiviral response and α/β interferon induction in mice lacking β interferon. *J. Virol.* 74:3404–3409.
38. Taniguchi, T., and A. Takaoka. 2001. A weak signal for strong responses: interferon-α/β revisited. *Nat. Rev. Mol. Cell. Biol.* 2:378–386.
39. Barnes, B.J., P.A. Moore, and P.M. Pitha. 2001. Virus-specific activation of a novel interferon regulatory factor, IRF-5, results in the induction of distinct interferon α genes. *J. Biol. Chem.* 276:23382–23390.
40. Eloranta, M.L., K. Sandberg, and G.V. Alm. 1996. The interferon-α/β responses of mice to herpes simplex virus studied at the blood and tissue level in vitro and in vivo. *Scand. J. Immunol.* 43:356–360.
41. Matsuno, K., H. Fujii, and M. Kotani. 1986. Splenic marginal-zone macrophages and marginal metallophils in rats and mice. *Cell Tissue Res.* 246:263–269.
42. Seiler, P., P. Aichele, B. Odermatt, H. Hengartner, R.M. Zinkernagel, and R.A. Schwendener. 1997. Crucial role of marginal zone macrophages and marginal zone metallophils in the clearance of lymphocytic choriomeningitis virus infection. *Eur. J. Immunol.* 27:2626–2633.
43. Guleria, I., and J.W. Pollard. 2001. Aberrant macrophage and neutrophil population dynamics and impaired Th1 response to Listeria monocytogenes in colony-stimulating factor 1-deficient mice. *Infect. Immun.* 69:1795–1807.
44. Howell, D.M., S.B. Feldman, P. Kloser, and P. Fitzgerald-Bocarsly. 1994. Decreased frequency of functional natural interferon-producing cells in peripheral blood of patients with the acquired immune deficiency syndrome. *Clin. Immunol. Immunopathol.* 71:223–230.
45. Soumelis, V., I. Scott, F. Gheyas, D. Bouhour, G. Cozon, L. Cotte, L. Huang, J.A. Levy, and Y.J. Liu. 2001. Depletion of circulating natural type 1 interferon-producing cells in HIV-infected AIDS patients. *Blood.* 98:906–912.